

TECHNICAL REPORT 97-08

**Coprecipitation of radionuclides:
basic concepts, literature review
and first applications**

October 1997

E. Curti

PSI, Würenlingen and Villigen

TECHNICAL REPORT 97-08

**Coprecipitation of radionuclides:
basic concepts, literature review
and first applications**

October 1997

E. Curti

PSI, Würenlingen and Villigen

Der vorliegende Bericht wurde im Auftrag der Nagra erstellt. Der Autor hat seine eigenen Ansichten und Schlussfolgerungen dargestellt. Diese müssen nicht unbedingt mit denjenigen der Nagra übereinstimmen.

Preface

The Waste Management Laboratory at the Paul Scherrer Institute is performing work to develop and test models as well as to acquire specific data relevant to performance assessment of Swiss nuclear waste repositories. These investigations are undertaken in close co-operation with, and with the partial financial support of, the National Cooperative for the Disposal of Radioactive Waste (Nagra). The present report is issued simultaneously as PSI-Bericht and Nagra Technical Report.

ISSN 1015-2636

"Copyright © 1997 by Nagra, Wettingen (Schweiz) / Alle Rechte vorbehalten.

Das Werk einschliesslich aller seiner Teile ist urheberrechtlich geschützt. Jede Verwertung ausserhalb der engen Grenzen des Urheberrechtsgesetzes ist ohne Zustimmung der Nagra unzulässig und strafbar. Das gilt insbesondere für Übersetzungen, Einspeicherung und Verarbeitung in elektronischen Systemen und Programmen, für Mikroverfilmungen, Vervielfältigungen usw."

Abstract

Coprecipitation of radionuclides with solid alteration products is currently not analysed quantitatively in safety assessments for nuclear waste repositories, although this process is thought to be an important mechanism for limiting nuclide concentrations in solution. This is due to the fact that neither the solid phases controlling coprecipitation nor the parameter values necessary to describe this process are known sufficiently.

This introductory report provides basic knowledge on this subject and a review of experimental data from the literature. Emphasis is placed on experiments of trace metal coprecipitation with calcite, because this mineral is a dominating alteration product of cement in the Swiss L/ILW repository. This resulted in a database of *partition coefficients*, which allow to describe empirically the distribution of trace elements between calcite and solution and thus to quantify coprecipitation processes.

Since laboratory data on coprecipitation with calcite are lacking for many safety-relevant radioelements, their partition coefficients were inferred with the help of estimation techniques. Such techniques rely on empirical correlations, which relate the uptake of trace metals in calcite (measured in laboratory tests) with selected chemical properties of the coprecipitated metals (e.g. ionic radius, sorption properties, solubility products of the pure trace metal carbonates). The combination of these correlations with independent geochemical evidence allows the extrapolation of radioelement-specific partition coefficients, which are then used for the quantitative modelling.

In a first step the potential role of radionuclide coprecipitation during cement degradation in the L/ILW repository planned at Wellenberg is assessed. The results of model calculations indicate for many radionuclides that a large fraction of the total inventory would remain trapped in the secondary calcite formed during cement degradation, considerably reducing their solution concentration. Such calculations confirm the large potential of coprecipitation as a solubility-limiting mechanism for many radionuclides and suggest that including this process in future safety analyses could lead to a significant decrease in doses.

Zusammenfassung

Die Mitfällung von Radionukliden in sekundären Festkörpern wurde bis heute bei Sicherheitsanalysen für nukleare Endlager nicht quantitativ analysiert, obwohl dieser Prozess als wichtiger Mechanismus zur Begrenzung der Nuklidkonzentration in der Lösung gilt. Dies ist darauf zurückzuführen, dass weder die Festphasen, welche solche Mitfällungsprozesse bestimmen, noch die für deren Beschreibung nötigen Parameterwerte genügend bekannt sind.

Dieser einführende Bericht vermittelt Grundkenntnisse über dieses Thema und gibt eine Übersicht experimenteller Daten aus der Literatur. Der Schwerpunkt wurde auf Mitfällungsexperimente von Spurenmetallen in Calcit gelegt, weil dieses Mineral eine dominierende Sekundärphase der Zementdegradierung im Schweizerischen SMA-Endlager ist. Daraus entstand eine Datenbank von *Verteilungskoeffizienten*, welche die Verteilung von Spurenelementen zwischen Calcit und Lösung empirisch beschreiben und damit den Mitfällungsprozess quantifizieren.

Da von vielen sicherheitsrelevanten Radioelementen Labordaten über die Mitfällung mit Calcit fehlen, wurden die entsprechenden Verteilungskoeffizienten mit Hilfe verschiedener Abschätzungstechniken abgeleitet. Diese Techniken beruhen auf empirischen Korrelationen, welche die (in Laborexperimenten gemessene) Aufnahme von Spurenmetallen in Calcit mit ausgewählten chemischen Eigenschaften des Spurenmetalls wie dem Ionenradius, den Sorptionseigenschaften oder der Löslichkeit des reinen Karbonates verbinden. Die Kombination solcher Korrelationen mit unabhängigen geochemischen Daten erlaubt die Extrapolation radioelement-spezifischer Verteilungskoeffizienten, welche dann in die quantitative Modellierung einfließen.

In einem ersten Schritt wird die potentielle Rolle der Radionuklidmitfällung während der Zementdegradierung im geplanten SMA Endlager Wellenberg bewertet. Die Ergebnisse von Modellrechnungen zeigen für viele Radionuklide, dass ein wesentlicher Anteil des entsprechenden Gesamtinventars im Laufe der Zementdegradierung durch den sekundär ausgefällten Calcit eingefangen wird. Dadurch werden die Lösungskonzentrationen dieser Radionuklide stark reduziert. Die Rechnungen bestätigen das grosse Potential der Mitfällung als löslichkeitslimitierenden Mechanismus für viele Radionuklide und weisen darauf hin, dass die Berücksichtigung dieses Prozesses in künftigen Sicherheitsanalysen zu signifikant kleineren Dosen führen kann.

Résumé

La coprécipitation de radionucléides dans les phases solides d'altération n'a pas été jusqu'à présent prise en compte quantitativement dans les analyses de sûreté pour les dépôts de déchets nucléaires. Pourtant, ce processus est considéré comme un mécanisme majeur limitant la concentration des radionucléides en solution. Ceci est dû à une méconnaissance des phases solides contrôlant la coprécipitation et des valeurs des paramètres nécessaires pour la décrire.

Ce rapport introductif donne des connaissances de base à ce sujet et inclut une analyse détaillée des données expérimentales accessibles dans la littérature. En particulier, les expériences sur la coprécipitation des métaux en trace avec la calcite ont été largement considérées, puisque ce minéral est l'un des principaux produits d'altération du ciment dans le dépôt final de déchets de basse et moyenne activité. Cette recherche a permis de mettre au point une banque de données contenant des *coefficients de partage* qui permettent de décrire de manière empirique la distribution des éléments traces entre la calcite et la solution et donc de quantifier le processus de coprécipitation.

Pour beaucoup de radioéléments importants, ces coefficients de partage ne sont pas connus sur la base de données de laboratoire. Donc, ils ont été déduits à l'aide de techniques d'estimation. Ces techniques s'appuient sur des corrélations empiriques, permettant de relier l'incorporation des métaux en trace dans la calcite (mesurée par des expériences de laboratoire) avec des propriétés spécifiques des métaux coprécipités (comme le rayon ionique, les propriétés d'adsorption et les produits de solubilité des carbonates purs des métaux en trace). En combinant ces corrélations avec des données géochimiques indépendantes il est alors possible d'extraire les coefficients de partage spécifiques des radioéléments, qui sont ensuite utilisés dans la modélisation quantitative.

Un modèle préliminaire a été développé afin de déterminer le rôle potentiel que la coprécipitation des radionucléides pourrait jouer pendant l'altération du ciment dans le dépôt pour déchets de basse et moyenne activité planifié à Wellenberg. Les résultats de la modélisation montrent qu'une proportion importante de l'inventaire de certains radionucléides sera incorporée dans la calcite secondaire produite pendant l'altération du ciment. Ceci permettrait ainsi de réduire largement la concentration en solution de ces radionucléides. Ces calculs confirment le potentiel remarquable de la coprécipitation comme mécanisme limitant la solubilité des radionucléides. La prise en compte de ces processus dans les analyses de sûreté futures devrait donc diminuer considérablement les doses.

Riassunto

La coprecipitazione di radionuclidi nei prodotti di alterazione solidi non è stata fino ad oggi trattata quantitativamente nelle analisi di sicurezza per depositi di scorie nucleari, nonostante tale processo sia ritenuto un meccanismo essenziale nel limitarne la concentrazione in soluzione. Ciò è dovuto al fatto che nè le fasi solide controllanti la coprecipitazione nè i valori dei parametri necessari per descriverla sono noti in misura sufficiente.

Questo rapporto introduttivo raccoglie nozioni fondamentali su questo tema e comprende un'analisi dettagliata di dati sperimentali accessibili nella letteratura. In special modo, sono stati presi in considerazione esperimenti sulla coprecipitazione di metalli in traccia nella calcite, dato che questo minerale è uno dei principali prodotti di alterazione del cemento nel deposito finale di bassa e media radioattività. Questa ricerca ha dato origine ad una banca di dati per *coefficienti di ripartizione*, attraverso i quali è possibile descrivere empiricamente la distribuzione di elementi in traccia tra calcite e soluzione, quantificando così il processo di coprecipitazione.

Poichè mancano dati di laboratorio per molti radioelementi importanti, i relativi coefficienti di ripartizione sono stati dedotti con l'aiuto di tecniche di stima. Tali tecniche si basano su correlazioni empiriche, che mettono in relazione l'incorporazione dei metalli in traccia nella calcite (misurata tramite test di laboratorio) con proprietà specifiche dei metalli coprecipitati (per esempio il raggio ionico, le proprietà di assorbimento, i prodotti di solubilità dei carbonati puri dei metalli in traccia). Combinando queste correlazioni con dati geochimici indipendenti è possibile estrapolare coefficienti di ripartizione per radioelementi specifici, che vengono poi impiegati ai fini della modellizzazione quantitativa.

Un modello preliminare è stato sviluppato nell'intento di accertare il ruolo potenziale della coprecipitazione di radionuclidi durante la degradazione del cemento nel deposito a bassa e media radioattività pianificato a Wellenberg. I risultati della modellizzazione indicano che importanti frazioni dell'inventario di molti radionuclidi dovrebbero rimanere imprigionate nella calcite secondaria prodotta durante l'alterazione del cemento, riducendo così in misura considerevole la concentrazione di tali radionuclidi in soluzione. Questi calcoli confermano che i processi di coprecipitazione hanno un notevole potenziale quale meccanismo limitante la solubilità dei radionuclidi e suggeriscono che le dosi potrebbero venir ridotte in misura significativa se tali processi verranno considerati nelle analisi di sicurezza future.

Table of content

Preface	II
Abstract	III
Zusammenfassung	IV
Résumé	V
Riassunto	VI
Table of content	VII
1. Introduction	1
2. The Retention of Trace Elements in Minerals	4
2.1 Sorption and Precipitation	4
2.2 Coprecipitation	4
3. The formal treatment of coprecipitation	8
3.1 Solid solution models	8
3.1.1 The thermodynamic approach	8
3.1.2 Binary ideal solid solutions	8
3.1.3 Ideal solid solution model: comparison with experimental data	10
3.2 Empirical relationships for coprecipitation	14
3.2.1. The heterogeneous partition coefficient	14
3.2.2. The homogeneous partition coefficient	16
3.2.3. Homogeneous and heterogeneous coprecipitation	17
3.2.4. Relation of the partition coefficients to thermodynamic solubility products	22
4. Solid solution formation in carbonate minerals	24
4.1 Why carbonates ?	24
4.2 Experimental techniques	24
4.3 Compilation of partition coefficients	26
4.4 Factors affecting the coprecipitation of metals	32
4.4.1 Ionic radius and charge	32
4.4.2 Crystal structure of the host phase	36
4.4.3 Precipitation/ recrystallisation rate	38
4.4.4 Temperature	41
4.4.5 Correlation with the solubility products of pure carbonates	43
4.4.6 Correlation with adsorption	45
4.4.7 Influence of pH and ionic strength	48
4.4.8 Influence of complex formation	48
4.4.9 Concentration and competition effects	50

5.	Mechanisms of solid solution formation	52
6.	Trace element geochemistry of selected radionuclides	56
6.1	Preliminary notes	56
6.2	Nickel	56
6.3	Caesium	61
7.	Radionuclide coprecipitation in the LLW / ILW repository	65
7.1	Preliminary remarks	65
7.2	Calcite formation during cement degradation	65
7.3	Extrapolation to safety-relevant radionuclides	66
7.3.1	Americium, curium	66
7.3.2	Nickel	67
7.3.3	Caesium	68
7.3.4	Strontium, radium	68
7.3.5	Selenium	68
7.3.6	Zirconium, tin, molybdenum, technetium	69
7.3.7	Palladium	69
7.3.8	Thorium, protactinium, uranium, neptunium, plutonium	70
7.4	A model to estimate radionuclide coprecipitation with calcite in the L/ILW repository near-field	72
7.5	Model development	73
7.6	Model parameters	76
7.7	The effect of stable and natural radioactive isotopes	79
7.8	Results: is sorption or coprecipitation more efficient?	83
7.9	Generalisation of the model	86
7.10	Coprecipitation of ^{14}C with calcite	90
7.11	Conclusions	91
8.	Summary, conclusions and recommendations	92
8.1	Models for the quantitative description of coprecipitation processes	92
8.2	Factors affecting radionuclide coprecipitation	92
8.3	Estimation of partition coefficients for radionuclides	94
8.4	The role of coprecipitation as a retention mechanism	94
8.5	A road map for future work	95
8.6	Concluding remarks	96
	Acknowledgements	98
	References	99

1. Introduction

The main purpose of safety analyses for radioactive waste repositories is to assess the radiological hazards arising from the disposal of radioactive waste in geological formations. Safety analyses (e.g. NAGRA 1994a) are normally carried out using a chain of computational models, which rely on a sufficient understanding of the processes affecting in a significant way the release and transport of radionuclides initially present in the waste matrix. Some potentially beneficial processes, however, are not modelled, although they are known to occur and to have a large influence on radionuclide mobility, because they are not sufficiently understood to be approached quantitatively and are considered to contribute only positively to the safety case.

One of the processes not included explicitly in the safety analyses computations carried out up to date for the repositories planned in Switzerland is coprecipitation, i.e. the incorporation of *trace amounts* of radioelements in solid alteration products formed in the repository system. *Coprecipitation* must be clearly distinguished from the *precipitation of pure radioelement phases*. In the latter case, a given radioelement is concentrated in a specific solid, of which the radioelement is a major constituent. In contrast, coprecipitation implies that the radioelement is dispersed in trace concentrations as a foreign constituent of alteration products.

Precipitation of radionuclides is usually modelled assuming that the aqueous phase tends towards equilibrium with pure solids, i.e. with solids in which the corresponding radioelement is a major constituent. This approach, which leads to the definition of radioelement-specific "solubility limits" (used in model calculations for safety analyses), is convenient and justified in some instances, but has important limitations (see e.g. BERNER 1995, pp.2-3 for a detailed discussion).

A major practical problem is that in general little is known of the thermodynamic properties of many radioelements. Thoroughly reviewed and consistent thermodynamic databases exist only for a few elements of interest (essentially U and Am, see GRENTHE et al. 1992; SILVA et al. 1995) and even these cannot be considered to be complete. An additional difficulty lies in the selection of appropriate solubility-limiting solids. In order to be reliable, saturation equilibria should be calculated only for solids which demonstrably form in the chemical environment of interest. A single radioelement may form various solids; it is not always easy to determine which of these solids will effectively precipitate under repository conditions. Metastable, and possibly amorphous, phases may be favoured in low-temperature environments. As a consequence, the most stable (i.e. least soluble) phase will not nucleate, leading to higher elemental solubilities than those calculated assuming thermodynamic equilibrium.

Thus, the uncritical use of thermodynamic databases associated with geochemical codes may easily produce meaningless results. For example, a solubility limit for nickel could be calculated from a variety of Ni-phases commonly reported in thermodynamic databases. These include Ni-silicates and Ni-sulphides which have *never* been found in low-temperature natural environments. Speciation calculations in which one of these minerals is assumed to be at saturation equilibrium with the solution may result in unreasonable Ni concentrations which clearly disagree with ground water concentration data (see BERNER 1995, p.18). As a consequence, the modeller may have to make

very conservative assumptions about the solubility limit for this element to be used in safety analyses (NAGRA 1994a).

Most radionuclides occur, even within high-level radioactive waste, in very small concentrations and have to be considered as *trace elements*. It is well-known from the mineralogical literature that trace elements do not usually form pure solids, unless they are extremely insoluble. More commonly, they are found as finely dispersed contaminants in solids precipitated from the major elements present in the system. Thus, a coprecipitation model is usually more successful in determining the solubility of minor elements than the classical pure phase approach, as demonstrated in a few cases in the laboratory (BRUNO et al. 1995, BRUNO et al. 1996).

Unfortunately, knowledge of coprecipitation reactions is currently limited and it is not possible to incorporate this process in safety assessment models. The difficulties are not of a formal nature, as a variety of quantitative approaches exist. The major problem is the lack of data on the coprecipitation of radioelements with the solids expected to form in the repository environment. In the past decades, the efforts of geochemists working in the field of radioactive waste management were predominantly focused on investigations of radionuclide sorption, a key process contributing to the retardation of radionuclide transport. Although the importance of coprecipitation as a complementary radionuclide retention mechanism is acknowledged by most scientists, very little effort has been made up to date in order to understand and quantify this process.

Among the potentially beneficial processes neglected in safety analyses, radionuclide coprecipitation is estimated to be one of the most important (NAGRA 1994a, p. 169). This report is meant to be a *first step* to fill this gap. The main objective is to provide basic knowledge and guidelines for future work relevant to the problems of radioactive waste management. The objectives of this report are:

- to define and classify the processes identified with the generic term “coprecipitation” and to differentiate them from “sorption” processes (chapter 2);
- to present and develop formal tools for the quantitative treatment of coprecipitation reactions (chapter 3);
- to review the extensive literature on metal coprecipitation with carbonate minerals, in order to identify the chemical factors governing the coprecipitation of trace metals and radionuclides during alteration processes in the repository (chapter 4);
- to understand, on a microscopic scale, the mechanisms involved in solid solution formation (chapter 5);
- to give a generic overview of the behaviour of Ni and Cs during coprecipitation reactions (chapter 6);
- to evaluate the potential role of coprecipitation for the safety of the Swiss L/ILW repository and to give recommendations for future work (chapter 7).

The choice of carbonate minerals for a detailed evaluation is primarily dictated by the fact that extensive coprecipitation data exist only for this mineral group. Fortunately, calcite and other carbonates are ubiquitous and they will play an important role in the Swiss repository environment. Particularly, large amounts of calcite are predicted to form in the L/ILW repository during cement-ground water interaction (NEALL 1994). For other minerals which may form as secondary alteration products in the repository near-field (clay minerals, zeolites, hydrous oxides), *quantitative* coprecipitation studies are rare (e.g. BRUNO et al. 1995) and a systematic analysis like that carried out for carbonate minerals is not currently possible.

2. The Retention of Trace Elements in Minerals

2.1 Sorption and Precipitation

The scavenging of dissolved chemical species from a solution requires interaction with solid phases. Two broad process types can be distinguished: *precipitation* and *sorption*. Precipitation requires the formation of new solids, into which chemical species removed from solution are transferred. Changes in solute concentrations due to precipitation depend on the amount of precipitated solid. Sorption processes, in contrast, do not require the formation of new solids; the species removed from solution are taken up on pre-existing mineral surfaces, so that changes in solute concentrations are proportional to the exposed surface area of the mineral (COREY 1981).

The concepts of sorption and precipitation can be differentiated more finely. Depending on scientific roots and taste of the researchers, a considerable number of contradictory definitions, and consequently much confusion, has been created. To avoid misunderstandings, a summary of the definitions used in this report for sorption and coprecipitation processes is given in Table 2-1.

2.2 Coprecipitation

Coprecipitation is a special case of precipitation. It occurs whenever foreign solutes are trapped in the body of a precipitating solid of stoichiometric composition. For example, a crystal growing from a solution containing only sodium, chloride and water, will result in a pure mineral with formula NaCl (*halite*). If the solution contains other cations, like K^+ and Cs^+ , a small fraction of them will be included in the mineral. The mineral formula will then be $(Na_x K_y Cs_z)Cl$, and we say that potassium and caesium ions coprecipitate with *halite*. In this case x is approximately 1, while y and z will be very small, implying that only traces of K^+ and Cs^+ are included in the solid.

At high temperatures, the miscibility of different components in solids increases. In the limiting case completely miscible solid solutions are formed, like the olivine - forsterite series (Mg_2SiO_4 - Fe_2SiO_4). At low temperatures, however, coprecipitation of foreign components is normally limited to a few mole percent. Since we are interested in low-temperature conditions (prevailing in radioactive waste repositories), in this report the term coprecipitation refers only the uptake of *trace elements* in solids at low temperature; high-temperature miscibility phenomena are thus disregarded.

A coprecipitate may form either through precipitation of a new phase from a supersaturated solution or through rearrangement (recrystallisation or ageing¹) of a

¹ Recrystallisation (also termed Ostwald ripening) is the transformation of a solid compound made of many small crystals into an equivalent amount of few large crystals of the same compound. Ageing is the process by which an initially amorphous precipitate becomes crystalline, or by which a crystalline metastable phase is converted in a more stable phase.

pre-existing phase at saturation. In contrast to coprecipitation from a supersaturated solution, recrystallisation and ageing proceed almost without net changes in the mass of the solid, since these processes are essentially phase transformations.

Table 2-1: Classification and definition of sorption and coprecipitation processes.

<p>SORPTION</p> <p>The reversible uptake of ions, atoms or molecules on a mineral surface</p>	<p>SPECIFIC ADSORPTION = SURFACE COMPLEXATION</p>	<p>The uptake of dissolved species on a mineral surface through formation of covalent bonds.</p>
	<p>ION EXCHANGE</p>	<p>The uptake of ions on a mineral surface with the simultaneous displacement of a previously adsorbed ions.</p>
	<p>PHYSICAL ADSORPTION</p>	<p>The uptake of molecules to a mineral surface through Van der Waals forces.</p>
<p>COPRECIPITATION</p> <p>The trapping of foreign chemical components in a solid of stoichiometric composition</p>	<p>ISOMORPHOUS REPLACEMENT (SOLID SOLUTION)</p>	<p>The incorporation of foreign ions in crystal lattice sites usually occupied by a major ion of the solid.</p>
	<p>INCORPORATION IN CRYSTAL DEFECTS</p>	<p>Incorporation of foreign ions, atoms or molecules outside the crystal lattice positions (e.g. in vacancies or dislocations). For an amorphous compound, any incorporation at atomic scale.</p>
	<p>NON-UNIFORM INCORPORATION</p>	<p>The trapping of discrete particles (e.g. colloids) in a growing solid.</p>

In spite of these differences, there is no need for a terminological distinction of coprecipitation, since also recrystallisation and ageing involve precipitation of a new solid

(they proceed through dissolution of the primary solid and simultaneous reprecipitation of thermodynamically more stable crystals). The driving force for recrystallisation processes is the small difference in free energy between the primary precipitate and the recrystallised solid: a finely divided precipitate is less stable, and hence slightly more soluble, than a coarse-grained solid because its surface tension contributes significantly to the total free energy. There are good reasons to believe that recrystallisation and ageing may lead to permanent structural rearrangements at the surface layers of the solids (STIPP et al. 1992; STIPP et al. 1994), which ultimately leads to a phenomenon generically termed *surface precipitation* or *surface mineralisation*. Such processes are frequently misunderstood as sorption processes (the so-called *irreversible adsorption*, which implies that the “adsorbed” chemical species cannot be desorbed after such restructuring of the surface has taken place).

The following precipitation mechanisms can be distinguished:

- *homogeneous nucleation*, by which a solid phase is generated directly from a homogeneous solution. This mechanism usually requires a high degree of supersaturation and is thought to be of secondary importance in natural processes.
- *heterogeneous nucleation*, by which a new mineral is generated on top of a pre-existing mineral surface. Heterogeneous nucleation is facilitated if the crystalline structures of substrate and precipitate are similar (i.e. silicates will tend to nucleate on existing silicates, sulphides on sulphides, and so on). This mechanism is the most frequent in geological environments, where a large variety of minerals with different surface structures exist, offering adequate substrates for the growth of new solids.

The distribution of trace elements in the solids varies according to the incorporation mechanism. One can distinguish between:

- *isomorphous replacement*: the trace ions are fixed at lattice sites usually occupied by regular ions (e.g. Ni^{2+} for Ca^{2+} in calcite). This mechanism is favoured in the case of chemical affinity between the trace ion and the substituted ion (similar ionic radii and charges, analogous electronic configurations). Only isomorphous replacement produces true *solid solutions*, as described by thermodynamic mixing models.
- *incorporation in crystal defects*: the coprecipitated trace ions are incorporated on sites of crystal defects (vacancies, dislocations).
- *non-uniform incorporation*: trace components may be incorporated into a solid through physical isolation of discrete particles from the solution. This may be the case of colloidal particles sticking on the surface of a growing mineral, which become covered by successive layers of the precipitating host solid, or of fluid inclusions.

The latter two mechanisms are typical of high precipitation rates, while isomorphous replacement prevails at low recrystallisation/precipitation rates (for instance, when the precipitation rate does not exceed the rate at which sorption equilibria are established).

The classification of coprecipitation phenomena given above is not an established, generally accepted scheme. However, a review of the literature on coprecipitation revealed such a terminological confusion², that it seemed necessary to make some order. This was achieved by reducing the categories of coprecipitation phenomena to three basic categories, each characterised by a clear definition.

Finally, it must be pointed out that there are trace element retention processes which, by their own nature, cannot be unequivocally assigned to either the category "sorption" or "coprecipitation". For example, the phenomenon of "internal adsorption" (the adsorption of trace elements on the walls of sealed microcavities in a growing solid) is macroscopically a coprecipitation process (HAHN 1936) although on the microscopic scale it has to be considered as a reversible sorption process (the adsorbed ions would desorb if they had access to the bulk solution).

² As an example, obsolete terms like "occlusion", "internal adsorption", "partial precipitation", "anomalous mixed crystals", "replacement" occur in the literature on coprecipitation.

3. The formal treatment of coprecipitation

3.1 Solid solution models

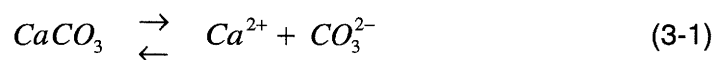
3.1.1 The thermodynamic approach

Various models based on chemical thermodynamics have been developed to predict the equilibrium distribution of mixed chemical components in isomorphous solid solutions and in the coexisting aqueous solutions (see e.g. NORDSTROM & MUNOZ 1985, p.152, GLYNN & REARDON 1990). Although the laws of chemical thermodynamics offer a solid theoretical framework for the development of rigorous solid solution models, their applicability is currently limited. Such models tend to become complicated as soon as the number of components exceeds two. Further, they frequently operate with complex thermodynamic functions, generally requiring a number of undetermined experimental parameters. It is thus not surprising that solid solution models often fail in predicting the solubility of impure solids and the equilibrium concentrations of the relevant chemical species (see e.g. GRAUER 1988, p.2; NORDSTROM & MUNOZ 1985, p. 236).

The problem is not the thermodynamics itself, but the complexity of the processes taking place during the formation of mixed solids. For instance, a specific cation may be incorporated in a clay mineral at different lattice sites, or it may be distributed either randomly or in an ordered way within the crystal. This affects the configuration entropy and hence the free energy of the mineral. This example shows that the knowledge of the chemical composition of the mineral may not be sufficient to describe an impure solid: also detailed crystallographic information is needed for the correct treatment of solid solution thermodynamics.

3.1.2 Binary ideal solid solutions

The dissolution of a pure calcite in water can be described by the following chemical reaction:



Dissolution proceeds until thermodynamic equilibrium (saturation) is reached between solid and aqueous solution. This condition corresponds to a state of minimum free energy, which is expressed by a fixed value of the activity product at equilibrium:

$$K_{\text{calcite}} = \frac{(Ca^{2+})(CO_3^{2-})}{a_{\text{calcite}}^{CaCO_3}} = (Ca^{2+})(CO_3^{2-}) \quad (3-2)$$

where:

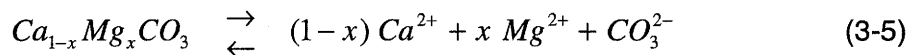
K_{calcite} is the thermodynamic solubility product of *pure* calcite,
 $a_{\text{calcite}}^{CaCO_3}$ is the activity of calcium carbonate in calcite (1 in pure calcite),
 $(Ca^{2+}), (CO_3^{2-})$ are the activities of the calcium and carbonate ions in solution.

The right-hand side of Equation (3-2) is simplified because the activity of the component forming a pure mineral is, by definition, equal to unity. The simplest solid solution involves mixing of *two* components at a *single* crystallographic site (e.g. isomorphous substitution of Mg^{2+} for Ca^{2+} in calcite). The solubility of a solid solution generally differs from that of the end-member minerals. This experimental fact is accounted for in thermodynamics by adjusting the activities in the solid to values less than unity. A common practice in dealing with solid solutions is to assume that the components mix ideally³, in which case the activity of each component is assumed to be equal to its mole fraction. The activity products of calcite and magnesite in a solid solution containing x moles of Mg^{2+} per mole calcite are then given by:

$$(Ca^{2+})(CO_3^{2-}) = a_{\text{calcite}}^{CaCO_3} K_{\text{calcite}} = (1-x) K_{\text{calcite}} \quad (3-3)$$

$$(Mg^{2+})(CO_3^{2-}) = a_{\text{calcite}}^{MgCO_3} K_{\text{magnesite}} = x K_{\text{magnesite}} \quad (3-4)$$

where the quantities in Equation (3-4) are analogous to those defined for Equations (3-2) and (3-3)⁴. Equations (3-3) and (3-4) express the activity products $(Ca^{2+})(CO_3^{2-})$ and $(Mg^{2+})(CO_3^{2-})$ in a solution at equilibrium with a Mg-calcite of composition $Ca_{1-x}Mg_xCO_3$. The congruent dissolution reaction and the *stoichiometric equilibrium constant*, $K_{ss}(x)$, for the solid solution of the specified composition are defined as follows:



$$K_{ss}(x) = (Ca^{2+})^{1-x} (Mg^{2+})^x (CO_3^{2-}) \quad (3-6)$$

³ Ideal mixing implies that the enthalpy of mixing is zero, i.e. that there is no heat exchange when two or more components mix to form a solid solution. Although this assumption greatly simplifies the thermodynamic description of solid solutions and is thus very popular, it is frequently inaccurate, as demonstrated later in this chapter.

⁴ The term $x K_{\text{magnesite}}$ in Equation (3-4) is equivalent to the *conditional solubility constant* defined by BRUNO et al. (1995) to describe coprecipitation of U(VI) with iron hydroxide.

Equation (3-6) can be related to Equations (3-3) and (3-4) in order to express $K_{ss}(x)$ as a function of the mole fraction of Mg in the solid and of the solubility products of the pure end-members:

$$\begin{aligned} K_{ss}(x) &= (Ca^{2+})^{1-x} (Mg^{2+})^x (CO_3^{2-}) = \\ &= [(Ca^{2+})(CO_3^{2-})]^{1-x} [(Mg^{2+})(CO_3^{2-})]^x = \\ &= [(1-x)K_{calcite}]^{1-x} [x K_{magnesite}]^x \end{aligned} \quad (3-7)$$

Equations (3-5), (3-6) and (3-7) may be used: (a) to predict the change in solubility due to magnesium contamination in calcite, or (b), to calculate the equilibrium composition of the solid solution and coexisting aqueous phase. From the point of view of this report, effects due to changes in the solubility of the solid will in general be negligible: since radionuclides will coprecipitate only in trace amounts, x will be very small, implying that both the second term of the product on the right-hand side of Equation (3-7) and the term $(1-x)$ approach unity. Therefore the solubility of a calcite with very small amounts of magnesium or other cations will not differ significantly from that of pure calcite⁵. The second application is the main concern, since we are primarily interested in the distribution of trace radionuclides between impure alteration solids and aqueous solution. Thus, only this aspect of solid solution models will be considered in the further discussion.

3.1.3 Ideal solid solution model: comparison with experimental data

In this section, experimental data on the coprecipitation of Mg^{2+} , Sr^{2+} , Fe^{2+} and Mn^{2+} with calcite will be compared with ideal solid solution models for calcite-magnesite ($CaCO_3$ - $MgCO_3$), calcite-strontianite ($CaCO_3$ - $SrCO_3$), calcite-siderite ($CaCO_3$ - $FeCO_3$) and calcite-rhodochrosite ($CaCO_3$ - $MnCO_3$) mixed crystals.

In order to obtain a convenient graphic representation, Equation (3-4) is divided by Equation (3-3), which leads to the following expression:

$$\frac{(Mg^{2+})}{(Ca^{2+})} = \frac{\gamma_{Mg^{2+}} \alpha_{Mg^{2+}} [Mg]_{tot}}{\gamma_{Ca^{2+}} \alpha_{Ca^{2+}} [Ca]_{tot}} = \frac{\gamma_{Mg^{2+}} [Mg^{2+}]}{\gamma_{Ca^{2+}} [Ca^{2+}]} = \frac{K_{magnesite}}{K_{calcite}} \frac{x}{1-x} \quad (3-8)$$

⁵ Nevertheless, one should be aware that also non-radioactive elements will coprecipitate with calcite (e.g. stable isotopes of Fe and Ni). If the total solution concentrations of such elements are sufficiently high, changes in calcite solubility may become significant and should therefore be considered in speciation calculations.

where $\gamma_{Mg^{2+}}$, $\gamma_{Ca^{2+}}$ are individual ion activity coefficients, $\alpha_{Mg^{2+}}$, $\alpha_{Ca^{2+}}$ are the corresponding fractions of uncomplexed metal, $[Mg]_{tot}$, $[Ca]_{tot}$ denote total elemental concentrations and $[Mg^{2+}]$, $[Ca^{2+}]$ are free ion concentrations, all in molal units. Assuming identical activity coefficients for like-charged species (e.g. Davies approximation), then Equation (3-8) simplifies to:

$$\frac{[Mg^{2+}]}{[Ca^{2+}]} \cong \frac{K_{magnesite}}{K_{calcite}} \frac{x}{1-x} \quad (3-9)$$

Using the equilibrium constants given in PEARSON et al. (1992) ($K_{magnesite} = 10^{-8.04}$, $K_{strontianite} = 10^{-9.29}$ and $K_{calcite} = 10^{-8.48}$ at 25°C) Equation (3-9) has been plotted in Figure 3-1 for the calcite-magnesite and for the calcite-strontianite solid solutions together with selected experimental data. In both cases the ideal solid solution model is inadequate, since it predicts, at a given $[Me^{2+}] / [Ca^{2+}]$ ratio, much larger trace metal concentrations in calcite than effectively observed.

The data on the coprecipitation of Mn^{2+} and Fe^{2+} (DROMGOOLE & WALTER 1990) also appear to be inconsistent with the ideal solid solution model (Figure 3-2). In this case, the experimental data do not define linear arrays as in the case of Sr^{2+} and Mg^{2+} , but are distributed horizontally, parallel to the x-axis. This peculiar arrangement is the result of variations in the precipitation kinetics imposed to these experiments: the amount of Mn^{2+} or Fe^{2+} coprecipitated at a given $[Me^{2+}] / [Ca^{2+}]$ ratio in solution increases as the calcite precipitation is made slower. These plots may show that the predictions of the thermodynamic model are approached if the effects of fast kinetics are progressively turned off. Nevertheless, discrepancies remain even at the slowest precipitation rates imposed in these experiments⁶. Unlike the preceding cases (Sr^{2+} and Mg^{2+}), the $[Me^{2+}] / [Ca^{2+}]$ ratios do not coincide with the total elemental concentrations given by the solution analyses, because the formation of carbonate and chloride complexes is no longer negligible (these experiments were carried out in 0.1 M $CaCl_2$ solutions at pCO_2 reaching 1 atm while the experiments with Sr^{2+} and Mg^{2+} were carried out in dilute solutions). The Mg^{2+} and Mn^{2+} solution concentrations were thus determined with the help of speciation calculations⁷.

⁶ The "slowest precipitation rates" in the experiments of DROMGOOLE & WALTER (1990) approximate the recrystallisation rates in the experiments of KATZ et al. (1972) and KATZ (1973), i.e. $\sim 10^{-7}$ mol $m^{-2} s^{-1}$.

⁷ In Figure 3-1, the quantities on the ordinate coincide with the elemental metal/calcium ratios, since no significant complexation occurs in the solutions used in the corresponding experiments. Speciation calculations for the Mn and Fe data, on the contrary, predict important complexation with chloride and carbonate species. The stability constants used in the speciation calculations are: $\log K (MnCO_3^0) = \log K (FeCO_3^0) = 5$, obtained from a provisional correlation of stability constants through the Irving-Williams series (Hummel, personal communication), $\log K (MnHCO_3^+) = \log K (FeHCO_3^+) = 12.3$, $\log K (MnCl^+) = 0.61$, $\log K (FeCl^+) = 0.14$ (PEARSON et al. 1992). All constants refer to the complex formation reaction at 25 °C and are extrapolated to zero ionic strength.

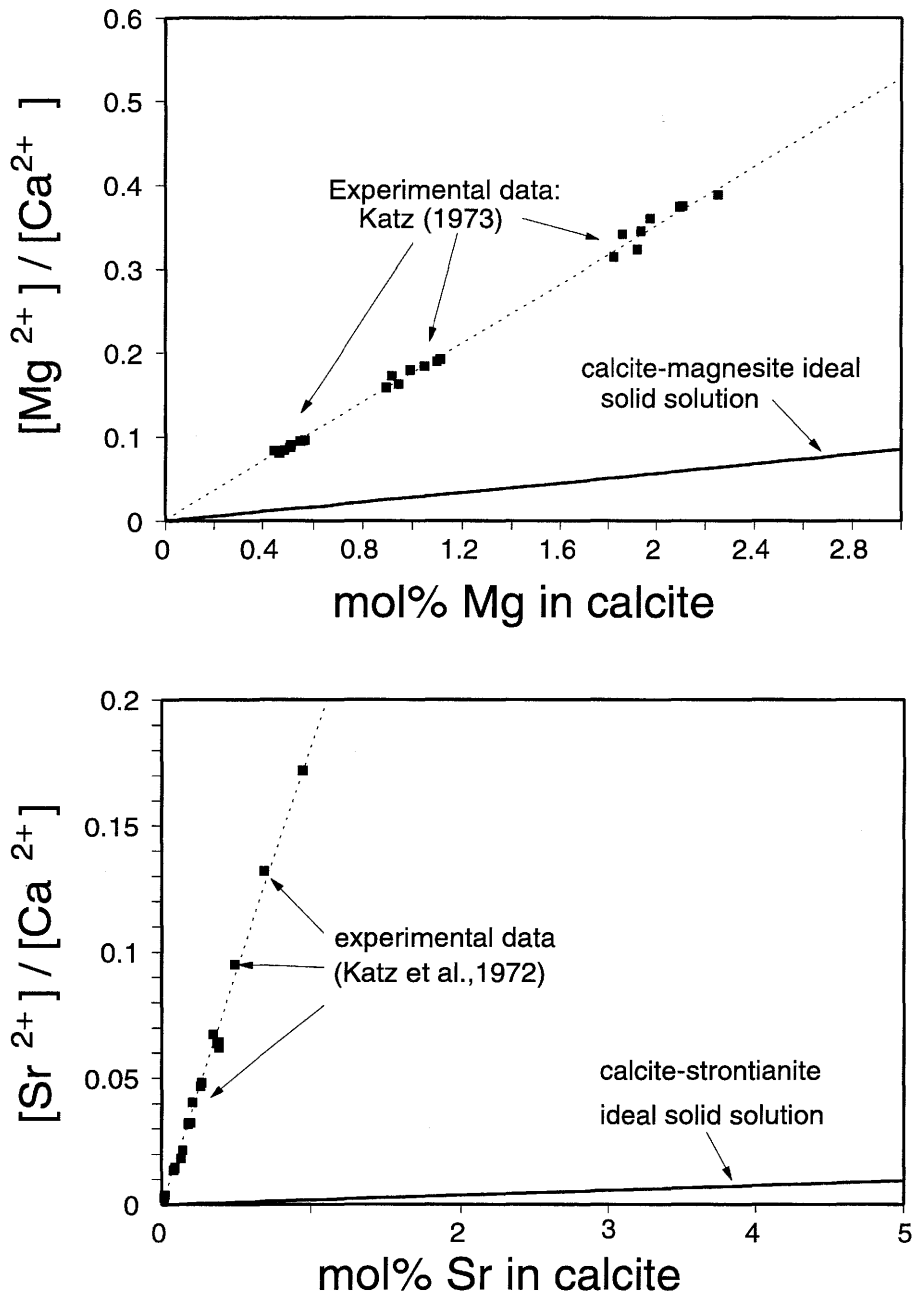


Figure 3-1: Comparison between experimental data on the coprecipitation of Mg^{2+} and Sr^{2+} with calcite and ideal solid solution models. The selected data (KATZ et al. 1972, KATZ 1973) are particularly accurate, as indicated by their excellent linear distribution. They were obtained from experiments in which aragonite, previously doped with Mg^{2+} or Sr^{2+} , had been recrystallised to calcite. This method guarantees slow reaction rates, ensuring that all reactions involved in the coprecipitation process are close to equilibrium. Despite these favourable conditions, the solid solution model fails in reproducing the experimental data.

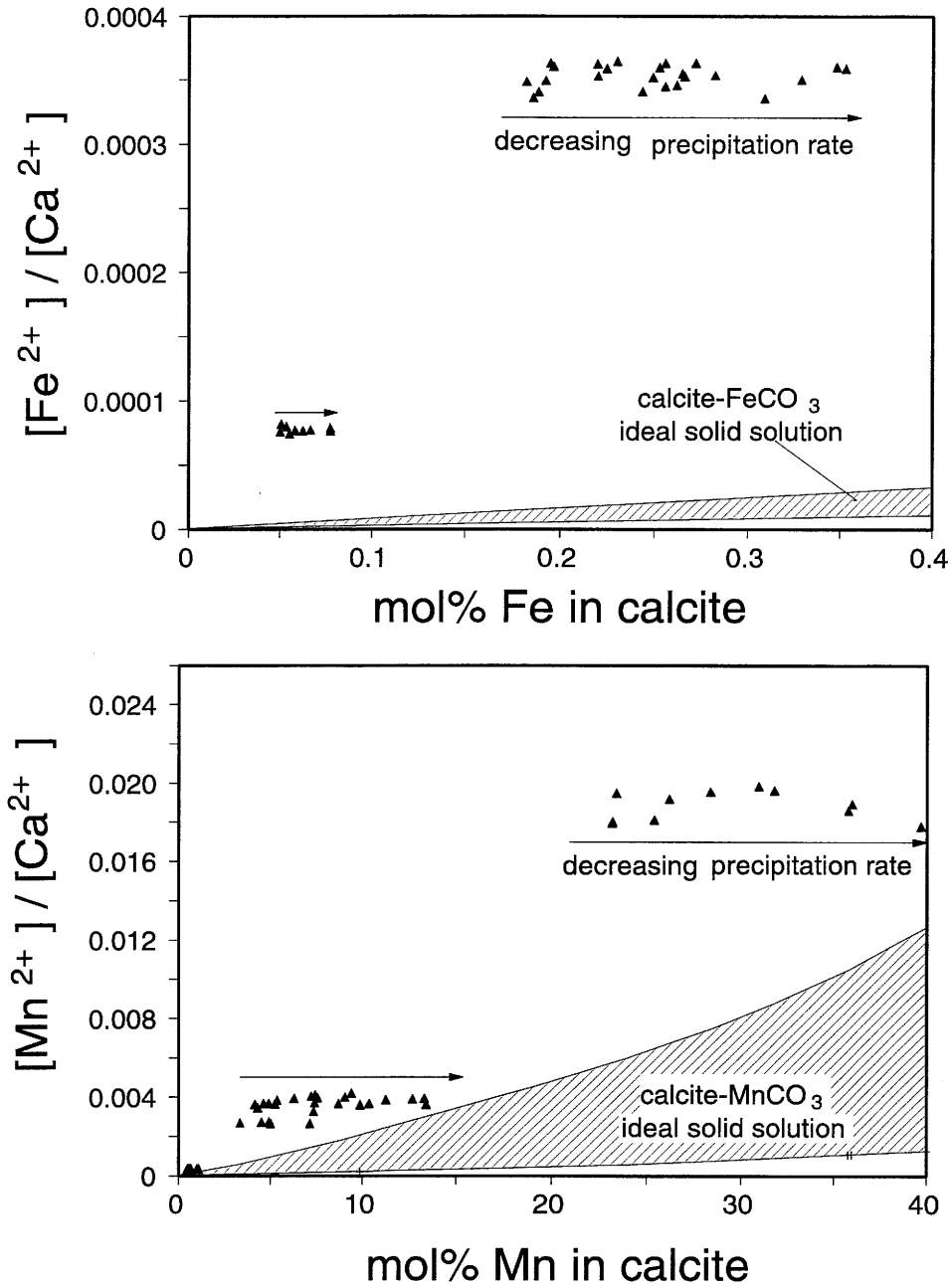


Figure 3-2: Comparison between experimental data on the coprecipitation of Fe^{2+} and Mn^{2+} with calcite (DROMGOOLE & WALTER 1990) and ideal solid solution models. Unlike in Figure 3-1, the solid solution models define regions (stippled areas) due to considerable uncertainties in the solubility products of the iron and manganese carbonates. The solubility products recommended by GRAUER (1994) were used ($pK_{S0} = 10.7 \pm 0.5$ for $MnCO_3$ and $pK_{S0} = 10.8 \pm 0.2$ for $FeCO_3$). The horizontal distribution of the experimental data results from variations in the rate of calcite precipitation. In both cases, the ideal solid solution models overestimate the amount of metal incorporated at a given metal/calcium ratio in solution.

These observations indicate a further limitation of thermodynamic solid solution models: such models seem to be appropriate only for systems in which precipitation is slow. In many laboratory situations precipitation rates may be sufficiently high to prevent some reactions involved in the process of trace element incorporation (e.g. the adsorption of the trace element to the mineral surface) from reaching equilibrium. The data in Figure 3-2 exemplify the dependence and sensitivity of coprecipitation processes on the kinetics of mineral formation. Thus, when modelling radionuclide uptake in secondary phases, the effect of precipitation kinetics should be considered. This question will be addressed later in more detail (see section 4.4.3).

In contrast to the findings presented above, BRUNO et al. (1995) (see also READ et al. 1996) were able to show that coprecipitation of uranyl with ferric iron hydroxide follows reasonably well an ideal mixing law over a comparable range of mole fractions (up to 3 mole % U in $\text{Fe}(\text{OH})_3$), suggesting that this simplest solid solution model may, at least in some cases, be suitable to predict coprecipitation phenomena in oxyhydroxides.

It cannot be excluded that more refined thermodynamic models may succeed in predicting the coprecipitation of trace elements with carbonates. However, this question is presently of secondary importance compared to the need for a synthesis of published experimental data and will be addressed in a future report. There exists an extensive literature on laboratory studies of metal coprecipitation with carbonate minerals which still needs to be reviewed. A primary aim of this report is to examine these data and to discover dependencies on measurable chemical properties of the coprecipitated elements. The objective is to identify, by means of empirical correlations, which chemical and physical factors mostly influence coprecipitation processes in low-temperature aqueous solutions. To this purpose, an alternative phenomenological approach, which relies on empirical distribution laws, will be adopted to treat coprecipitation. This approach will be introduced in the following sections.

3.2 Empirical relationships for coprecipitation

3.2.1. The heterogeneous partition coefficient

An early definition of empirical laws governing the distribution (partition)⁸ of coprecipitating chemical species between solid and aqueous solution is given in DOERNER & HOSKINS (1925). It is instructive to quote their introductory note, because it states with clarity the essential feature which makes radionuclide coprecipitation a beneficial process for radioactive waste disposal:

⁸ In the literature both the terms "distribution coefficient" and "partition coefficient" are encountered as synonyms describing the distribution of a trace element between solid and aqueous solution following coprecipitation. The term "distribution coefficient" is, however, equivocal, since it is also used in the treatment of sorption processes. In this report the term "distribution coefficient" will refer exclusively to sorption processes, while the term "partition coefficient" will be used only in conjunction with coprecipitation.

" It has been generally recognized that when a solution of radium and barium chlorides is treated with an excess of sulphuric acid, both the barium and radium are precipitated quantitatively, even though the concentration of radium is so small that its true solubility as sulfate is far from being reached. In every case the amount of radium left in solution is many time less than would be expected from the solubility of pure radium sulfate."

Doerner and Hoskins recognised that the precipitation of a phase formed from major components in solution (barium sulphate) may scavenge efficiently a minor component (Ra^{2+}) even if its concentration in solution is much less than the solubility of the corresponding pure phase (radium sulphate). This is precisely the beneficial effect which modellers would like to include when predicting the migration of soluble radionuclides for safety analyses.

In their experiments, DOERNER & HOSKINS (1925) added sulphuric acid to solutions with predetermined concentrations of dissolved radium and barium, causing the precipitation of impure barium sulphate. By varying appropriately the concentrations of dissolved species and allowing for slow precipitation, they could show that the mole ratio of radium to barium incorporated in the *surface layer* of the solid was proportional to the molar ratio in solution, according to the following relation:

$$\frac{\{T\}_{surface}}{\{C\}_{surface}} = \lambda \frac{[T]}{[C]} \quad (3-10)$$

where :

- $\{ \}_{surface}$ denotes mole fractions at the surface of the solid [-]
- $[\]$ denotes total concentrations in solution [M]
- T is the trace element (radium in this case)
- C is the carrier element (barium in this case)
- λ is a proportionality factor [-]

The proportionality factor λ is called *heterogeneous partition coefficient*. The qualification "heterogeneous" means that the crystal is not in a state of internal equilibrium, i.e. only the surface layer of the solid contacting the aqueous solution obeys the relation stated by Equation (3-10). If this law applies, the composition of a crystal precipitating from a solution will not be, in general, uniform. For any impure solid precipitating in a closed system, the concentration of the trace element will vary from the core towards the rim of the crystal, generating *zoned crystals*. Compositional zonation will not develop, however, if of both carrier and trace elements are buffered to constant solution concentrations, or if the value of λ is equal to one (see later in this chapter).

Equation (3-10) was found to apply to many solids precipitating in low-temperature geologic environments and is thus considered to be appropriate for waste management studies. This “law” was first enunciated before the turn of the century by BERTHELOT (1872) and NERNST (1891) but most recent works refer to the definition given by DOERNER & HOSKINS (1925). Therefore it is cited in the literature both as *Berthelot-Nernst law* and *Doerner-Hoskins law*.

3.2.2. The homogeneous partition coefficient

If equilibrium is maintained with the *bulk* of the solid, not just with its surface, then the distribution of a trace element coprecipitating with an impure solid will be uniform within the solid and adjust continuously to any change of the carrier/trace concentration ratio in solution. In this case, the coprecipitating components follow a different partition law:

$$\frac{\{T\}_{bulk\ solid}}{\{C\}_{bulk\ solid}} = D \frac{[T]}{[C]} \quad (3-11)$$

where D is the *homogeneous partition coefficient*. Homogeneous coprecipitation always results in crystals with a spatially uniform, but time-dependent, distribution of the trace elements. That is, if we would monitor the concentration of a trace element at many locations of the crystal during its growth, we would measure at any given instant everywhere the same concentration, which however changes with time.

In spite of their identical form, Equations (3-10) and (3-11) lead to different results. Criteria for the distinction between D and λ will be presented in section 3.2.3⁹. The homogeneous partition law rarely applies to low-temperature systems. This is not surprising considering the slow rates at which atoms and ions diffuse through a crystal lattice at temperatures below 100 °C (volume diffusion). Since diffusion coefficients for volume diffusion increase exponentially with temperature (see KLEBER 1975, p.220), fast internal equilibration within crystals, leading to a homogeneous composition in the crystal, may be expected only at high temperatures. There are nevertheless simple compounds in which the ionic mobility is so high that homogeneous precipitates are obtained in the laboratory even under atmospheric conditions¹⁰. On the other hand, zoned crystals are common among feldspars grown in contact with a magmatic phase, indicating that heterogeneous crystals may form even at high temperature.

From the definitions given in Equation (3-10) and (3-11), the following rules can be derived, which help to understand qualitatively the meaning of the partition coefficient:

⁹ Strictly, there is no need to introduce two different symbols, D and λ , to describe homogeneous and heterogeneous coprecipitation, because the distinction between the two processes is based on the behaviour of the trace element in the crystal, after coprecipitation occurred, and not on differences in the coprecipitation mechanisms. However, these symbols are so deep-seated in the literature, that it is preferable to keep them in this report.

¹⁰ mainly soluble salts precipitated under peculiar laboratory conditions, see HAHN (1936).

- $\lambda, D > 1$:the trace element is enriched in the solid (i.e. the trace/carrier element ratio is higher in the solid than in solution);
- $\lambda, D < 1$:the trace element is depleted in the solid (i.e. the trace/carrier element ratio is lower in the solid than in solution);
- $\lambda, D = 1$:the trace element is neither enriched nor depleted in the solid (i.e. the trace/carrier element ratios in solution and in the solid are equal).

3.2.3. Homogeneous and heterogeneous coprecipitation

Because of technical difficulties in measuring trace concentrations in small amounts of precipitated solids, DOERNER & HOSKINS (1925) derived a simple equation to calculate the heterogeneous partition coefficient (λ) from solution concentration data alone.

We assume a closed system consisting of a fixed volume of well-mixed solution containing two dissolved coprecipitating species (Figure 3-3). If these species distribute themselves according to the heterogeneous partition law, then the following relation must hold for any *small* increment, Δm , of the mass of the solid:

$$\frac{\{T\}_{surface}}{\{C\}_{surface}} = \frac{-\Delta[T]}{-\Delta[C]} = \lambda \frac{[T] + \Delta[T]}{[C] + \Delta[C]}. \quad (3-12)$$

For $\Delta m \rightarrow 0$, $\Delta[T]$ and $\Delta[C]$ also tend to zero and the following differential equation is obtained:

$$\frac{d[T]}{d[C]} = \lambda \frac{[T]}{[C]} \quad (3-13)$$

Setting as initial conditions $[T] = [T]_0$ and $[C] = [C]_0$, the solution of Equation (3-13) is:

$$\ln \frac{[T]}{[T]_0} = \lambda \ln \frac{[C]}{[C]_0} \quad (3-14)$$

Equation (3-14) allows the calculation of λ from the initial and final solution concentrations of the carrier and trace species, without resorting to the analysis of trace element concentrations in the solid. An equivalent expression can be easily derived for the homogeneous coprecipitation law:

$$\frac{\{T\}_{bulk\ solid}}{\{C\}_{bulk\ solid}} = \frac{[T]_0 - [T]}{[C]_0 - [C]} = D \frac{[T]}{[C]} \quad (3-15)$$

Equations (3-12) to (3-15) are not generally valid and apply only to closed systems, where no exchange of the species T and C with an external reservoir occurs. These equations are useful as criteria to distinguish between heterogeneous and homogeneous coprecipitation in suitable experiments. If the heterogeneous law applies, then the calculated value of λ will remain constant for a series of experiments with different initial concentrations of carrier and trace element, while D will vary in the same series of experiments. Conversely, if the homogeneous law applies, then D will remain constant and λ will vary.

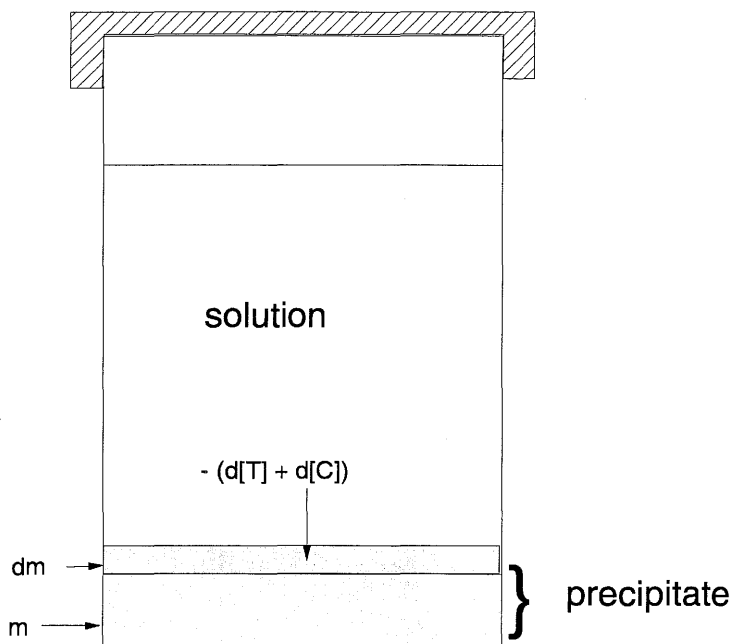


Figure 3-3: Schematic illustration of the experimental set-up for which the equations developed in section 3.2.3 are valid: a *closed* system consisting of a supersaturated solution from which the components C and T coprecipitate.

Figure 3-4 shows a comparison between the homogeneous and heterogeneous coprecipitation models based on Equations (3-14) and (3-15). The relative concentration of trace element *in solution* $[T]/[T]_0$, is plotted as a function of the relative concentration of carrier element *in solution* $[C]/[C]_0$.

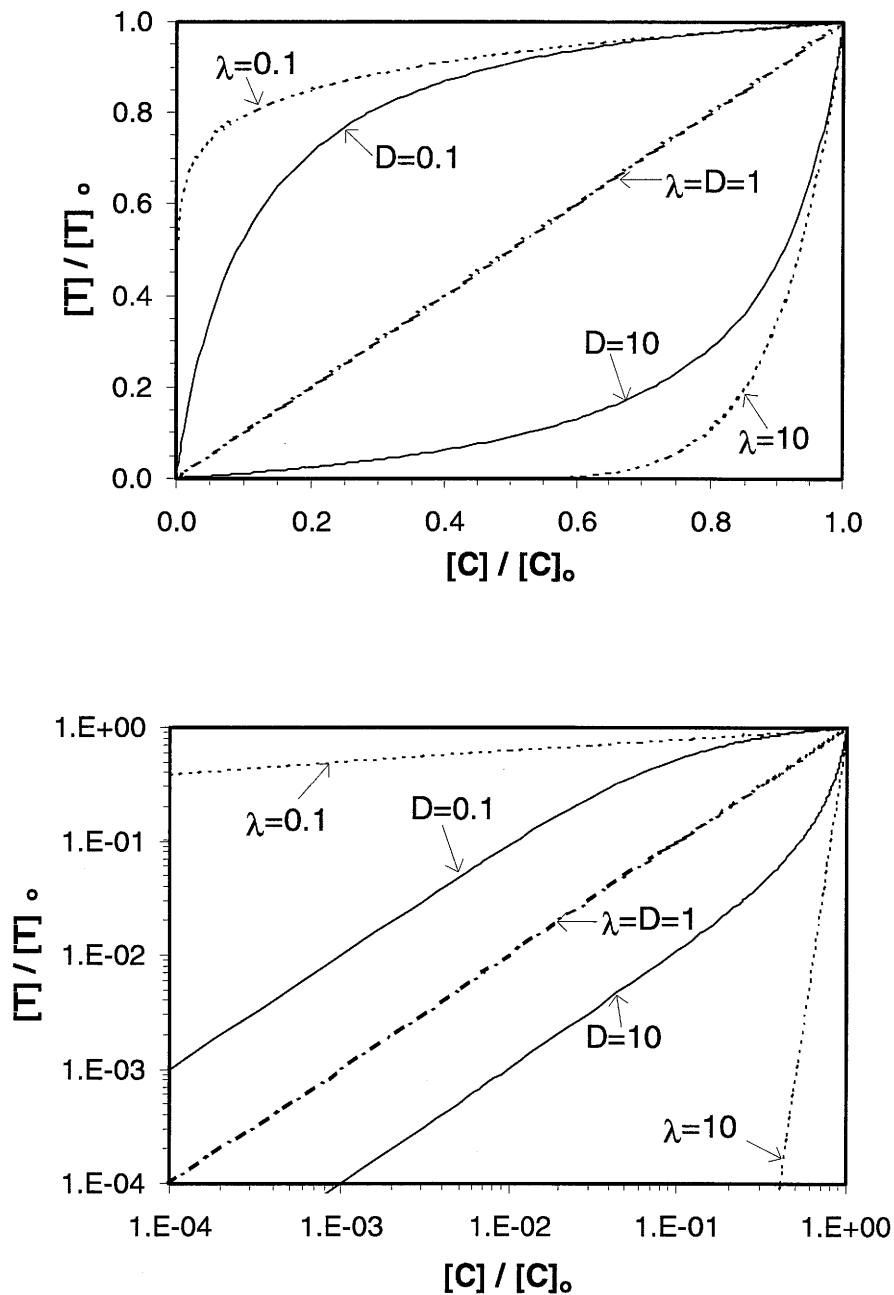


Figure 3-4: Comparison between heterogeneous and homogeneous coprecipitation in a closed system for 3 values of the partition coefficient. The upper plot is drawn on linear scale while the lower plot is logarithmic. For $\lambda, D > 1$ heterogeneous coprecipitation withdraws the trace element T more efficiently from solution than homogeneous coprecipitation. The opposite is true for $\lambda, D < 1$, while the two models converge for $\lambda, D = 1$.

The latter quantity expresses the degree of precipitation, i.e. the fraction of C remaining in solution after the precipitation of $C_o - C$ moles of the carrier component per litre of solution. The plot should be "read" from right to left, since $[C]/[C]_o = 1$ marks the beginning of precipitation and $[C]/[C]_o = 0$ correspond to the (merely hypothetical) end of the precipitation, when all of the carrier component has been withdrawn from solution¹¹. The curves obtained from both models are shown for three partition coefficients. The results indicate that for values of $\lambda = D > 1$ heterogeneous coprecipitation is more effective than homogeneous coprecipitation in scavenging the trace element from solution. The opposite is true for $\lambda = D < 1$: in this case homogeneous coprecipitation is more efficient. Finally, for $\lambda = D = 1$ the homogeneous and heterogeneous partition laws are indistinguishable.

Comparing the various curves in Figure 3-4, it can be concluded that substantial differences between the two coprecipitation models arise only under the following circumstances: a) for large values of the partition coefficient ($\lambda, D \gg 1$), when precipitation is sufficiently advanced (at $[C]/[C]_o \sim 0.6$ for $\lambda, D = 10$), heterogeneous coprecipitation would remove the trace element quantitatively from solution, while a considerable fraction of the trace element would remain dissolved if homogeneous coprecipitation took place; b) for small values of the partition coefficient ($\lambda, D \ll 1$), when the carrier's precipitation is very advanced (at $[C]/[C]_o < 0.1$ for $\lambda, D = 0.1$) homogeneous coprecipitation would remove the trace element from solution much more efficiently than heterogeneous coprecipitation does. For instance, with a partition coefficient of 10 and 40% precipitation ($[C]/[C]_o = 0.6$), heterogeneous coprecipitation withdraws from solution more than 99% of the trace element inventory, while homogeneous coprecipitation would leave about 10% of the trace element inventory dissolved. In other cases, the differences arising from the two mechanisms are small.

It is instructive to analyse the logarithmic plot in Figure 3-4 carefully, because it reveals some features which are important from the point of view of radioactive waste management and not evident in the linear plot. The logarithmic plot is useful to depict situations where almost the entire initial carrier inventory has been precipitated, that is the typical case of precipitation of an insoluble phase in a closed (not buffered) system. The important point is the following: if the final carrier concentration is less than $\sim 10\%$ of the initial concentration, then differences in the final trace element (i.e. radionuclide) concentration due to the coprecipitation mechanism may reach orders of magnitude. If, say, 90% of the carrier inventory precipitates and the value of the partition coefficient is 10, homogeneous coprecipitation would leave about 1% of the initial radionuclide concentration in solution, which may still represent a dangerous radioactivity level. Under the same conditions, heterogeneous coprecipitation, which would be more expected under repository conditions, would leave in solution a formal concentration equal to $1/10^{20}$ the initial radionuclide concentration. This is practically equivalent to a complete scavenging of the radionuclide¹².

¹¹ In practice, the state $[C]/[C]_o = 0$ is never reached, since each solid has a finite solubility.

¹² It is important to remember that all the arguments developed here refer to an idealised laboratory situation, namely a closed system where no external supply of carrier/trace element can buffer solution concentrations. In a repository environment, waste materials and rocks may conceivably buffer carrier and trace radionuclides to \sim constant solution concentrations. Under such circumstances, these differences between heterogeneous and homogeneous coprecipitation with respect to the scavenging of trace elements would disappear.

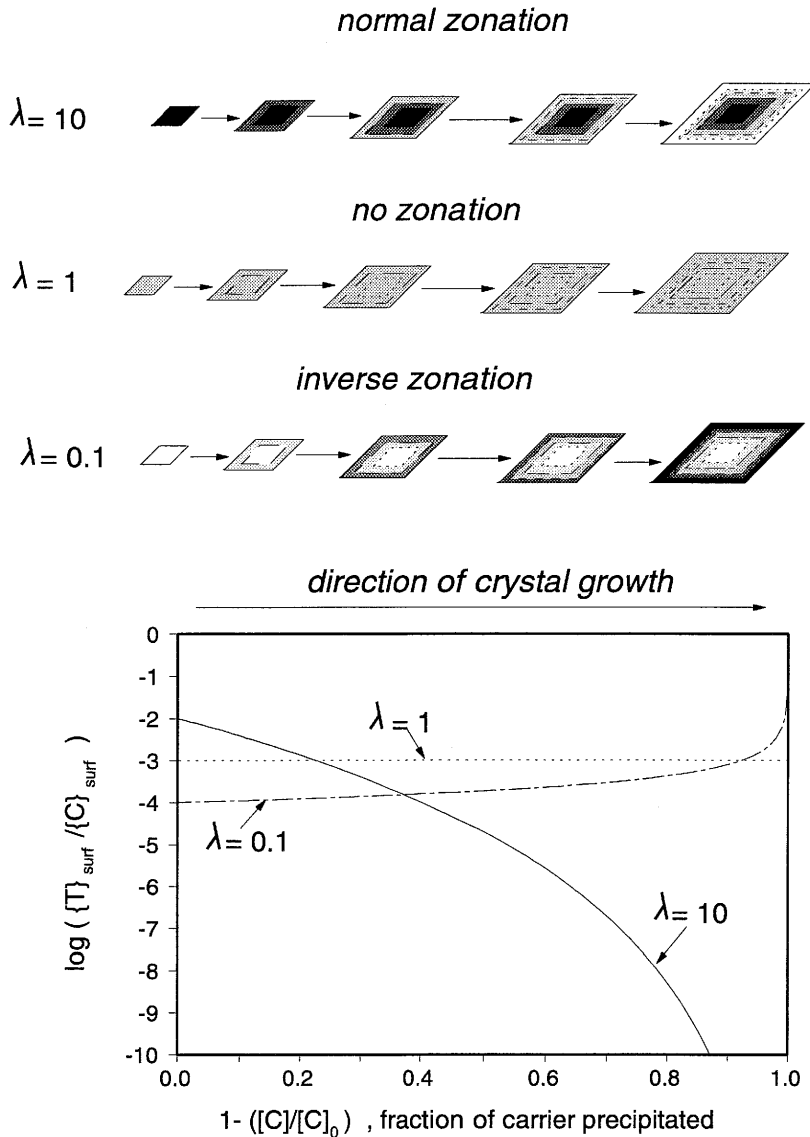


Figure 3-5: Composition of a binary coprecipitate (expressed as the ratio of trace to carrier element in the solid, $\{T\}_{\text{surf}} / \{C\}_{\text{surf}}$) as function of the fraction of carrier precipitated from the solution in a closed system. The calculations are based on Equation (3-16) and assume initial concentrations of 10^{-6} M for the trace element and 10^{-3} M for the carrier. The sketches above the plots illustrate the different kinds of compositional zoning arising from different values of the partition coefficient (darkening in the shading corresponds to increasing trace element concentrations).

A substantial difference between homogeneous and heterogeneous coprecipitation is that the former mechanism produces solids with uniform composition, whereas heterogeneous precipitation will in general lead to compositionally zoned precipitates. There are two possible exceptions to this rule: for $\lambda=1$ or when both trace element and carrier

concentrations are kept constant in solution (buffered solutions). In the latter case, heterogeneous coprecipitation will also produce uniform crystals. For closed systems, it is possible to derive from Equations (3-10) and (3-14), through simple algebraic manipulations, an expression for the composition of the solid surface as a function of the amount of carrier precipitated:

$$\log \frac{\{T\}_{surface}}{\{C\}_{surface}} = \log \lambda + (\lambda - 1) \log \left[\frac{[C]}{[C]_0} \right] + \log \left[\frac{[T]_0}{[C]_0} \right]. \quad (3-16)$$

Equation (3-16) is plotted in Figure 3-5. The plot shows, for three values of λ , the mole ratio of trace to carrier element at the mineral surface as a function of the fraction of carrier precipitated. The initial conditions are $[C]_0 = 10^{-3}$ and $[T]_0 = 10^{-6}$ M. For $\lambda > 1$, the solid becomes increasingly depleted of the trace element as precipitation progresses, giving rise to normally zoned crystals (i.e. the core has a larger trace element concentration than the rim). For $\lambda < 1$, in contrast, the trace element concentration in the solid increases in the course of precipitation, leading to inversely zoned crystals (i.e. the rims have a larger trace element concentration than the core). Finally, for $\lambda = 1$ the solid composition is uniform because neither the carrier nor the trace element are removed preferentially from solution. The $\{T\}/\{C\}$ ratio is at any time constant and equal to the ratio in solution:

$$\frac{\{T\}}{\{C\}} = \frac{[T]}{[C]} = \frac{[T]_0}{[C]_0}.$$

The curves shown in Figure 3-5 may be used (as a complement to those depicted in Figure 3-4) to model the results of experiments in which the composition of the solids is measured in addition to the composition of the solution.

3.2.4. Relation of the partition coefficients to thermodynamic solubility products

The phenomenological partition coefficients (D , λ) can be formally related to the thermodynamic solubility products of the end-member solids forming a solid solution, as illustrated by the following equations. The formalism is exemplified here for a generic divalent metal (Me^{2+}) forming a binary solid solution with calcium carbonate. Starting with Equation (3-8) and using activities in the solid instead of the mole fractions, one obtains:

$$\frac{(Me^{2+})}{(Ca^{2+})} = \frac{K_{MeCO_3} a_{MeCO_3}}{K_{CaCO_3} a_{CaCO_3}} = \frac{K_{MeCO_3} f_{MeCO_3} x}{K_{CaCO_3} f_{CaCO_3} (1-x)}, \quad (3-17)$$

where a_{MeCO_3} , a_{CaCO_3} are the activities of the indicated components in the solid solution and f_{MeCO_3} , f_{CaCO_3} are the corresponding activity coefficients (which are equal to one in ideal solid solutions). The free ion activities (Me^{2+}) , (Ca^{2+}) can be expressed as products of the individual activity coefficients of the free ions, $\gamma_{Me^{2+}}$, $\gamma_{Ca^{2+}}$, the fractions of uncomplexed metal $\alpha_{Me^{2+}}$, $\alpha_{Ca^{2+}}$ and the total metal concentrations in solution, $[Me]_{tot}$, $[Ca]_{tot}$:

$$(Me^{2+}) = \gamma_{Me^{2+}} \alpha_{Me^{2+}} [Me]_{tot} \quad (3-18)$$

$$(Ca^{2+}) = \gamma_{Ca^{2+}} \alpha_{Ca^{2+}} [Ca]_{tot}. \quad (3-19)$$

Substituting Equations (3-18) and (3-19) into Equation (3-17), rearranging and setting $x \equiv x_{Me}$, $(1-x) \equiv x_{Ca}$:

$$\frac{K_{CaCO_3} \gamma_{Me^{2+}} \alpha_{Me^{2+}} f_{CaCO_3}}{K_{MeCO_3} \gamma_{Ca^{2+}} \alpha_{Ca^{2+}} f_{MeCO_3}} = \frac{[Ca]_{tot} x_{Me}}{[Me]_{tot} x_{Ca}} \equiv D, \lambda. \quad (3-20)$$

Equation (3-20) provides a link between empirical partition coefficients and thermodynamic solid solution models, which in principle enables the comparison between the two approaches. Although the derivation of Equation (3-20) is straightforward, its application is far from being trivial. The calculation of the activity coefficients and of the fractions of uncomplexed metals needs precise knowledge of the relevant ion pairing and solubility equilibria and of their dependence on ionic strength. Moreover, and this is the major difficulty, the activity coefficients of the components in the solid (f_{MeCO_3} , f_{CaCO_3}) must be known. The main task of advanced thermodynamic solid solution models is the calculation of such activity coefficients.

4. Solid solution formation in carbonate minerals

4.1 Why carbonates ?

Simple carbonate minerals were chosen to exemplify trace element incorporation essentially for the following reasons. First, carbonates are a unique mineral group for which extensive coprecipitation data are available. In addition, these minerals are likely to be important secondary solids in both HLW and L/ILW repositories. Finally, such carbonates have only one possible lattice site for cation substitution, thereby simplifying the interpretation of experimental data (unlike clay minerals, which have multiple sites).

Large amounts of calcite are expected to form in the L/ILW repository near-field. Following the reaction with dissolved carbonate species, originating from the degradation of organic materials and from advected ground water, up to 80% of the calcium released during cement degradation could ultimately precipitate as calcite (NEALL 1994, p. 40). In addition, carbonate minerals are abundant in the marls hosting the repository. These carbonates will interact with dissolved radionuclides and could form mixed surface precipitates (see DAVIS et al. 1987 and chapter 5 of the present report).

Calcite and other carbonates will also be present in appreciable amounts in the bentonite backfill of the HLW repository (1.4 - 3.8 weight % according to MÜLLER-VONMOOS & KAHR 1983) and more could precipitate due to the interaction of calcium released from the glass and carbonate species dissolved in the ground water.

4.2 Experimental techniques

In the past 30 years, many experimental investigations were carried out, aiming to quantify the incorporation of trace metals during the precipitation of calcite and other carbonates, were carried out. Different experimental techniques have been used, which have become increasingly accurate in the course of the years.

Some of the earlier experiments were quite inaccurate, as key chemical parameters were not properly controlled. In these experiments, the solid phase was precipitated from strongly oversaturated solutions (*free nucleation technique*), causing rapid and uncontrolled mineral precipitation. In addition, the effects of adsorption on container walls and on mineral surfaces were not accounted for (see e.g. THORNER & NICKEL 1976). This technique has been abandoned, because the reactions involved in the process of trace element incorporation proceed in this case far from equilibrium conditions, leading often to irreproducible results.

Later experiments were designed and carried out with more care taken in precise control of chemical variables (see e.g. MUCCI & MORSE 1983). An improved technique (*calcite to aragonite recrystallisation*) utilised the small difference between calcite and aragonite solubilities to impose a slow, constant rate of precipitation (KATZ et al. 1972,

KATZ 1973). With this method, aragonite powder is put in contact with an aqueous solution and starts to dissolve, while an equivalent amount of calcite, which is the stable phase at ambient temperature and pressure, precipitates at its expense. As long as some aragonite is present, the solution remains slightly but constantly oversaturated with respect to calcite, resulting in a slow, fixed rate of calcite formation until all the aragonite has disappeared. A drawback of this method is the possible contamination with trace elements due to the dissolution of impure aragonite. Either the trace element content of the aragonite is analysed carefully and the results then corrected accordingly, or the initial trace element concentrations in solution are large enough to justify neglecting them.

A decisive improvement was made by letting the mineral precipitate on a solid substrate (*heterogeneous nucleation technique*). In this case, the coprecipitation reaction takes place in a solution containing a suspension of the same mineral which is to be precipitated. The newly formed carbonate nucleates on the surfaces of suspended "crystal seeds", forming characteristic overgrowths. The coprecipitated trace element is present in the overgrowth, but not in the seeds. This method is often used in conjunction with a *chemostat*, technical equipment designed to buffer the solution composition during the entire experiment. Typically, the chemostat adjusts solution concentrations to the desired levels through an automatic feedback system which adds appropriate amounts of titrant in response to decreases in pH induced by calcite precipitation. DROMGOOLE & WALTER (1990) employed this technique to investigate the uptake of Mn^{2+} and Fe^{2+} by calcite. During the experiments, the pH was monitored and continuously adjusted to a constant value (± 0.002 pH-units) through dynamic addition of $NaHCO_3/Na_2CO_3$ titrant. The calcium and trace metal concentrations were kept constant through addition of appropriate amounts of $CaCl_2/MeCl_2$ solution. In this way, the species removed from solution due to the precipitation of calcite (carbonate, calcium and trace metal) were continuously replaced, so that the experiments ran at constant oversaturation and fixed Ca^{2+} , Me^{2+} concentrations. Chemostatic techniques, which were originally developed for kinetic studies of carbonate precipitation, are now routinely used for coprecipitation studies.

Carbonate precipitation may be initiated in different ways. For instance, by stirring a solution previously saturated with a high partial pressure of CO_2 (CROCKET & WINCHESTER 1966) under normal atmospheric conditions. Through the stirring, excess CO_2 gas is released, leading to an increase of pH and thus of the carbonate ion activity. The solubility product of the carbonate mineral is then exceeded and precipitation occurs. An alternative method is to introduce crystal seeds (normally of the same mineral which is to be precipitated) in an oversaturated solution (MUCCI & MORSE 1983, DROMGOOLE & WALTER 1990). The seeds induce instantaneous nucleation of the new phase on top of the seed surface.

Radiotracers are routinely used in coprecipitation studies to determine the distribution of trace elements between solid and solution. The great advantage of radiochemical methods lies in their high analytical sensitivity, which makes possible to study the uptake of a trace element by a solid phase at extremely low concentration levels. Investigations carried out with inactive trace elements either rely on high initial concentrations of the trace metal to give precise results (e.g. KATZ 1973) or typically lead to rather imprecise partition coefficients (e.g. ZHONG & MUCCI 1995).

In summary, although the experimental techniques developed to study the coprecipitation of trace metals in carbonate minerals are not trivial, a great deal of experience is now available. There is no doubt that these methods could be adapted successfully to study the coprecipitation of radionuclides with carbonates. The extension of these methods to other secondary solids, however, will depend heavily on the ability to control their growth under laboratory conditions at low temperatures. For instance, it is very difficult to control precipitation of clay minerals at room temperatures.

4.3 Compilation of partition coefficients

Based on an extensive literature survey, data on metal coprecipitation with carbonates have been compiled in Table 4-1. The collected data stem exclusively from experimental investigations. Rather than presenting the data in the form of a simple list of partition coefficients, a more extensive presentation was preferred, including important information on the experimental conditions. Knowledge of variables like pH, ionic strength, precipitation rate, temperature, and concentration ranges in solution are essential for the critical evaluation and comparison of the tabulated partition coefficients, as will become evident in the following discussion (section 4.4).

The quality of the selected data is not uniform. For instance, results derived from free nucleation experiments were included, like the data of KITANO & OOMORI (1971) and MEECE & BENNINGER (1993) on the incorporation of hexavalent uranium. These data were considered because of the special interest in this element within the context of radioactive waste disposal. In spite of the inaccuracies plaguing both works, the resulting partition coefficients for calcite roughly agree ($D < 0.2$). Although these results are only qualitative, there can be no doubt that uranyl ions do not coprecipitate efficiently with calcite.

Table 4-1 : Compilation of literature data on the coprecipitation of trace elements in carbonate minerals.

trace cation or anion (ionic radius) ^k	precipitating solid	pH	initial solution concentrations ^d , ionic strength, [M]	precipitation rate ^a [mol m ⁻² s ⁻¹]	temperature [°C]	partition coefficient ^b (D or λ) [-]	Ref.
Fe ²⁺ (0.78 Å)	calcite	5.5 - 6.7	[Fe] ~ 10 ⁻⁵ - 10 ⁻⁴ [Ca] ~ 10 ⁻¹ I = 0.03 - 0.25	~3 x 10 ⁻⁷	10	2.3	(4)
				~7 x 10 ⁻⁶	10	1.5	(4)
				~2 x 10 ⁻⁷	25	3.5	(4)
				~6 x 10 ⁻⁶	25	2.0	(4)
				~2 x 10 ⁻⁷	25	7.7	(4)
				~3 x 10 ⁻⁵	25	2.8	(4)

trace cation or anion (ionic radius) ^k	precipitating solid	pH	initial solution concentrations ^d , ionic strength, [M]	precipitation/ recrystallisa- tion rate ^a [mol m ⁻² s ⁻¹]	temperature [°C]	partition coefficient ^b (D or λ) [-]	Ref.	
Mg²⁺ (0.72 Å)	calcite	6.9 - 8.6	[Mg] ~10 ⁻³ - 10 ⁻²	g ~ 10 ⁻⁷	25	0.06	(1)	
			[Ca] ~10 ⁻² - 10 ⁻¹		35	0.07	(1)	
			I = 0.3		50	0.08	(1)	
					70	0.10	(1)	
					90	0.12	(1)	
	calcite	7.7 - 8.2	[Mg] ~10 ⁻² - 10 ⁻¹ [Ca] = 5 x 10 ⁻³ - 10 ⁻² I = 0.7	2x10 ⁻⁸ - 3x10 ⁻⁷	25	0.01 - 0.03	(14)	
Co²⁺ (0.75 Å)	calcite	7.3 - 7.5	[Co] ~10 ⁻⁹	~7 x 10 ⁻¹⁰	25	~ 8	(3)	
			[Ca] ~10 ⁻²	~6 x 10 ⁻⁸	25	4.2 ± 0.2	(2)	
			I = 0.7	~ 10 ⁻⁷	25	3.7	(3)	
				~3 x 10 ⁻⁶	25	1.9 ± 0.1	(2)	
	siderite	7.0 - 7.3	[Co] ~10 ⁻⁵ [Fe] ~ 5 x 10 ⁻⁴ I = 0.2	fast (free nucleation)	22-24	0.5 - 0.9	(17)	
Zn²⁺ (0.74 Å)	calcite	~ 8 ^c	[Ca] ~ 10 ⁻³	~10 ⁻⁷ - 2x10 ⁻⁶	25	5.7 ± 0.3	(6)	
			[Zn] ~ 10 ⁻⁷ - 10 ⁻⁶		35	4.1 ± 0.1	(6)	
			I = 0.001 ^c		50	3.2 ± 0.2	(6)	
	calcite	~7 - 8.5	[Ca] ~ 10 ⁻²	fast (free nucleation)	20	50 ± 4	(21)	
			[Zn] ~ 10 ⁻⁶ - 10 ⁻⁵		25	20 - 30	(22)	
			I ~ 0.03					
			7.3 - 7.5		[Zn] ~ 10 ⁻¹⁰	~6 x 10 ⁻⁸	25	80 ± 20
		[Ca] ~ 10 ⁻²	3 x 10 ⁻⁶	25	55 ± 5	(2)		
		I = 0.7						
Cu²⁺ (0.73 Å)		~7 - 8.5	[Ca] ~ 10 ⁻²	fast (free nucleation)	20	25 ± 2	(21)	
			[Cu] ~ 3-6 x 10 ⁻⁶		25	~25 - 40	(22)	
			I ~ 0.03-0.06					

trace cation or anion (ionic radius)	precipitating solid	pH	initial solution concentrations ^d , ionic strength, [M]	precipitation/ recrystallisa- tion rate ^a [mol m ⁻² s ⁻¹]	temperature [°C]	partition coefficient ^b (D or λ) [-]	Ref.	
Mn²⁺ (0.83 Å)	calcite	5.5 - 6.7	[Mn] ~ 10 ⁻⁴ - 10 ⁻³	~8 x 10 ⁻⁸	10	12.2	(4)	
			[Ca] ~ 10 ⁻¹	~6 x 10 ⁻⁶	10	3.1	(4)	
			I = 0.03 - 0.25	~10 ⁻⁷	25	15.8	(4)	
				5 x 10 ⁻⁶	25	4.1	(4)	
				2 x 10 ⁻⁷	50	24.9	(4)	
				2 x 10 ⁻⁵	50	8.0	(4)	
Cd²⁺ (0.95 Å)	calcite	7.3 - 7.5	[Mn] ~ 10 ⁻¹⁰	~6 x 10 ⁻⁸	25	16.1 ± 0.5	(2)	
			[Ca] ~ 10 ⁻²	~10 ⁻⁷	25	14.8	(3)	
			I = 0.7	3 x 10 ⁻⁶	25	5.4 ± 0.3	(2)	
Cd²⁺ (0.95 Å)	calcite	7.3 - 7.5	[Cd] ~ 10 ⁻¹⁰	~6 x 10 ⁻⁸	25	24 ± 4	(2)	
			[Ca] ~ 10 ⁻²	~10 ⁻⁷	25	21.3	(3)	
			I = 0.7	3 x 10 ⁻⁶	25	9.5 ± 1.0	(2)	
Cd²⁺ (0.95 Å)	calcite	6.5 - 8.0	[Cd] ~ 10 ⁻⁷ - 10 ⁻⁶	2 x 10 ⁻¹² to 5 x 10 ⁻¹¹	25	1210-1780 (~20-200) ^b	(5)	
			I = 0.001 - 0.1	(saturated solution)				
Cd²⁺ (0.95 Å)	calcite	6.0 - 6.3	[Ca] ~ 10 ⁻²	5 x 10 ⁻⁶	25	200 - 3040 (8 - 110) ^b	(20)	
			[Cd] ~ 3 x 10 ⁻⁶ - 7 x 10 ⁻⁵	to 6 x 10 ⁻¹⁰				
			I ~ 0.03					
^eUO₂²⁺ (~3.5 Å)	calcite	8.3 - 9.0	[U] ~ 10 ⁻⁶	~10 ⁻⁷ - 2 x 10 ⁻⁶	22-27	< 0.2	(7) ^f	
			[Ca] ~ 10 ⁻²					
	aragonite			I ~ 0.7 (seawater)			~ 2 - 10	(7) ^f
^eUO₂²⁺ (~3.5 Å)	calcite	6.3 - 8.6	[U] ~ 4 - 8 x 10 ⁻⁵	unknown	20	~ 0.01-0.2	(12)	
			[Ca] ~ 10 ⁻²					
	aragonite		I ~ 0.2 - 0.6			0.3 - 1.2	(12)	
				unknown	20			

trace cation or anion (ionic radius)	precipitating solid	pH	initial solution concentrations ^d , ionic strength, [M]	precipitation/ recrystallisa- tion rate ^a [mol m ⁻² s ⁻¹]	temperature [°C]	partition coefficient ^b (D or λ) [-]	Ref.
Sr ²⁺ (1.18 Å)	calcite	7.3 - 7.5	[Sr] = 3x10 ⁻⁷	~6 x 10 ⁻⁸	25	0.037 ± 0.005	(2)
			[Ca] ~10 ⁻²	~10 ⁻⁷	25	0.04	(3)
			I = 0.7	3 x 10 ⁻⁶	25	0.094 ± 0.004	(2)
	calcite	7.2 - 7.3	[Ca] ~10 ⁻²	8 ~10 ⁻⁷	40-98	0.05 - 0.08	(8)
			[Sr] = 10 ⁻⁵ - 10 ⁻³				
			I = 0.03 - 0.6				
			[Ca] ~5 x 10 ⁻³				
	calcite	7.7 - 8.2	[Sr] = 9 x 10 ⁻⁵	2x10 ⁻⁸ - 3x10 ⁻⁷	25	0.15 - 0.39	(14)
			[Ca] = 5 x 10 ⁻³ - 10 ⁻²				
			I = 0.7				
calcite	?	?	?	25	0.04 - 0.2	(15)	
calcite	6.0 - 6.3	[Sr] = 7 x 10 ⁻⁵	~10 ⁻⁵ - 10 ⁻⁸	25	0.02 - 0.14	(20)	
		[Ca] ~10 ⁻²					
		I ~ 0.03					
aragonite	?		?	?	0.9 - 1.6	(16)	
Ba ²⁺ (1.18 Å)	calcite	?	[Ca] ~10 ⁻³ - 10 ⁻²	h ~5x10 ⁻⁷	25	0.06 ± 0.01	(9)
			[Ba] = 10 ⁻⁵ - 4 x 10 ⁻⁵	~10 ⁻⁵			
	calcite	6.0 - 6.2	[Ca] ~10 ⁻²	~3 x 10 ⁻⁸ - 10 ⁻⁵	25	0.01 - 0.05	(20)
			[Ba] = 7 x 10 ⁻⁵ - 1 x 10 ⁻⁴				
			I = 0.03				
Na ⁺ (1.02 Å)	calcite	~8 - 8.4	[Ca] ~10 ⁻²	3x10 ⁻¹⁰ to 6x10 ⁻⁹	25	0.0002 - 0.004	(10)
			[Na] ~0.5				
			I = 0.7 (seawater)				

trace cation or anion (ionic radius)	precipitating solid	pH	initial solution concentrations ^d , ionic strength, [M]	precipitation/ recrystallisa- tion rate ^a [mol m ⁻² s ⁻¹]	temperature [°C]	partition coefficient ^b (D or λ) [-]	Ref.
Na ⁺ (1.02 Å)	calcite	6.1 - 8.3	[Ca] ~ 10 ⁻² [Na] ~ 10 ⁻² - 0.5 I=0.04 - 0.5	unknown (free nucleation)	25	0.001 - 0.006	(18)
	calcite	?	?	?	?	2x10 ⁻⁵ to 3x10 ⁻⁵	(19)
K ⁺ (1.38 Å)	calcite	6.1 - 8.3	[Ca] ~ 10 ⁻² [K] ~ 0.005 - 0.03 I=0.04 - 0.5	unknown (free nucleation)	25	5x10 ⁻⁵ to 10 ⁻³	(18)
Li ⁺ (0.76 Å)	calcite	6.1 - 8.3	[Ca] ~ 10 ⁻² [Li] ~ 0.03 - 0.15 I=0.04 - 0.5	unknown (free nucleation)	25		(18)
Ln ³⁺ (0.87-1.03 Å)	calcite	6.7 - 8.3	[Ca] ~ 10 ⁻² [Ln]=10 ⁻⁸ - 7x10 ⁻⁷ I= 0.7 (seawater)	3x10 ⁻¹⁰ to 6x10 ⁻⁹	25	60 -4250	(10)
La ³⁺						500 - 4180	(10)
Ce ³⁺						560 - 4250	(10)
Pr ³⁺						430 - 4010	(10)
Nd ³⁺						320 - 1840	(10)
Sm ³⁺						260 - 2280	(10)
Eu ³⁺						210 - 1390	(10)
Gd ³⁺						140 - 1450	(10)
Tb ³⁺						280 - 390	(10)
Dy ³⁺						230 - 270	(10)
Ho ³⁺						110 - 150	(10)
Er ³⁺						80 - 120	(10)
Yb ³⁺						60 - 70	(10)
Ln ³⁺	calcite	6.3 - 8.5	[Ca] ~ 10 ⁻² [Ln]=10 ⁻¹² - 2 x 10 ⁻⁹ I= 0.1 (NaCl)	unknown (free nucl.)	21 - 26	~2.5 - 10	(13)
	aragonite	6.3 - 8.5	[Ca] ~ 10 ⁻² [Ln]= 10 ⁻¹² - 3 x 10 ⁻¹⁰ I= 0.1 (MgCl ₂)	(free nucl.)	21 - 26	~2.5 - 5	(13)

trace cation or anion (ionic radius)	precipitating solid	pH	initial solution concentrations ^d , ionic strength, [M]	precipitation/recrystallisation rate ^a [mol m ⁻² s ⁻¹]	temperature [°C]	partition coefficient ^b (D or λ) [-]	Ref.
SeO ₄ ²⁻ (~2.8 Å)	calcite	7.4 - 7.6	ⁱ [CO ₃ ²⁻] ~ 5 x 10 ⁻³ [Se] ~ 10 ⁻² I = 0.6	unknown	25	ⁱ 6 x 10 ⁻⁶ to 5 x 10 ⁻⁵	(11)

References:

- | | |
|---------------------------------|---------------------------------|
| (1) KATZ et al. (1972) | (12) KITANO & OOMORI (1971) |
| (2) LORENS (1978) (Table 7) | (13) TERAKADO & MASUDA (1988) |
| (3) LORENS (1981) | (14) MUCCI & MORSE (1983) |
| (4) DROMGOOLE & WALTER (1990) | (15) PINGITORE & EASTMAN (1986) |
| (5) DAVIS et al. (1987) | (16) KINSMAN & HOLLAND (1969) |
| (6) CROCKET & WINCHESTER (1966) | (17) THORNBUR & NICKEL (1976) |
| (7) MEECE & BENNINGER (1993) | (18) OKUMURA & KITANO (1986) |
| (8) KATZ (1973) | (19) VEIZER (1983a) |
| (9) PINGITORE & EASTMAN (1984) | (20) TESORIERO & PANKOW (1996) |
| (10) ZHONG & MUCCI (1995) | (21) KITANO et al. (1968) |
| (11) STAUDT et al. (1994) | (22) KITANO et al. (1980) |

Notes:

^aWhere possible, partition coefficients are reported for the minimum and maximum precipitation rates used in the specific study, as well as for the precipitation rate nearest to 10⁻⁷ mol m⁻² s⁻¹. The latter figure serves as a common reference value for comparison purposes.

^bThe values of the partition coefficients are given as reported in the literature. In most cases partition coefficients are expressed in terms of total elemental concentrations, in agreement with the classical definition. In two instances (references 5 and 20 above) the authors gave values corresponding to a modified definition of the partition coefficients, which relies on free ion concentrations. In such cases, recalculated partition coefficients based on total metal concentrations are given in parentheses. Statistical errors are reported as specified in the original works, whenever available. Because most of the experiments were carried out at constant or nearly constant carrier element concentration ([C]/[C]₀ ~ 1.0 with reference to Figure 3.4), interpretation of the laboratory data with both heterogeneous and homogeneous coprecipitation model leads approximately to the same partition coefficients. For this reason it is not necessary to distinguish between λ and D values in this compilation.

^cValue modelled with the help of speciation calculations based on the concentration data given in the source reference.

^dOnly total initial elemental concentrations are reported. In most experiments, the final concentrations of the carrier were in the same order of magnitude as the initial concentrations.

^eIt is not clear whether hexavalent uranium is incorporated as a free cation or as uranyl ion (UO₂²⁺). In the former case, the partition coefficient for incorporation in calcite should be larger than that for uptake in aragonite, since the ionic radius of U⁶⁺ is clearly smaller than the critical ionic radius dividing hexagonal from orthorhombic carbonate structures. Exactly the opposite is observed, suggesting incorporation as uranyl ion.

^fThese data should be taken with care, since: a) in the experiments on calcite coprecipitation aragonite was also formed and the distribution coefficient for U in calcite was determined through a linear extrapolation to 100% calcite; b) adsorption corrections for calcite were made on the base of only 2 sorption measurements on *aragonite*; c) The adsorption tests were carried out at pH-values 1 to 1.5 units below those established in the coprecipitation experiments.

^g Estimated with help of Figure 1 in LORENS (1981) , from the degree of supersaturation (SI=1.4) during the calcite-aragonite transformation.

^h Crude estimate on the base of data in the source reference.

ⁱ The total carbonate concentration is given here instead of that of calcium because selenate replaces carbonate groups in calcite (see REEDER et al. 1994). Accordingly, the partition coefficients were calculated from the data in the source reference assuming CO_3^{2-} as the carrier species.

^k The ionic radii were taken from SHANNON (1976).

The main objective of Table 4-1 is to provide a condensed, but comprehensive compilation of partition coefficients for calcite and other carbonates, to be used for the systematic analysis and discussion of the data carried out in the following sections. The goal is to assess the chemical and physical factors on which the incorporation of trace elements in carbonates depend and to ascertain to which degree these factors affect partition coefficients. The hope is that useful correlations will emerge, which would allow the extrapolation of partition coefficients for safety-relevant radioelements.

4.4 Factors affecting the coprecipitation of metals

4.4.1 Ionic radius and charge

Among the various chemical factors thought to govern the formation of solid solutions, the most obvious are size and charge of the coprecipitated ions. Clearly, coprecipitated ions with similar radius and identical charge as the replaced ion should be incorporated more easily in the crystal lattice than those having different size and charge. For example, cations with a ionic radius considerably larger than that of Ca^{2+} (1.00 Å) should have very small partition coefficients in calcite, simply because they are too large to fit into the calcium sites.

Table 4-2 presents a summary of partition coefficients ordered by increasing size of the coprecipitated ions, which partially confirms these expectations, although the data cover a wide parameter space in terms of pH, ionic strength and precipitation kinetics. Some of the predictions made above are met: for instance, the highest partition coefficients were measured for cations with a ionic radius closely approaching that of Ca^{2+} and the lowest are found for cations which are too large to fit in the octahedrally coordinated calcium sites.

In contrast, an incongruent ionic charge does not seem to prevent effective coprecipitation with calcite, as proved by the very high partition coefficients measured for some non-divalent cations, notably the trivalent rare earths. This surprising behaviour may be explained by invoking charge-balancing mechanisms. Either coupled substitution (e.g. substitution of 2 calcium sites by a monovalent plus a trivalent cation), or formation of point defects (for two trivalent cations an unoccupied calcium site), could facilitate the uptake of trivalent cations in calcite. ZHONG & MUCCI (1995) found a positive correlation between REE^{3+} partition coefficients and sodium concentration in solution, suggesting a coupled substitution $\text{Na}^+ + \text{REE}^{3+}$ for 2 Ca^{2+} as charge-balancing mechanism.

Table 4-2: Summary of partition coefficients for the incorporation of metals in calcite (all experiments carried out at temperatures below 100 °C). The cations are sorted by increasing ionic size in two groups. The first group includes divalent cations, while the second group includes cations with a different charge. The size of UO_2^{2+} was estimated from the molecule geometry and the radii of the constituent ions. Broken lines within the table separate cations with radius smaller than that of Ca^{2+} (1.00 Å) from ions having larger radii. Ionic radii are taken from SHANNON (1976).

trace cation or anion	ionic radius [Å]	partition coefficient (D or λ) [-]	Reference (see Table 4-1)
Mg^{2+}	0.72	0.06 - 0.12	(1)
Zn^{2+}	0.74	3.2 - 80	(2)(6)
Co^{2+}	0.75	1.9 - 8.0	(2) (3)
Fe^{2+}	0.78	1.5 - 7.7	(4)
Mn^{2+}	0.83	3.1 - 16	(2) (4)
Cd^{2+}	0.95	9.5 - ~ 200	(2) (3) (5) (20)
Sr^{2+}	1.18	0.02 - 0.14	(2) (8) (20)
Ba^{2+}	1.35	0.01 - 0.07	(9) (20)
UO_2^{2+}	3.5	0.01 - 0.2	(7) (12)
Yb^{3+}	0.87	60 - 70	(10)
Eu^{3+}	0.95	210 - 1390	(10)
Na^+	1.02	0.0002 - 0.004	(10)
La^{3+}	1.03	500 - 4180	(10)

A possible important consequence of coupled substitution is that the partition coefficients of trivalent cations may be considerably smaller in dilute solutions. The solutions used by ZHONG & MUCCI (1995) contained 0.5 M NaCl, ensuring that enough Na^+ cations could be incorporated into calcite to compensate the excess of positive charge caused by the uptake of REE cations, in spite of the very low partition coefficient of Na^+ . Indeed, simple calculations confirmed that the total amounts of REE^{3+} and sodium incorporated in Zhong and Mucci's calcite overgrowths are approximately equal, making the coupled substitution hypothesis quite plausible. According to this model, the partition coefficients of REE^{3+} cations should become smaller as the solution concentration of the charge-balancing monovalent cation decreases. For a sodium concentration of, say, 10^{-2} M instead of 0.5 M, then, if the

principle of electroneutrality holds, the D_{REE} -values indicated in Table 4-2 would decrease by a factor of fifty¹³.

Inspection of Table 4-1 reveals that three cations, Na^+ , Li^+ and Mg^{2+} , violate the “size rule”. Uptake of Na^+ in calcite is several orders of magnitude weaker than uptake of La^{3+} , in spite of their identical ionic radius (closely approaching that of Ca^{2+}) and although they have the same difference in charge with respect to Ca^{2+} . Also the large difference between the partition coefficients of Zn^{2+} and Mg^{2+} , which have similar radii and identical charge, cannot be understood in terms of ionic radii. Clearly, other factors are important in these cases, indicating that it is not possible to extrapolate unknown partition coefficients uniquely on the base of ionic size.

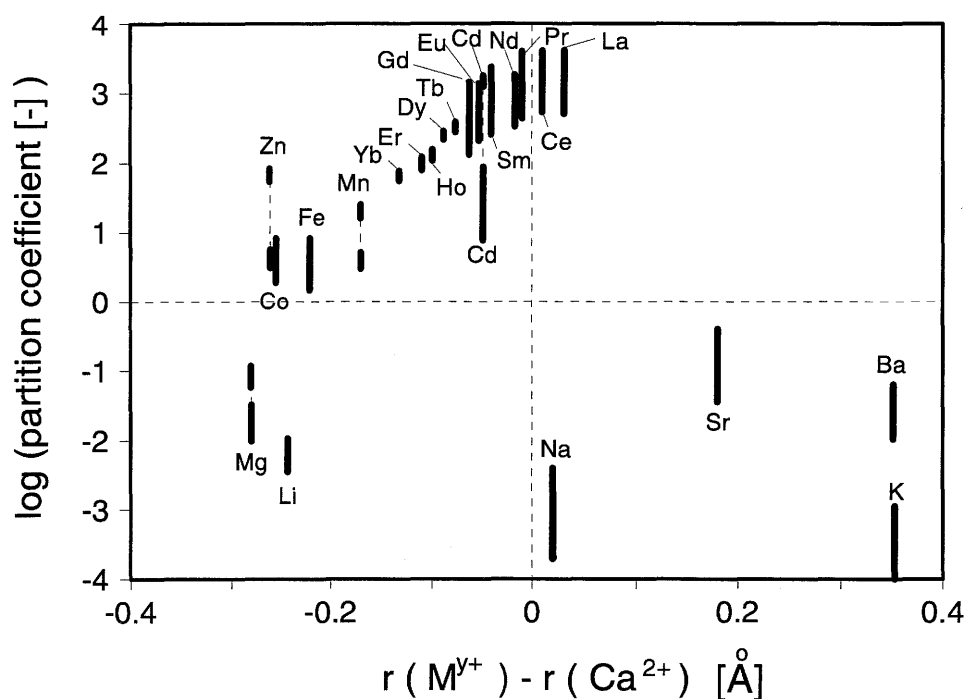


Figure 4-1: Graphical representation of the partition coefficients tabulated in Table 4-1 as a function of ionic radius.

¹³ Unfortunately, there is no investigation on the tolerance of charge imbalance in solid solutions. The possibility of reduced partition coefficients for trivalent and tetravalent actinides should, therefore, always be considered in view of applications to waste management problems. In the context of the model calculations for the Swiss L/ILW repository presented in chapter 7, no problem arises since radionuclide concentrations will be so small, that there will be enough sodium available to balance the charge of trivalent and tetravalent actinides coprecipitated with calcite.

BUSENBERG & PLUMMER (1985) studied the incorporation of Na^+ in calcite and aragonite. Their results suggest that sodium ions do not replace Ca^{2+} isomorphously. Sodium is apparently incorporated in interstitial positions: their data indicate that Na^+ is first adsorbed on structural crystal defects forming at the surface of calcite, the concentration of which is primarily determined by the rate of precipitation. These findings explain well the violation of the “size rule” observed for Na^+ .

The anomalous behaviour of Li^+ , Na^+ and Mg^{2+} is particularly evident in Figure 4-1, where the experimental data listed in Table 4-1 are plotted as a function of ionic radius. Although the measured partition coefficients may vary for a single ion by more than one order of magnitude (a consequence of the wide range of conditions under which the experiments ran) and despite the mentioned anomalies, a correlation emerges for the ions with radius smaller or slightly larger than that of calcium¹⁴.

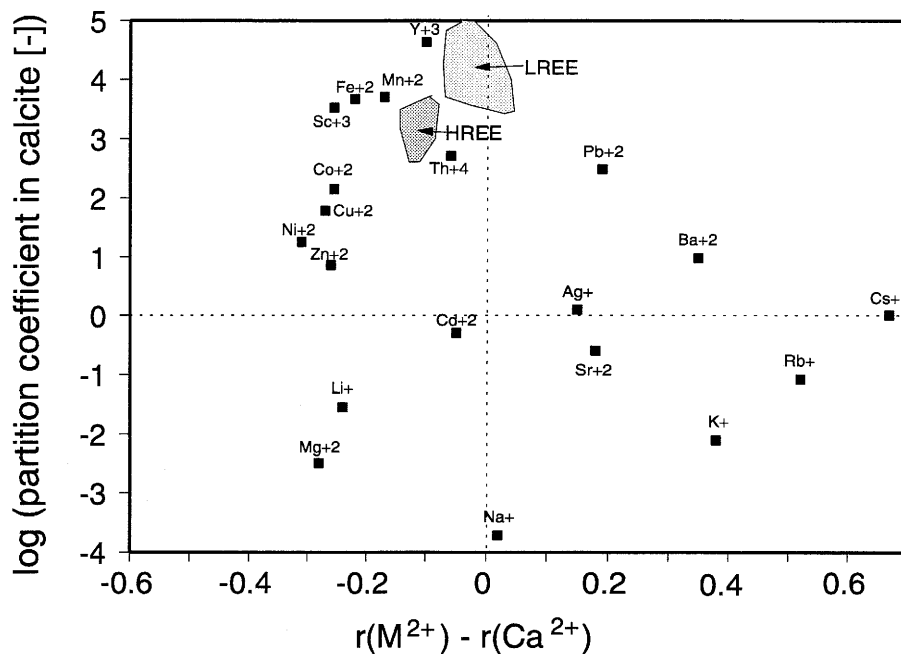


Figure 4-2: Partition coefficients of various cations, calculated from average elemental concentrations in seawater and in marine carbonates, as a function of ionic radius.

¹⁴ One should nevertheless realise that the correlation is defined to a large extent by partition coefficients of the rare-earths, for which most chemical properties vary smoothly with atomic number, due to the progressive filling of the internal 4f orbitals. The filling of the 4f orbitals leads to a regular decrease in ionic radius (“lanthanide contraction”), but leaves the external (valence) shells unchanged. As a consequence, coprecipitation of lanthanides is mainly governed by ionic size.

In addition to the values determined experimentally, partition coefficients were calculated for many cations from tabulated data of average elemental concentrations in seawater (KRAUSKOPF 1979) and in marine carbonate rocks (VEIZER 1983b). These are plotted in Figure 4-2 as a function of ionic radius. Despite the large uncertainties associated with such average concentrations, a rough correlation similar to that observed for the experimental data can be recognised. As in the case of the experimental data, most cations smaller or slightly larger than divalent calcium have partition coefficients exceeding one, the highest partition coefficients being those of light REEs (La-Gd). In addition, the three exceptions to this rule emerging from the experimental data, i.e. the very low partition coefficients for Mg^{2+} , Li^+ and Na^+ , are confirmed in Figure 4-2. Finally, the majority of cations larger than Ca^{2+} have small partition coefficients.

Some partition coefficients in Figure 4-2, however, violate the “size rule” and do not agree with the results of experimental studies. For instance, the partition coefficient for Cd^{2+} appears to be too small, while those for Ba^{2+} and Pb^{2+} are too high. In addition, the experimentally determined partition coefficients are generally smaller than those determined from the average concentration data.

4.4.2 Crystal structure of the host phase

Common anhydrous carbonates can be subdivided in two distinct crystal structure types: *rhombohedral* carbonates, in which the metals are octahedrally coordinated (6 oxygen ions as nearest neighbours) and *orthorhombic* carbonates, in which the metal ions have a 9-fold coordination. Octahedral coordination in carbonates is limited to metal ions with a radius smaller than the threshold value of $\sim 1.0 \text{ \AA}$; larger cations *must* have a higher coordination number for crystal-chemical reasons (KLEBER 1975). Thus, carbonates of divalent metals with ionic radius smaller than 1.0 \AA (e.g. Mn^{2+} , Fe^{2+} , Mg^{2+}) normally crystallise in the rhombohedral system, while those with a larger radius (e.g. Sr^{2+} , Ba^{2+}) form orthorhombic carbonates. Because the ionic radius of Ca^{2+} lies on the 1.0 \AA threshold, calcium carbonate can crystallise in both structure types: as *calcite*, the rhombohedral form, or *aragonite*, the orthorhombic form¹⁵.

The *polymorphism* of carbonate minerals explains why cations like Sr^{2+} and Ba^{2+} do not coprecipitate efficiently with calcite. These cations are simply too large for octahedral coordination. Thus they are preferentially incorporated in calcite either in crystal defects or through incorporation as discrete particles, which results in low partition coefficients. Following the same geochemical logic, it can be predicted that cations larger than Ca^{2+} should coprecipitate more effectively with aragonite than with calcite, while the reverse should hold for ions smaller than Ca^{2+} . Indeed, experimental data (e.g. KINSMAN & HOLLAND 1969) indicate that Sr^{2+} partition coefficients in aragonite are significantly larger than in calcite (by at least a factor of 4). Other data (VEIZER 1983a) report Ba^{2+} partition coefficients in aragonite exceeding those in calcite by at least one order of magnitude and Mg^{2+} , Mn^{2+} and Cd^{2+} partition coefficients in aragonite that are considerably smaller than in calcite.

¹⁵ A third, though rare, form of calcium carbonate is the hexagonal mineral *vaterite*.

A factor which might influence the extent of isomorphous substitution in carbonate minerals of the same structure type is the dimension of the unit cell, which depends on the size of the carrier cation. For instance, the unit cell of siderite (FeCO_3), a mineral which could form as a corrosion product of steel, is about 30% smaller than that of calcite, due to the smaller size of Fe^{2+} compared to Ca^{2+} . Accordingly, partition coefficients in siderite should increase as the radius of the coprecipitating cation approaches the size of Fe^{2+} . This prediction is only partially confirmed by the data of THORNER & NICKEL (1976), who studied the coprecipitation of divalent metals with siderite (Table 4-3). Although the highest partition coefficients were found for the ions most similar in size to Fe^{2+} (i.e. Cu^{2+} , Mn^{2+} and Co^{2+}), there are evident inconsistencies. For instance, in all experiments copper was removed quantitatively from solution, leading to partition coefficients at least two orders of magnitude larger than for Mn^{2+} , although both cations have ionic radii differing from that of Fe^{2+} by the same small amount (0.05 Å). In addition, the incorporation of Mg^{2+} was by many orders of magnitude weaker than that of Cu^{2+} , in spite of their very similar ionic radii.

Table 4-3: Partition coefficient of various divalent metals in siderite (from THORNER & NICKEL 1976).

cation	ionic radius / [Å]	$r(\text{M}^{2+}) - r(\text{Fe}^{2+}) / [\text{Å}]$	$D_{M^{2+}}^{\text{siderite}}$
Ca^{2+}	1.00	+ 0.22	0.07 - 0.12
Mn^{2+}	0.83	+ 0.05	4.0 - 19.9
Co^{2+}	0.75	- 0.03	0.52 - 0.92
Cu^{2+}	0.73	- 0.05	> 400
Mg^{2+}	0.72	- 0.06	0.0006 - 0.013
Ni^{2+}	0.69	- 0.09	0.07 - 0.20

A similar incongruent behaviour of Cu^{2+} and Mg^{2+} is found when the data on coprecipitation of these two metals with calcite are examined. According to KITANO et al. (1968) and KITANO et al. (1980) (see also VEIZER 1983a) Cu^{2+} partition coefficients in calcite are much higher (~25 - 40) than for Mg^{2+} (~ 0.01 - 0.1, see Table 4-1). Neither metal fits into the correlation with ionic size defined by most other metals, either for calcite or for siderite. This indicates, again, that additional factors must control their coprecipitation behaviour.

An additional factor influencing metal coprecipitation is *crystal morphology*. The partition coefficient of a specific ion may vary among faces of the same crystal, a phenomenon known as *sectoral zoning* (PAQUETTE & REEDER 1995). Sectoral zoning of selenate (SeO_4^{2-}) and sulphate ions (SO_4^{2-}) in calcite was investigated by STAUDT et al. (1994). They found variations by a factor of 2 to 4 in the concentration of these anions across different crystal faces of calcite grown under carefully controlled conditions (chemostatic technique). The results of similar experiments conducted by PAQUETTE & REEDER (1995) demonstrated that the partition coefficients of Sr^{2+} , Mn^{2+} and Mg^{2+} in calcite also may vary significantly from face to face (by factors of up to ~ 1.5, 9 and 13, respectively).

Sectoral zoning is thought to be a consequence of peculiarities in the *surface topographies* of the various crystal faces. STAUDT et al. (1994) and PAQUETTE & REEDER (1995) argue that differential incorporation of trace metals is due to subtle differences in the coordinative environments at the sites of crystal growth. On each face, the coordination polyhedron of a trace metal in the process of being incorporated is slightly different. On the faces offering a geometrically favourable coordinative environment, trace metals are incorporated more easily than on faces where the coordination geometry is unfavourable, which results in face-dependent partition coefficients. Although significant, the effect of sectoral zoning on the partition coefficients of trace metals coprecipitated with calcite seems to be less than one order of magnitude and is thus not considered to be a critical issue.

4.4.3 Precipitation/ recrystallisation rate

Several studies indicate unequivocally that the uptake of trace ions in calcite depends strongly on precipitation kinetics (LORENS 1978, LORENS 1981, DROMGOOLE & WALTER 1990, MUCCI & MORSE 1983, MUCCI 1986).

Lorens (LORENS 1978, LORENS 1981) carried out the first and still most thorough investigation of the role of kinetics. He found that the partition coefficients of several divalent metals (Mn^{2+} , Cd^{2+} , Co^{2+} and Zn^{2+}) decrease systematically with increasing rate of calcite precipitation, while the partition coefficient of Sr^{2+} increased with increasing precipitation rate (see Figures 4-3 and 4-4). Lorens' data indicate a maximum variation in the partition coefficient of a single cation of approximately half order of magnitude.

However, if the data of DAVIS et al. (1987) on the uptake of Cd in calcite are merged with those of TESORIERO & PANKOW (1996), LORENS (1978) and LORENS (1981) (see Figure 4-4), this figure increases to three orders of magnitude. The high partition coefficients determined by DAVIS et al. (1987) arise from experiments during which calcite recrystallised very slowly, resulting in rates up to 3 orders of magnitude less than the slowest rate in Lorens' experiments.

The data presented in Figure 4-4 would suggest that the high Cd-partition coefficients of DAVIS et al. (1987) are due to the very slow kinetics imposed during their experiments. However, these authors calculated partition coefficients on the base of free ion concentrations, so that they are not directly comparable to the other partition coefficients reported in Figure 4-4. Unfortunately, it is not possible to recalculate the Davis et

al. data precisely to the usual form of partition coefficients, since some essential details of their calculations are not known. Nevertheless, it is possible, on the basis of the information supplied in their paper, to make rough estimates of the Doerner-Hoskins partition coefficients (shaded rectangle in Figure 4-4). If these estimates are integrated with the other values, it appears that the Cd partition coefficients first increase with decreasing precipitation rate and then remain more or less constant below a precipitation rate of $\sim 10^{-9} \text{ mol m}^{-2} \text{ s}^{-1}$.

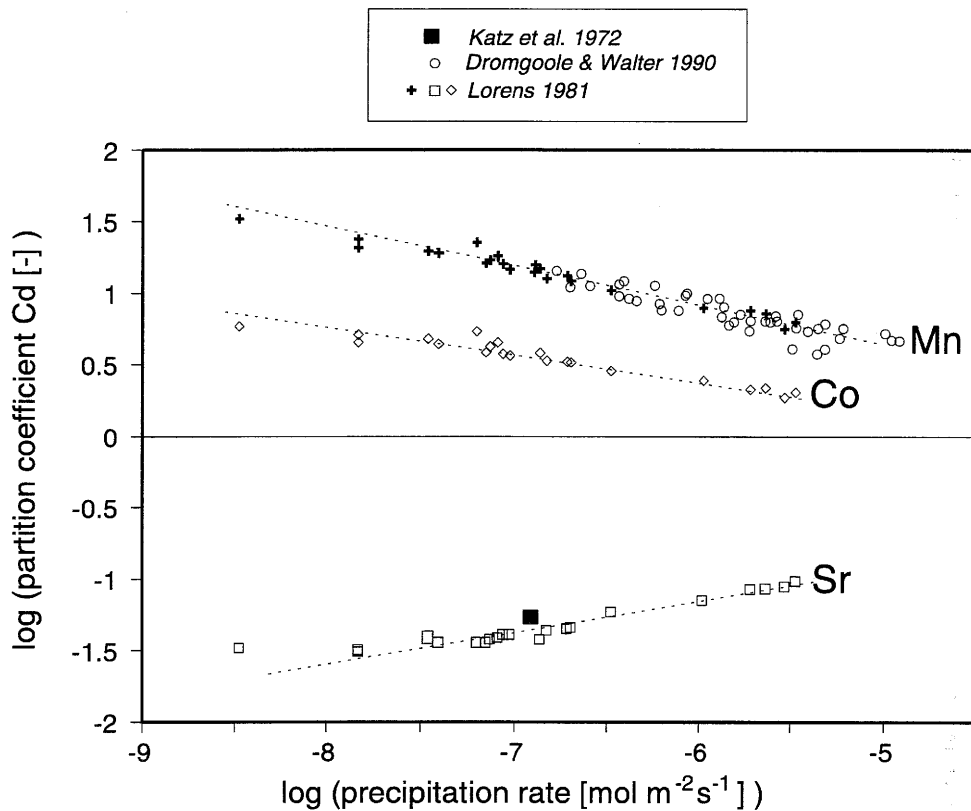


Figure 4-3: Dependence of partition coefficients for divalent cations in calcite on the precipitation rate.

The latter hypothesis is substantiated by TESORIERO & PANKOW (1996), who recalculated Lorens' partition coefficients using free ion concentrations. Their Figure 6 shows that the free ion partition coefficients by DAVIS et al. (1987) are comparable to the highest free ion partition coefficients measured in their own experiments, which were carried out at faster precipitation rates. It seems thus that there is a threshold value of the precipitation rate, below which all reactions involved in the incorporation of a trace element are in a state of mutual equilibrium. Below this limiting value, partition coefficients do not increase further. Similar effects were observed also for Sr and Ba (see TESORIERO & PANKOW 1996).

The different behaviour of Sr^{2+} with respect to other cations (Figure 4-3) can be explained as follows. Mn^{2+} , Cd^{2+} , Co^{2+} and Zn^{2+} , being smaller than Ca^{2+} , are incorporated more easily into calcite than the exceedingly large Sr^{2+} ion. Thus, if precipitation is sufficiently slow to guarantee equilibrium conditions, cations with radii smaller than Ca^{2+} will have distinctly larger partition coefficients than Sr^{2+} or other large ions. At high precipitation rates, however, not all reactions involved in the incorporation process will be at equilibrium. For instance, adsorption reactions will not be fast enough to keep pace with precipitation. At very fast precipitation rates, all trace cations dissolved in a thin film of solution in contact with the growing mineral surface will be indiscriminately trapped by a layer of newly formed precipitate, before adsorption reactions can “sort them out” according to their affinity for the calcite surface. Ideally, then, no matter which size they have, all cations should be incorporated into calcite with the same trace ion to calcium ion ratio as the solution, i.e. the partition coefficient should approach unity for all coprecipitated ions. Figure 4-3 shows a trend consistent with this argument. With increasing precipitation rate the partition coefficients of all cations tend to unity, but even at the highest rates ($\sim 10^{-5} \text{ mol m}^{-2} \text{ s}^{-1}$) differences in the values of the partition coefficients remain substantial.

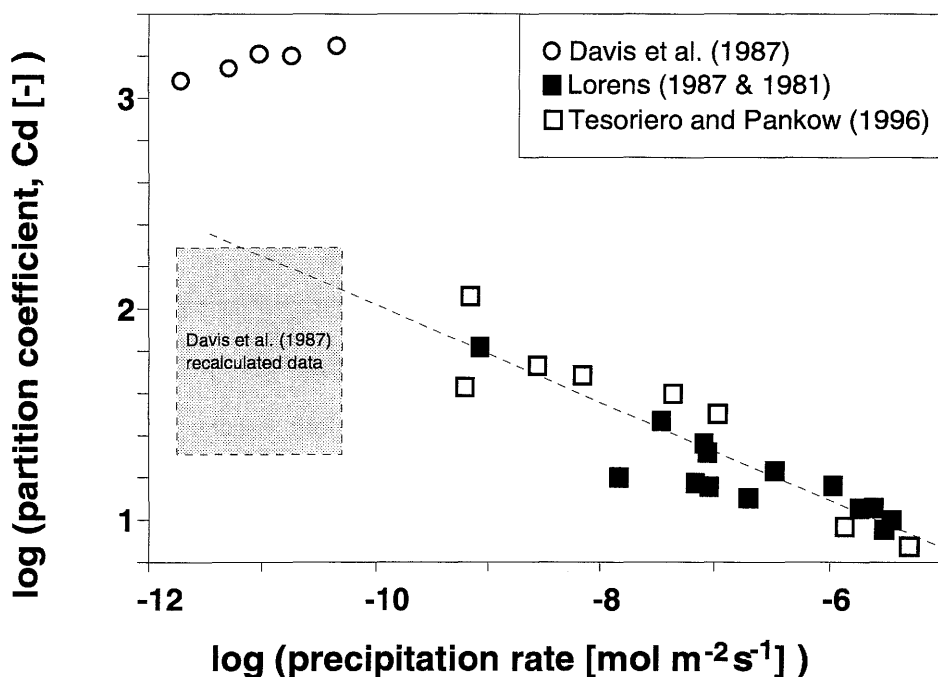


Figure 4-4: Cadmium partition coefficients as a function of the precipitation / recrystallisation rate of calcite (see text for comments).

In summary, the available data demonstrate that the rate of precipitation has a considerable effect on the uptake of trace metals in calcite. The variation of the partition coefficients observed for a given ion is usually within one order of magnitude over a large range of precipitation rates. It is possible that larger differences will emerge if the kinetic conditions applied in laboratory tests are extended to faster rates. In contrast, partition coefficients do not increase indefinitely as the precipitation/recrystallisation becomes progressively slower: apparently, a limiting value of the partition coefficient is reached at sufficiently low precipitation rates, which is not exceeded if the rate of mineral growth decreases further.

Under repository conditions, precipitation rates are expected to be slower than those imposed in most laboratory experiments, since a large degree of oversaturation should not be reached in systems where solute transport (by diffusion or advection) is slow. This would minimise the need for reaction rate-dependent partition coefficients when modelling radionuclide coprecipitation in repository systems. Nevertheless, given the potential influence of the precipitation rate on partition coefficients in calcite, it will be important to define precisely the range of possible precipitation rates for carbonate precipitation under repository conditions (e.g. through modelling studies or with the help of data from natural analogues).

4.4.4 Temperature

Systematic studies of the effect of temperature on the uptake of metals in carbonate minerals are rare since most coprecipitation studies were carried out at 25°C¹⁶. Nevertheless, a few investigations exist in which coprecipitation experiments were carried out over temperatures ranging from 10 to 100°C, i.e. in a range covering the temperatures prevailing in Swiss radioactive waste repositories.

Among these studies, the experiments of CROCKET & WINCHESTER (1966) on the incorporation of Zn in calcite had to be discarded, since they were performed using a free nucleation technique, which causes the calcite to grow at variable rates. In this kind of experiment, a very rapid growth soon after nucleation of the solid phase is followed by progressively slower precipitation as saturation equilibrium is approached, so that the effects of precipitation kinetics on the uptake of zinc interfere with those due to temperature variations.

The effect of such interference is illustrated by the negative correlation between temperature and the Zn partition coefficients determined by CROCKET & WINCHESTER (1966). The partition coefficients were found to decrease with increasing temperature (from 5.7 at 25°C to 3.2 at 50°C), a behaviour contradicting common geochemical evidence (as a rule, miscibility in minerals increases with temperature). On the other hand, rates of reaction are also temperature-dependent (following Arrhenius' law), thus the rate of calcite precipitation will increase exponentially with temperature, resulting in a decrease of the partition coefficients. Hence, the negative correlation of the Zn²⁺ partition coefficients with temperature may be ascribed to the overcompensating effect of the precipitation kinetics.

¹⁶ This is due to the fact that most investigators of coprecipitation in carbonates are marine geologists.

If the data of CROCKET & WINCHESTER (1966) are excluded, there remain the experimental works of DROMGOOLE & WALTER (1990), KATZ (1973) and KATZ et al. (1972) to investigate the effect of temperature. These experiments were carried out under controlled precipitation conditions and in solutions of well-defined constant composition, so that it is possible to select data which really describe the effect of temperature. As expected, they consistently indicate a weak, but significant, increase of the partition coefficients with temperature (Figure 4-5). In all cases, the maximum variation of the partition coefficient over the temperature interval considered is much less than one order of magnitude. Considering the restricted range of possible temperatures in the Swiss repository environments (from ambient to 60°C in the HLW repository, virtually unchanged from ambient in the L/ILW repository), these results indicate that uncertainties in the temperature are not critical for the estimation of partition coefficients in view of safety analyses.

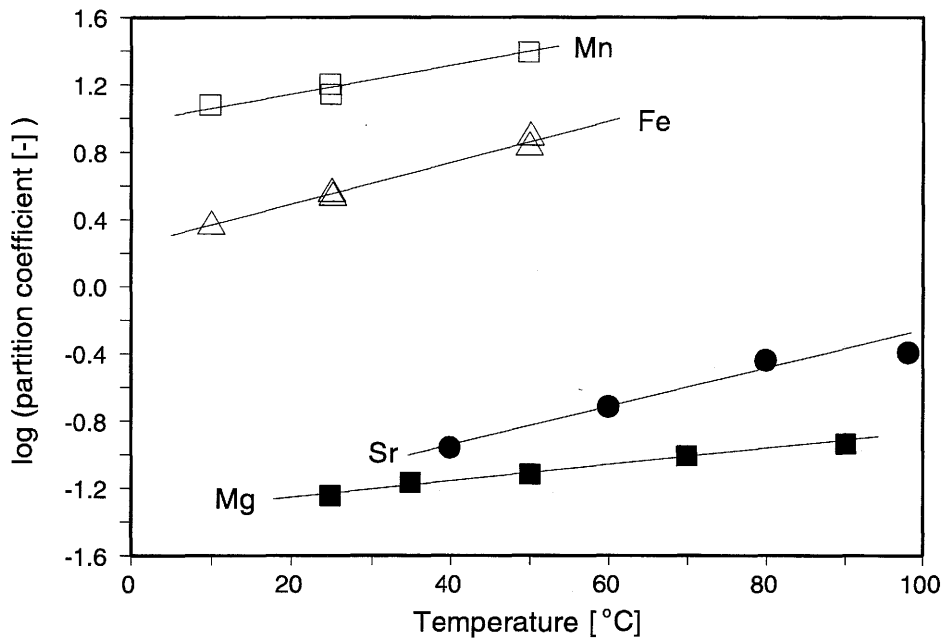


Figure 4-5: Effect of temperature on the partition coefficients of four divalent cations in calcite. Each correlation includes only data corresponding to experiments performed at the same rate of calcite precipitation (in all cases $R \sim 10^{-7} \text{ mol m}^{-2} \text{ s}^{-1}$) and in solutions of uniform composition. The plotted data were selected from DROMGOOLE & WALTER (1990) (Mn, Fe), KATZ (1973) (Mg) and KATZ et al. (1972) (Sr).

4.4.5 Correlation with the solubility products of pure carbonates

Since the earliest times of radiochemistry, coprecipitation techniques have been used to purify newly discovered actinides and fission products (HAHN 1936, HYDE 1954). The basic principle of such techniques consisted in removing a specific trace element from solution by repeatedly precipitating a solid for which the trace element showed a strong affinity. The trace element became progressively enriched in the host solid through *fractional crystallisation*¹⁷. This procedure was employed by the pioneers of radiochemistry to concentrate naturally occurring radioactive elements like Ra and Po (CURIE 1912, pp. 142-191) and later to isolate the first artificial actinides (e.g. Pu, Np).

In order to make these enrichment techniques efficient and predictable, the radiochemists developed a broad empirical knowledge of coprecipitation. They found out which type of solids would be suitable for their purposes and worked out rules governing the partitioning of radioactive species between solution and solid. One of the most useful rules is known as *Fajans' precipitation rule*. According to the definition given in HAHN (1936), it states that "*the lower the solubility of the compound formed by the radioelement with the anion of the precipitate, the greater is the amount of radioelement carried down as cation*". Fajans' rule thus predicts that the partition coefficient of a trace cation, of which the pure carbonate is insoluble, should be larger than that of a cation which forms, when precipitated as pure solid, a soluble carbonate. Accordingly, the trivalent rare earths and Cd^{2+} , which form insoluble carbonates, should partition strongly in calcite, while Mg^{2+} , Li^+ , K^+ and Na^+ , which form soluble to very soluble carbonates, are expected to have the lowest partition coefficients.

An inspection of the data compiled in Table 4-1 and of Figure 4-6 fully confirms the validity of Fajans' rule for the incorporation of metals in calcite. Particularly, the very small partition coefficients of K^+ , Li^+ , Na^+ and Mg^{2+} , which do not follow the correlation with ionic radius, are found to be consistent with this rule. Moreover, the large partition coefficient calculated for Pb^{2+} in marine carbonates (Figure 4-2) can be now understood: lead carbonate, with a solubility product of about 10^{-13} M^2 (GRAUER 1994), is much less soluble than strontianite, which has a solubility product of about 10^{-9} M^2 (PEARSON et al. 1992). Accordingly, a partition coefficient for lead in calcite much larger than for Sr^{2+} would result applying Fajans' rule, in spite of the similarity of the ionic radii (it would plot in the region populated by the rare earths in Figure 4-6).

These findings suggest that Fajans' rule may be a suitable tool for the estimation of unknown partition coefficients. If the correlation with the solubility products of pure carbonates is generally valid, then the rule should apply to coprecipitation with other carbonates, not only with calcite. A consistently increasing order of partition coefficients (from D_{Na^+} to $D_{\text{La}^{3+}}$) with decreasing solubility of the pure carbonates should also emerge for, say, siderite or aragonite. In spite of the scarcity of data available on other minerals and the uncertainties affecting them, this prediction is confirmed, since: a) partition coefficients for coprecipitation with siderite increase in the order $\text{Mg}^{2+} < \text{Ca}^{2+} \sim \text{Ni}^{2+} < \text{Co}^{2+} < \text{Mn}^{2+} < \text{Cu}^{2+}$ (Table 4-3), which is roughly

¹⁷ *Fractional crystallisation* involves many sequential precipitation steps. At each step, a precipitate enriched in the desired trace element is obtained. The depleted solution is then discarded, while the precipitate is redissolved for the next precipitation step. By this procedure, one starts with a large amount of raw material to obtain very small final amounts of purified trace element.

consistent with the decreasing order of the solubility products of the carbonates of the listed elements and b) the same pattern of partition coefficients found for trace metals in calcite, though less pronounced, is observed for aragonite (see Table 3-1 in VEIZER 1983a): for instance, very low partition coefficients were measured for Mg^{2+} and Na^+ as well, and the partition coefficient of Sr^{2+} was found, as in calcite, to be smaller than those of Mn^{2+} or Cd^{2+} .

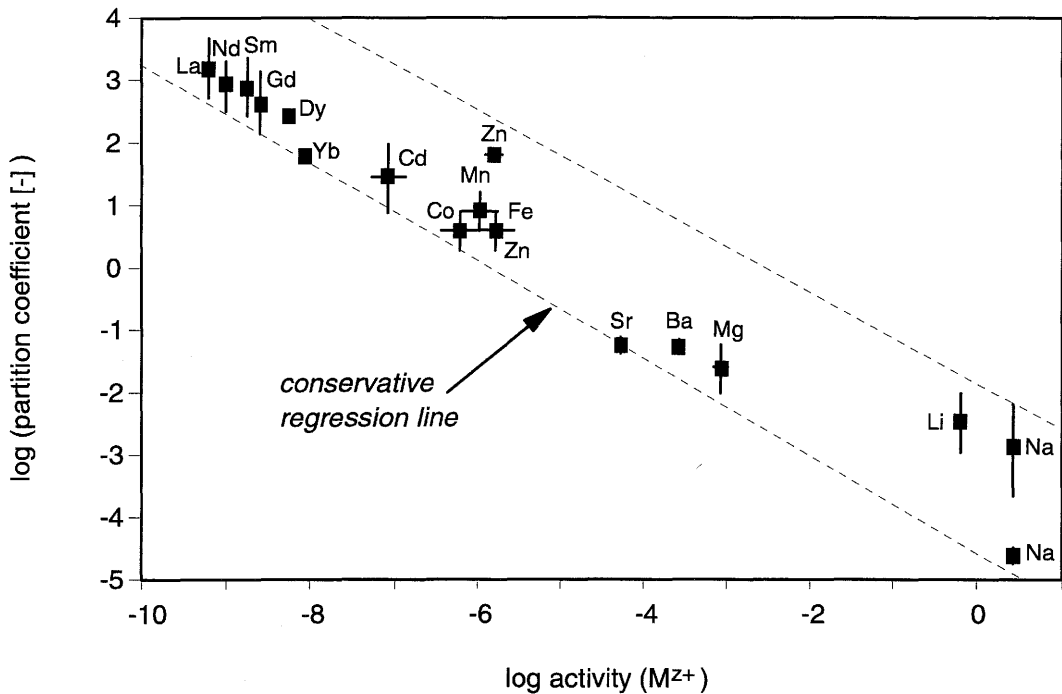


Figure 4-6: Correlation between partition coefficients of various trace metals in calcite and the solubility of the corresponding pure carbonates. Because carbonates have different stoichiometries ($Me(I)_2CO_3$, $Me(II)(CO_3)$ and $Me(III)_2(CO_3)_3$), it is not possible to use directly the solubility products for this correlation. The data were thus normalised to the equilibrium activity of the free metal ions in a solution saturated with the corresponding pure solids, assuming an arbitrary carbonate ion activity of 10^{-5} . The solubility products are taken from the compilations of GRAUER (1994) (Mn, Fe, Co, Ni, Zn, Cd, Pb carbonates), SMITH & MARTELL (1976) (La, Nd, Sm, Gd, Dy, Yb carbonates) and PEARSON et al. (1992) (Mg carbonate). The solubility products of Na and Li carbonate were estimated from the data given by WEAST (1977).

Fajans' rule is actually an expression of a basic principle of solid solution thermodynamic models, which also state a dependence between the concentrations of chemical components mixed in the solid and the solubility products of the corresponding pure solids. In the case of thermodynamic models, this dependence is described by activity coefficients in the solid, calculated with the help of special thermodynamic functions

and parameters. Fajans' rule, instead, is a purely empirical tool. There is no attempt to derive the observed dependence of the partition coefficients from thermodynamic principles.

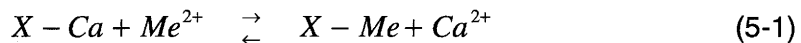
4.4.6 Correlation with adsorption

Coprecipitation reactions necessarily proceed via an intermediate adsorption step. Consequently, adsorption equilibria will be important in determining to what extent a trace element is incorporated in a solid during coprecipitation. Notably, one has to assume that weakly sorbing species should have very small partition coefficients, since they can hardly be incorporated into a solid if they cannot stick on its surface. The reverse need not be true, although strong adsorption certainly facilitates the uptake of coprecipitating species into the solid's lattice. A small partition coefficient may result for strongly sorbing species if one of the subsequent steps in the process of transferring adsorbed species into a lattice site is hindered for some reason (e.g. due to an exceedingly large ionic radius).

In Figure 4-7 partition coefficients for trivalent rare earths in calcite are plotted against the corresponding distribution coefficients (K_d [$\text{m}^3 \text{kg}^{-1}$], calculated from the adsorption data of ZHONG & MUCCI 1995). In spite of the large uncertainties affecting the partition coefficients, a positive correlation is evident.

Figure 4-8 shows the partition coefficients of some divalent metals in calcite plotted against the corresponding conditional selectivity constants (determined at a ionic strength of 0.1 M and in the pH-range 7-9 over a large metal concentration range, see ZACHARA et al. 1991). Also in this case a rough positive correlation emerges.

The selectivity constants describe equilibrium for cation exchange reactions of the type:



where $X -$ represents an exchangeable site on the sorbent surface. Equation (5-1) thus defines a mass action constant (see Equation (3-10) for the nomenclature):

$$K_{ex} = \frac{[Ca^{2+}]}{[Me^{2+}]} \left(\frac{\{Me\}}{\{Ca\}} \right)^n \quad (5-2)$$

For all but one of the metals investigated in ZACHARA et al. (1991), the exponential factor n is equal to unity (exception: $n=1.86$ for Zn). In all cases where $n=1$, K_{ex} is *formally equivalent* to the heterogeneous partition coefficient, λ , since Equation (5-2) can be rearranged as follows (compare with Equation (3-10)):

$$\frac{\{Me\}}{\{Ca\}} = K_{ex} \frac{[Me^{2+}]}{[Ca^{2+}]} \quad (5-3)$$

A basic difference is, however, that partition coefficients for coprecipitation are mostly based on *total concentrations* of the dissolved metals, while selectivity constants for adsorption use *free ion concentrations*. It is clear that a re-evaluation of both selectivity constants and partition coefficients in terms of free-ion activities is the ultimate goal. This would provide a thermodynamically consistent basis for the comparison of coprecipitation and ion exchange constants and probably improve the correlations, as suggested by the data presented in section 4.4.8.

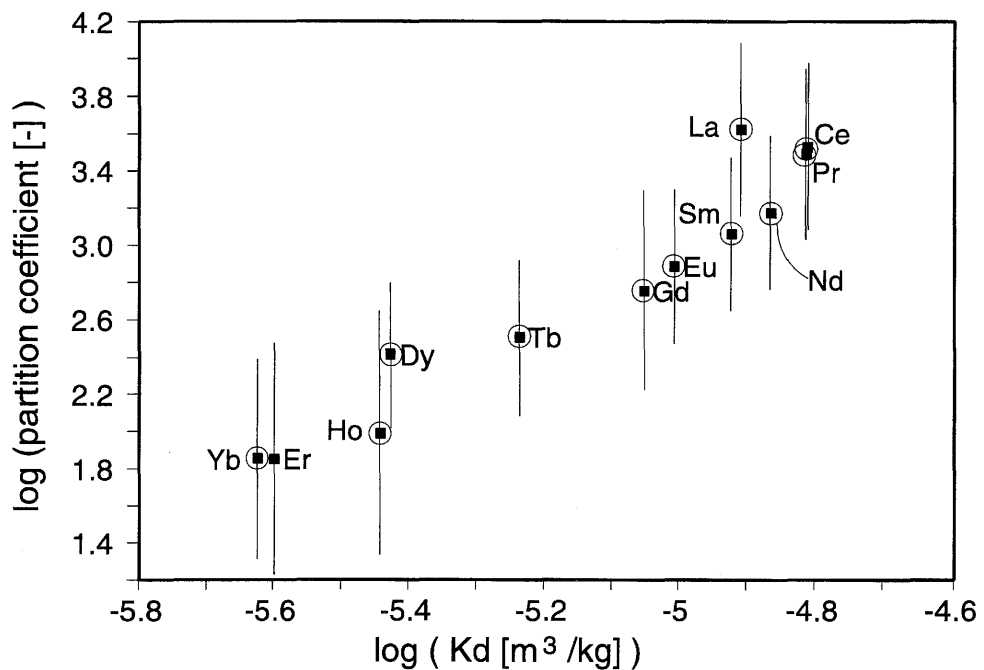


Figure 4-7: Correlation between partition coefficients of trivalent rare earths and sorption distribution coefficients, both based on the data of ZHONG & MUCCI (1995).

Pursuing the analogy between adsorption and coprecipitation, it is noteworthy that the correlation emerging in the log-log plot of Figure 4-8 has a slope approaching unity and an y-intercept of about zero, indicating that the values of partition coefficients tend to be equal to the selectivity constants. This approximation holds particularly if the partition coefficients given by DAVIS et al. (1987), which rely on free metal ion concentrations, are considered, and if only those partition coefficients are taken into account which are mostly unbiased by fast precipitation kinetics (these correspond, in Figure 4-8, to the highest partition coefficients in the ranges given for Co, Mn, Zn and Cd and to the lowest in the ranges given for Sr and Ba).

Although selectivity constants and partition coefficients do not necessarily quantify the same process, adsorption is a necessary intermediate step on the way to solid solution

formation. In a situation in which all reaction steps involved in the coprecipitation process are in mutual equilibrium and if some conditions are satisfied¹⁸, the relation $K_{ex} \sim \lambda$ may be expected to hold, as suggested by the data in Figure 4-8. In the author's opinion, it is not a coincidence that partition coefficients have the same form as selectivity constants: this analogy reflects the close relationship between adsorption and coprecipitation in carbonates.

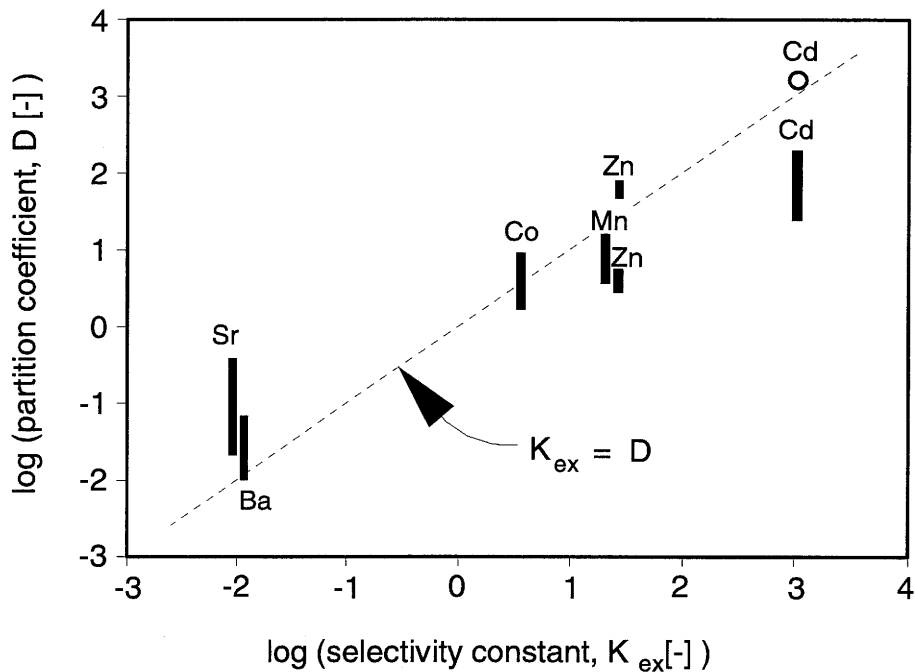


Figure 4-8: Correlation between selectivity constants (taken from ZACHARA et al. 1991), quantifying sorption of divalent metals on calcite, and partition coefficients. The open circle represents Cd partition coefficients defined using free ion concentrations, as given by DAVIS et al. (1987), while the solid bars give the ranges for partition coefficients determined using the Doerner-Hoskins definition, which utilises total metal concentrations.

¹⁸ Since selectivity constants are defined using the concentrations of free metal ions in solution, whereas empirical partition coefficients use total metal concentrations, the approximation $K_{ex} \sim \lambda$ cannot be reasonably expected to hold if one or both metals involved in the exchange reaction are strongly complexed.

4.4.7 Influence of pH and ionic strength

No systematic studies dealing with the effects of pH and ionic strength on the coprecipitation of trace metals with calcite have been found in the literature. The reasons for this are simple: a) since most investigators were interested in the uptake of trace metals by marine carbonates, most studies were carried out in seawater, which is essentially a medium of constant pH and ionic strength; b) in studies carried out before chemostatic techniques were developed it was not possible to buffer the pH and ionic strength at the desired values during the experiments.

Taking into account the considerations made in the previous section, it appears evident that pH and ionic strength *must* significantly affect the coprecipitation process, since both parameters have a profound effect on adsorption processes. Specifically, considering the data of ZACHARA et al. (1991) on the adsorption of transition metals, it can be expected that the partition coefficients for the coprecipitation of these metals with calcite will decrease strongly across adsorption edges, as pH decreases from ~8.5 to ~7. The determination of the pH-dependence of partition coefficients is therefore one of the most important outstanding tasks in the field of trace element coprecipitation.

4.4.8 Influence of complex formation

It is well-known that complex formation may affect the extent to which metals are adsorbed on a solid. The formation of stable complexes with strong organic ligands may significantly reduce the fraction of adsorbed metal on a specific solid surface. An effect of this type was observed for Am sorption on calcite. In the presence of iso-saccharinic acid, the distribution coefficient of Am was found to be orders of magnitude less than in the absence of complexing agents (TITS et al., in prep.). In view of the close relations between sorption and coprecipitation, it is reasonable to assume that any strong sorption effect attributable to metal complexation should be reflected in the corresponding coprecipitation process.

To the author's knowledge, the only study on this subject is the experimental work of KITANO et al. (1968), who investigated the coprecipitation of Zn^{2+} and Cu^{2+} with calcite and aragonite in the absence and presence of 19, mostly organic, ligands. The results from this investigation consistently indicate that the partition coefficients of Zn and Cu in calcite are significantly reduced in the presence of sufficient concentrations of the complexing agents.

The data summarised in Table 4-4 indicate that the partition coefficient of Zn^{2+} in calcite decreased by more than one order of magnitude as 1 M sodium chloride was added to the solution from which calcite was precipitated. Zinc is known to form strong chloride complexes; in the solutions used by KITANO et al. (1968), up to about 85% of the zinc dissolved is predicted to occur as $ZnCl^+$ (see caption of Table 4-4 for details on the calculations). The partition coefficient, λ , was found to correlate with the fraction of free zinc ion. If the partition coefficient is redefined using the free zinc ion concentration rather than the total zinc concentration in solution, the so modified coefficient turns out to be roughly constant ($\lambda^* \sim 30$).

These findings suggest that zinc chloride complexes are non-sorbing (in spite of the positive net charge of $ZnCl^+$), thus reducing the total amount of coprecipitated zinc. As an alternative explanation, one may assume that $ZnCl^+$ ions sorb on the calcite surface, but the Zn associated with this complex would not be incorporated in the mineral lattice due to the strong binding energy to the large Cl^- ligand, which would prevent the detachment of Zn^{2+} from the complex.

Table 4-4: Effect of complexation on the partition coefficient of zinc in calcite. As the fraction of free Zn^{2+} decreases due to complexation with chloride, the empirical distribution coefficient, λ , is reduced proportionally. The modified partition coefficient, λ^* , however, remains roughly constant. To determine the fraction of uncomplexed zinc, speciation calculations were carried out with MINEQL (WESTALL et al. 1976). Complexation with Cl^- was accounted for using the formation constant of GRAUER & SCHINDLER (1972). Complexation of zinc with carbonate species was not considered, because neither the formation constant of $ZnCO_3^0$ nor the CO_2 partial pressure during the experiments are known with sufficient accuracy.

added chloride [Cl^-] / M	fraction of uncomplexed zinc $\alpha = \frac{[Zn]_{free}}{[Zn]_{tot}}$	heterogeneous partition coefficient $\lambda = \frac{\{Zn\}[Ca]_{tot}}{[Zn]_{tot}\{Ca\}}$	modified partition coefficient $\lambda^* = \frac{\lambda}{\alpha} = \frac{\{Zn\}[Ca]_{tot}}{[Zn]_{free}\{Ca\}}$
0.000	1.00	50	50
0.028	0.86	25	29
0.085	0.66	20	30.3
0.38	0.30	8.5	28.3
0.51	0.25	5	20
1.0	0.14	4	28

As another example from the same study, the effect of the addition of citrate is briefly considered. Both zinc and copper form stable citrate complexes, whereby complexation with copper is considerably stronger than with zinc ($\log K_{Cu(cit)^-1} = 7.2$, $\log K_{Zn(cit)^-1} = 6.1$)¹⁹. The progressive addition of sodium citrate caused a decrease

¹⁹ Hummel, personal communication

of both Zn and Cu partition coefficients in calcite. Whereas the Zn partition coefficient was reduced from 50 to 19 upon addition of up to 7.8 mM citrate, the Cu partition coefficient decreased from 4.3 to zero (no detectable copper in calcite) after addition of 5.3 mM citrate. This behaviour is thus qualitatively consistent with the different stabilities of the Cu and Zn citrate complexes.

In the presence of other organic ligands, the uptake of copper and zinc in calcite was also reduced, with the reduction always larger for copper than for zinc. Whereas the partition coefficient of Zn decreased by less than a factor of 4 upon addition of considerable amounts of organic ligands (e.g. 1.5 g/L sodium citrate, 1.5 g/L sodium acetate, 3 g/L sodium acetate), reductions by more than 100 times were found for Cu in the presence of comparable amounts of citrate, glutamate, arginine, glycine and alanine. It is noteworthy that the decrease in the partition coefficient of Cu correlates with the stability of the corresponding organic complex: large reductions of the partition coefficients are found in the presence of ligands forming strong copper complexes (like citrate, glutamate, alanine, $\log K_1 \sim 7-8$), while the presence of weaker ligands (like succinate and acetate, $\log K_1 < 5$), has a more limited effect on copper uptake in calcite.

Although a quantitative modelling of the Kitano et al. experimental results is not possible, due to the limitations of the experimental technique they employed, the results of their investigation clearly indicate that complex formation with organic ligands may have a considerable, negative effect on the incorporation of radionuclides in solid phases. This topic is thus of primary importance for integration of coprecipitation reactions in safety assessment models.

4.4.9 Concentration and competition effects

Natural ground waters are multicomponent solutions containing a wide variety of trace elements. Due to their very low concentrations, trace elements are not expected to interfere with each other during simultaneous coprecipitation or adsorption. The partition coefficient of a given trace element should thus be independent of the concentration of other trace elements. Unfortunately, there are only a few studies which could help substantiating or disproving this assumption.

PINGITORE & EASTMAN (1986) showed that the addition of a few ppm Ba^{2+} in solution caused a depression of the Sr^{2+} partition coefficient in calcite from ~ 0.2 to 0.06, contradicting the argumentation presented above²⁰. These results may be explained by considering that both Ba^{2+} and Sr^{2+} are reluctant to be incorporated into calcite due to their exceedingly large ionic radii and weak sorption on the calcite surface. Probably, these ions are adsorbed on surface defects as is the case of the alkali ions (see BUSENBERG & PLUMMER 1985; OKUMURA & KITANO 1986). Since the availability of such surface defects is very limited, trace ions of this kind may interfere

²⁰ Considerable interference among trace elements has also been observed in the case of simultaneous adsorption of Cs, Co and Ce on granite alteration products (McKINLEY & WEST 1987): for instance, Cs distribution coefficients were found to vary by up to one order of magnitude as a function of the concentration of Co and Ce added to the spike solution.

with each other even if their solution concentration is very low. Such effects should not appear for ions which are adsorbed and incorporated at specific lattice sites.

Coprecipitating trace cations, however, also compete with calcium and other cations present in major concentrations. Therefore, it is likely that the partition coefficient of a trace element will depend on the relative concentrations of trace element and major competing ions in solution. Such effects have been indeed observed: the partition coefficients of trivalent rare earths in calcite were found to increase by up to one order of magnitude when their concentrations were raised from ~10 to ~100 nM, at constant calcium concentration (ZHONG & MUCCI 1995).

In other cases, partition coefficients appear to be insensitive to the trace metal / calcium concentration ratio. DROMGOOLE & WALTER (1990) observed that increasing the Mn/Ca ratio in solution by a factor of 50 (from 10^{-3} to 5×10^{-2}) caused the partition coefficient to decrease by a factor of only 2-3. Moreover, the partition coefficients measured by LORENS (1981) for the uptake of Mn in calcite are very similar to those of DROMGOOLE & WALTER (1990), although the experiments of the former were carried out at much lower Mn concentrations and Mn/Ca concentration ratios (see Table 4-1).

Although competition effects may affect considerably partition coefficients in calcite, the magnitude of such effects appears to be within one order of magnitude, judging from the available data. It is noteworthy and reassuring, for instance, that the partition coefficients of cations which have been repeatedly measured in different laboratories tend to be remarkably similar in spite of widely different concentration ranges used in the various experiments (e.g. Cd^{2+} , Mn^{2+} , Sr^{2+} , see Table 4-1). Therefore, there is a good degree of confidence that these partition coefficients can be used in generic safety assessment models.

5. Mechanisms of solid solution formation

The formation of a solid solution is a complex, multistep process which is poorly understood in terms of mechanisms at an atomic scale. Most coprecipitation studies are empirical and their main purpose is to determine distribution coefficients for a given trace element under the conditions of interest to the investigators. Consequently, studies aiming at elucidating the mechanisms through which dissolved trace ions are incorporated into mineral lattices are exceptional. Thanks to recent developments in surface analysis techniques, however, mineral-solution interfaces are becoming visible at the nanoscale, making it possible to observe structural changes on mineral surfaces following adsorption and lattice incorporation. Although some of these techniques are still in their infancy (specifically, Atomic Force Microscopy, or AFM), they undoubtedly have the potential of providing a detailed understanding of the mechanisms involved in coprecipitation processes. In this section, an attempt is made to combine information gained from surface analyses with that obtained from classical wet-chemical methods, in order to identify critical steps involved in coprecipitation reactions. These considerations are based on a few papers on the coprecipitation of Cd^{2+} and other metals with calcite.

The papers on the uptake of Cd^{2+} in calcite provide a unique case study giving detailed insight on processes taking place during the interaction of dissolved metal ions with a mineral surface. DAVIS et al. (1987) studied the uptake of Cd^{2+} by calcite in dilute, saturated solutions ($I < 0.1$, $\text{pH} = 7-9$). Since these experiments were carried out in solutions exactly saturated with calcite, kinetic effects can be excluded: the incorporation of Cd^{2+} took place during slow recrystallisation of the calcite, so that adsorption and incorporation reactions can be assumed to have proceeded in mutual equilibrium (in the case of fast calcite precipitation from a supersaturated solution, the reacting mineral surface could be covered by newly formed calcite before sorption equilibria are established). DAVIS et al. (1987) carried out preliminary experiments to determine the adsorption of Cd^{2+} on calcite. In a second series of tests, they induced desorption by adding appropriate amounts of the strong complexing agent EDTA in solution. They observed that the extent of Cd^{2+} desorption strongly depended on the time of previous adsorption. Desorption was almost quantitative if the EDTA was added after a short adsorption time (2 hours). In contrast, only a small fraction of the previously adsorbed Cd^{2+} would desorb after 4 days adsorption time. The desorbed fraction was found to decrease with adsorption time, i.e. the longer the duration of the interaction between Cd-spiked solution and calcite, the more "irreversible" Cd-adsorption became.

These observations were interpreted as evidence for the formation of a $(\text{Ca,Cd})\text{CO}_3$ solid solution on the calcite surface. In interpreting these results, Davis et al. postulated the existence of a thin, porous and amorphous hydrated layer separating the solution from the ordered calcite structure. The irreversibility of the adsorption reaction was explained by assuming that the adsorbed cadmium ions penetrated into the calcite lattice by diffusion through this porous layer. They argued that volume diffusion (i.e. diffusion through the ordered calcite lattice) would be too slow to explain the irreversibility of the Cd^{2+} adsorption.

This interpretation of Davis et al. was only partially confirmed by recent surface analyses (STIPP et al. 1992 and STIPP et al. 1994), which included atomic scale AFM

images of calcite surfaces immersed in water. For instance, the cadmium peaks obtained by X-ray photoelectron spectroscopy (XPS) on calcite samples previously exposed to a Cd-doped solution were found to decrease with increasing sample storage time. Since the samples were stored in dry air, this effect could only indicate penetration of the adsorbed Cd^{2+} cations into the crystal lattice, i.e. the formation of a solid solution. On the other hand, the AFM images revealed a periodic structure at the mineral surface consistent with the unit cell parameters of calcite, thus excluding the existence of the amorphous diffusion layer postulated by DAVIS et al. (1987).

The surface analytical data of STIPP et al. (1992) yielded even more details. In a series of experiments, thin layers of otavite (pure cadmium carbonate) were precipitated on top of calcite samples. XPS analyses carried out shortly after the experiments confirmed the presence of a pure CdCO_3 layer. However, after storing the sample for two months in vacuum, the intensity of the Cd peak appeared to be greatly reduced. These results indicate that: a) a $(\text{Ca,Cd})\text{CO}_3$ solid solution was formed, which is thermodynamically more stable than a mechanic mixture of pure otavite and calcite; and b), the formation of the solid solution is fast even in absence of an aqueous medium. Although it is not possible to identify the exact mechanism by which the cadmium ions migrate from the surface into the lattice of calcite, the AFM images taken at different time intervals suggest that a major role should be played by the rapid surface dynamics of calcite (rapid changes in the microtopography of the mineral surface due to recrystallisation).

Further insight into the process of metal coprecipitation with carbonates is provided by the investigation of ZACHARA et al. (1991). These authors studied the sorption and desorption of divalent metals on calcite in the mildly alkaline pH range. Several cations (Cd^{2+} , Zn^{2+} , Mn^{2+} , Co^{2+} , Ni^{2+}) sorbed strongly on calcite; however, substantial differences were observed in the desorption behaviour. Whereas, after 24 hours adsorption time, Co and Zn could be forced to desorb almost completely, it was not possible to remove more than 20-30 % of the sorbed Cd and Mn.

This contrasting behaviour was attributed by ZACHARA et al. (1991) to differences in the free energies of hydration (ΔG_{H}). Cations with large hydration energies like Zn^{2+} , Co^{2+} , Ni^{2+} ($\Delta G_{\text{H}} = -480$ to -500 kcal mol⁻¹) are solvated more easily than Cd^{2+} and Mn^{2+} , which have smaller energies of hydration ($\Delta G_{\text{H}} = -420$ to -440 kcal mol⁻¹). The former cations are thus adsorbed as hydrated cations, making them labile (i.e. they can easily desorb, but cannot be easily incorporated into the lattice). Cd^{2+} and Mn^{2+} , in contrast, are dehydrated when adsorbed, promoting subsequent incorporation into the crystalline lattice and at the same time inhibiting desorption (because the cations must be re-hydrated). This is a case of *surface mineralisation*, which is equivalent, in the terminology of sorption, to the concept of *irreversible adsorption* (see page 6 in this report).

In order to integrate the dehydrated cations into the crystal lattice, additional steps are required. In the absence of recrystallisation or precipitation of new calcite (a surface in equilibrium with the solution), the adsorbed trace metal must first displace a calcium ion from the top monolayer of the calcite crystal and subsequently penetrate into the bulk lattice. This last step may occur by volume diffusion, whereby the trace cation moves along dislocations and other defects.

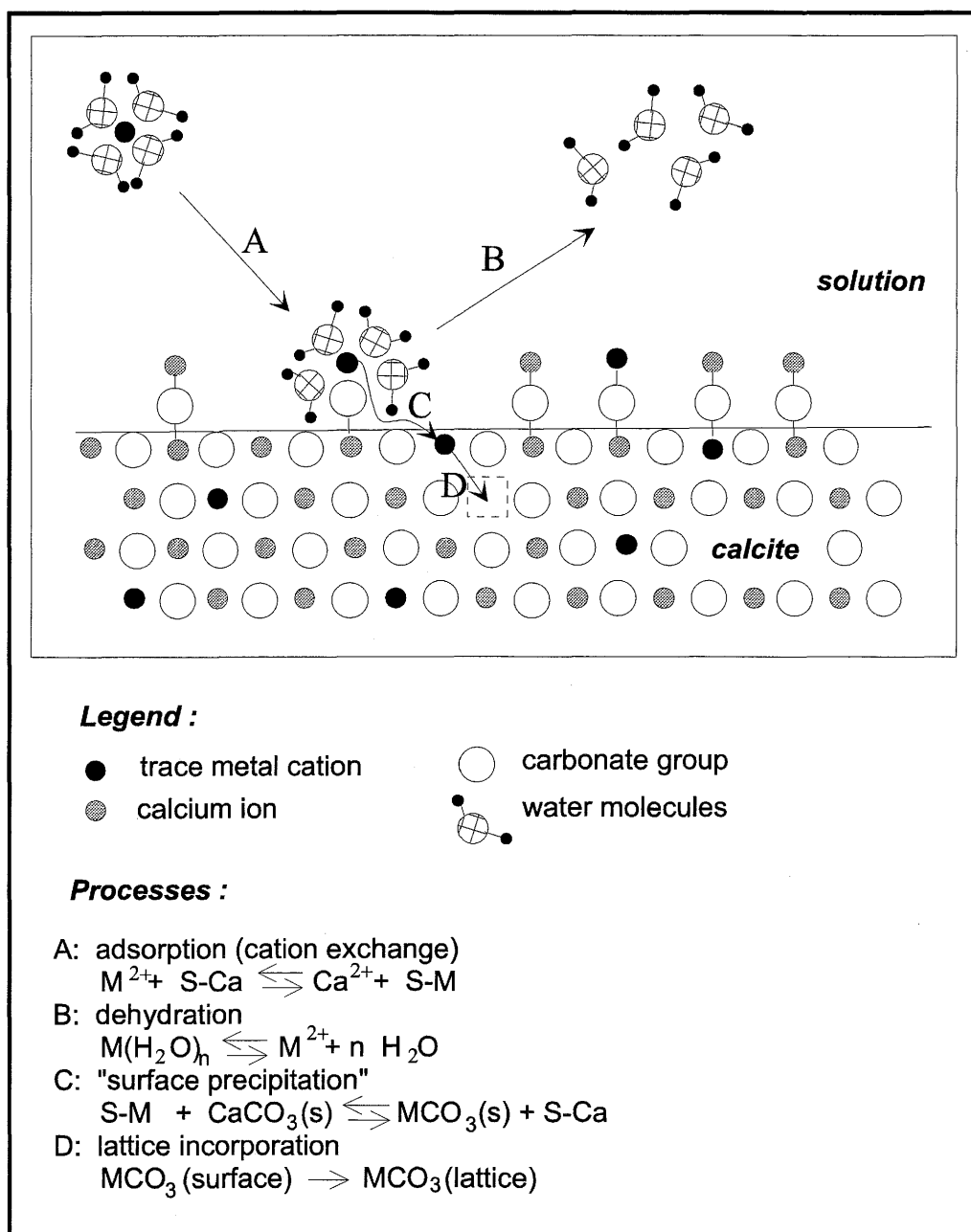


Figure 5-1: Atomistic model of solid solution formation in calcite. The whole process is separated in individual steps (A to D) which, however, are not strictly sequential. For instance, dehydration and surface precipitation (steps B and C) should be understood as a single dynamic process. For the sake of simplicity, step A was not represented completely (the displacement of the calcium ion, required by the ion exchange reaction, is not illustrated).

On the base of the information synthesised above, it is possible to devise a conceptual model for the overall process of trace metal coprecipitation with carbonate minerals, which could serve as a starting point for future interpretations. The model is illustrated in Figure 5-1 and can be subdivided in the individual steps:

- A. Adsorption through cation exchange with Ca^{2+} .
- B. Dehydration of the trace cation.
- C. Displacement of Ca^{2+} from the top monolayer and incorporation in the surface lattice ("surface precipitation").
- D. Incorporation into the lattice (by volume diffusion or other mechanism).

It must be emphasised that the model presented here is highly speculative and subject to considerable restrictions. It applies specifically to coprecipitation reactions in solutions saturated or slightly oversaturated with calcite, where sorption equilibria are maintained at all times. It does not describe entirely situations in which kinetic factors play a major role.

6. Trace element geochemistry of selected radionuclides

6.1 Preliminary notes

The previous chapters focused on the uptake of trace elements by carbonate minerals. Although carbonates are certainly important in repository environments, they are by no means the sole alteration products expected to form during the alteration of repository materials. For instance, the interaction of ground water with glass, bentonite and steel will produce a variety of secondary silicates, mainly zeolites and clay minerals, and Fe oxy-hydroxides in the HLW repository (GRAUER 1988). In the L/ILW repository, CSH-phases will be formed during the degradation of cement (TITS 1994, NEALL 1994). Considering the large variety of possible secondary solids, it would be desirable to take a "global picture" of the process of radionuclide coprecipitation. Unfortunately, no coprecipitation data exist for most relevant solid phases; it will therefore be possible to take only a very unfocussed, partial picture, limited to a few selected elements.

The elements treated in this preliminary review are Ni and Cs. These elements are radiologically relevant and their geochemistry is relatively well-understood. In addition, the coprecipitation of nickel and caesium is a particularly important issue considering that no solubility limits for these fission products were specified in the Kristallin-I safety analysis (NAGRA 1994a). Taking into account the coprecipitation of these elements could help in defining solubility limits for future safety analyses.

6.2 Nickel

It is a well documented geochemical fact that Ni has a strong tendency to concentrate in Mg- minerals. This trend begins during magmatic differentiation: the first rocks to crystallise in the course of a magmatic cycle are those richest in Mg (the so-called ultramafic rocks). Nickel is found to be strongly enriched in such rocks (KRAUSKOPF 1979, Table 20-5) and in their alteration products. The geochemical affinity of Ni for Mg is readily explained by their similar atomic properties. Both elements have electronic configurations which stabilise the (+II) oxidation state and which lead to similar ionic radii (Ni²⁺ : 0.69 Å, Mg²⁺ : 0.72 Å). It is thus not surprising that Ni²⁺ substitutes extensively for Mg²⁺ in a large number of minerals.

A geologic example of the Mg-Ni affinity is provided by the mineral associations in *nickel laterites*. Laterites are sedimentary rocks resulting from extreme weathering of well-drained silicic rocks in warm and humid flatlands. Under such conditions, the mobile elements in the soil are dissolved and washed out by tropical rains, leaving a residue in which the less soluble (immobile) components are concentrated. Typically, the residue is formed by Fe(III) and Al-minerals. If the parent formation happens to be an ultramafic rock, the end-product of weathering is a nickel laterite, a condensed horizon of ferric (hydrous) oxides containing a variety of Mg-Ni minerals, which may

be exploited as a nickel ore (see e.g. ROSEMBERG 1984, BESSET 1978, KUHNEL et al. 1978, MAKSIMOVIC 1978).

Before alteration starts, ultramafic rocks are enriched in Ni to a level comparable to that of Swiss vitrified nuclear waste (0.3 to 0.7 weight %) ²¹. The nickel in the laterite ore may reach a concentration of 2-3 weight % and is fixed in various minerals (see Table 6-1): Mg/Ni-clays like *chrysopras* and *nepouite*, the hydrated carbonate *takovite* (a member of the pyroaurite mineral group), the ferric hydrous oxide *goethite* and mixed amorphous metal oxides known with the generic name of *asbolite*. It is important to note that large amounts of Ni, far exceeding the levels of trace elements, may be incorporated in such minerals. Such phases may thus limit the solution concentration of Ni in Mg-rich environments.

The information derived from the mineral associations found in Ni-laterites indicates that during the alteration of repository materials nickel will be preferentially retained in secondary magnesian minerals. Coprecipitation of Ni with magnesium silicates or carbonates may control the solubility of this element in the near-field pore water. This process may be particularly important during the degradation of borosilicate glasses containing a significant percentage of Mg, like the British BNFL glasses. X-ray diffraction and microprobe analyses on samples of corroded BNFL glass revealed the formation of a secondary Mg-clay (*hectorite*, with the incomplete formula $\text{Mg}_{5.33}\text{Li}_{0.67}\text{Si}_8\text{O}_{20}(\text{OH})_4$, see ZWICKY et al. 1989).

Whereas nickel follows magnesium in silicate and other oxide phases, the two elements behave in a totally different way with respect to sulphide. Ni^{2+} forms a variety of sulphide minerals, which may in some circumstances concentrate to make massive ore bodies (economically much more important than the laterites). On the other hand, Mg^{2+} does not form sulphide minerals at all.

This discrepancy is consistent with the classical geochemical classification of metals into *siderophile* (those concentrated in the core of the earth), *chalcophile* (those typical of sulphide ores) and *lithophile* (those generally occurring in oxygen-bearing minerals). Magnesium is a lithophile element, while nickel has a chalcophilic character (although it is classified as siderophile). This classification, originally made by GOLDSCHMIDT (1954) is not entirely satisfactory, since it relies on phenomenological observations rather than on sound chemical arguments. A more satisfactory explanation for the incongruent behaviour of Ni and Mg with respect to sulphide is provided by the distinction between "hard" and "soft" metals (see e.g. STUMM & MORGAN 1996). Mg^{2+} is a typical hard cation, which means that it has a rigid, non-deformable electronic shell. Such cations tend to form electrostatic bonds, leading to the formation of strong complexes with oxygen-bearing ligands. In contrast, Ni^{2+} is a "soft" cation, i.e. one with easily deformable electronic shell which tends to form covalent bonds. Soft metals ions typically form stable complexes with sulphide ligands, which obviously facilitates the formation of solid sulphides.

²¹ There are, however, substantial differences between lateritisation and glass alteration. Lateritisation is a very selective process, leading in the final stages to a strong depletion of silica, which does not occur during glass alteration. In addition, the chemical compositions of the starting materials differ. Ultramafic rocks are much more Mg- and Fe-rich than borosilicate glasses, although their total silica content is very similar.

Table 6-1 : Ni concentrations in lateritic minerals from the Lokris ores (Greece), taken from ROSEMBERG (1984). *N* is the number of samples analysed. Formulas are given for ideal end-members except for nepouite, the stoichiometry of which refers to a specific analysis (p. 28 in NEWMAN 1987). The high concentrations found in quartz suggest that part of the nickel in this mineral may be present as inclusions of discrete Ni-rich phases.

Mineral	formula	Ni concentration (weight %)			N
		Minimum	Maximum	Mean	
hematite	Fe ₂ O ₃	0.1	0.7	0.4	6
goethite	FeOOH	0.6	1.3	1.2	5
quartz	SiO ₂	0.01	0.4	0.1	6
chlorite	Mg ₅ Al[Al Si ₃ O ₁₀](OH) ₈	0.1	3.4	2.2	4
chrysopras	(Mg,Ni) ₃ [Si ₄ O ₁₀](OH) ₂	-	-	3.8	1
nepouite	Ni _{4.03} Mg _{0.69} Fe ³⁺ _{0.12} Al _{0.06} Si ₄ (O,OH) ₁₈	-	-	25	1
takovite	Ni ₆ Al ₂ (OH) ₁₆ (CO ₃)·4H ₂ O	-	-	16.2	1
calcite	CaCO ₃	0.02	0.05	0.03	4

In spite of the large variety of Ni-sulphides existing in nature, it is unlikely that any of these phases would form in the HLW repository environment. First, Ni and sulphide concentrations in the waste materials and in the pore water may not be sufficiently large to cause precipitation of pure Ni-sulphides. Furthermore, most primary Ni-sulphides found in nickel ores (e.g. pentlandite, (Ni,Fe)₉S₈) are formed at high temperatures and are unstable at low temperatures²² (STANTON 1972). More likely, Ni radionuclides released from vitrified nuclear waste would coprecipitate with common low-temperature iron sulphides (like pyrite, FeS₂), if the sulphide concentration in the aqueous phase is sufficiently high to promote their formation.

The situation will be quite different in the planned L/ILW repository at Wellenberg, where large amounts (tons) of stable nickel will be present in addition to a large radiological inventory (~9100 moles ⁵⁹Ni and ⁶³Ni). Furthermore, important sulphide concentrations have been detected in the ground water (DEGUELDRE et al. 1997).

²² Primary nickel ore sulphides are progressively degraded to another Ni-sulphide (violarite). In the oxidation zone violarite becomes unstable and is replaced by Ni-carbonates like gaspeite (Ni,Fe)CO₃ and reevesite (Ni₆Fe₂CO₃(OH)₁₆·4H₂O). See KEELE & NICKEL (1974) for details.

According to the literature survey of THOENEN (1997), there is indisputable evidence that pure Ni sulphides can precipitate in low temperature aquatic environments. Primary millerite (NiS) was found, in conjunction with bacterial activity, in lacustrine sediments contaminated with metals discharged from mine tailing ponds at Sudbury (Ontario, Canada). To which extent the formation of pure Ni-sulphides could be a solubility limiting process is, however, still unclear.

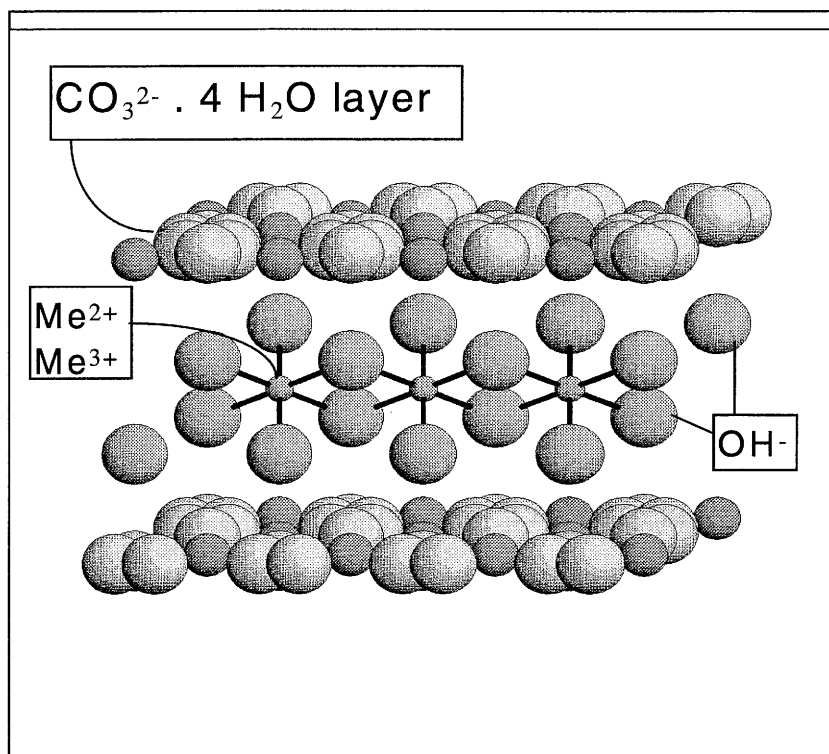


Figure 6-1: Structure of pyroaurite minerals. These hydrous carbonates consist of a “sandwich-like” succession of carbonate-water and metal-hydroxide layers. Several di- and trivalent metals may form continuous solid solutions: Mg²⁺, Ni²⁺, Fe²⁺ and Al³⁺, Fe³⁺. Pyroaurite minerals are common in carbonate-rich soils; they could represent effective traps for Ni radionuclides escaping from radioactive waste repositories.

Ni can also coprecipitate in low temperature environments with common iron sulphides like amorphous FeS, mackinawite (FeS) and pyrite (FeS₂) (see THOENEN 1997). Isomorphous substitution of Fe²⁺ by Ni²⁺ should be favoured by the similar radii of these two metal ions. Although it is presently not possible to specify the extent of isomorphous replacement of Ni²⁺ for Fe²⁺ in pyrite with the help of laboratory data, an indicative partition coefficient for Ni in pyrite has been determined using Ni concentrations determined in pyrites of sedimentary origin (KERSABIEC & ROGER 1977).

Table 6-2: List of natural solids with which Ni could coprecipitate in low temperature aqueous solutions. Only minerals which may contain Ni in large concentrations are specified, while those in which Ni is incorporated only as trace element are omitted.

Mineral name	Ideal formula	Mineral group	Ref.
nepouite-lizardite pecoraite-chrysotile	$(\text{Ni}, \text{Mg})_6 [\text{Si}_4\text{O}_{10}] (\text{OH})_8$	sheet silicate (serpentine)	(1)
brindleyite-berthierine	$(\text{Ni}, \text{Fe}, \text{Mg})_4 (\text{Al}, \text{Fe}^{3+})_{1.8} [\text{Al}_{1.4}\text{Si}_{2.6}] \text{O}_{10}(\text{OH})_8$	sheet silicate (serpentine)	(1),(3)
pimelite-kerolite	$(\text{Ni}, \text{Mg})_3 [\text{Si}_4\text{O}_{10}](\text{OH})_{2 \cdot n}\text{H}_2\text{O}$	sheet silicate (talc)	(1)
nimite	$(\text{Ni}, \text{Mg}, \text{Fe})_4 (\text{Al}, \text{Fe}^{3+})_{1.67} [\text{AlSi}_3\text{O}_{10}](\text{OH})_8$	sheet silicate (chlorite)	(1)
falcondoite	$(\text{Ni}, \text{Mg})_4 [\text{Si}_6\text{O}_{15}](\text{OH})_{2 \cdot n}\text{H}_2\text{O}$	sheet silicate (sepiolite)	(3)
Ni-nontronite	$(\text{M}^+)_{x+y} \cdot (\text{Fe}^{3+}_{4-y} (\text{Mg}, \text{Ni})_y) [\text{Si}_{8-x}\text{Al}_x\text{O}_{20}] (\text{OH})_4$	sheet silicate (smectite)	(3)
gaspeite	$(\text{Ni}, \text{Fe}, \text{Mg})\text{CO}_3$	carbonate	(4)
reevesite	$\text{Ni}_6\text{Fe}^{3+}_2(\text{OH})_{16}\text{CO}_3 \cdot 4\text{H}_2\text{O}$	carbonate (pyroaurite)	(3),(5)
takovite	$\text{Ni}_6\text{Al}_2(\text{OH})_{16}\text{CO}_3 \cdot 4\text{H}_2\text{O}$	carbonate (pyroaurite)	(2),(3)
carboydite	$\text{Ni}_{6.5}\text{Al}_{4.5}\text{Cu}_{0.4}(\text{OH})_{21.7}(\text{SO}_4)_{2.3}(\text{CO}_3)_{0.5} \cdot 3.7\text{H}_2\text{O}$	carbonate (pyroaurite)	(3)
cassidyite	$\text{Ca}_2(\text{Ni}, \text{Mg})(\text{PO}_4)_2 \cdot 2\text{H}_2\text{O}$	phosphate	(5)

References: (1) NEWMAN (1987), (2) BISH (1978), (3) BRINDLEY (1978), (4) KUHNEL et al. (1978), (5) WHITE et al. (1967).

These data indicate Ni concentrations ranging from 5 to 290 ppm for pyrites disseminated in various sedimentary rocks. Assuming average ground water concentrations of 2×10^{-7} and 7×10^{-5} for Ni and Fe(II), respectively²³, partition coefficients between 0.003 and 0.2 would result. Such partition coefficients are surprisingly small but are close to those determined experimentally for Ni in the iron carbonate siderite ($D = 0.07 - 0.2$, see Table 5-3) and for Mn in mackinawite ($D = 0.002 - 0.005$, see THOENEN 1997). Such low coefficients, if confirmed by experimental studies, would imply that only abundant pyrite precipitation could withdraw large amounts of Ni from solution.

To summarise, there are at least 4 classes of solids with which Ni could coprecipitate in a repository environment: 1) Mg silicates, particularly clay minerals, 2) Fe oxyhydroxides, 3) Fe, Mg carbonates and hydrous carbonates, particularly members of the pyroaurite group, with the general formula $(\text{Ni,Fe}^{2+},\text{Mg})_6 (\text{Al,Fe}^{3+})_2 (\text{OH})_{16} \text{CO}_3 \cdot 4\text{H}_2\text{O}$, and 4) Fe sulphides.

A list of low temperature solids with which Ni forms solid solutions is given in Table 6-2. Figure 6-1 shows the generic crystal structure of pyroaurite minerals.

6.3 Caesium

With a ionic radius of 1.67 Å, Cs^+ is the largest alkali cation and thus will hardly fit into the lattice sites of common alteration minerals. For this reason, Cs rarely forms pure minerals and it is found in solids almost exclusively as a dispersed trace element. It is enriched in evaporitic potassium salt deposits, from which it is extracted for industrial use, and in potassium clay minerals. Average concentrations for Cs are 200 ppm in carnallite ($\text{KCl} \cdot \text{MgCl}_2 \cdot 6\text{H}_2\text{O}$) deposits and 1000 ppm in clay sediments (PIETSCH, ed. 1938).

The formation of potassium salts and clays, however, is not possible in the Swiss radioactive waste repositories. Potassium salts are far too soluble and potassium clays are not stable under the conditions expected in the Swiss repositories, since temperatures over 80°C and high K concentrations in the ground water are required for illitisation²⁴ (GRAUER 1988). Cs, on the other hand, is also known to concentrate remarkably in *altered*, silica-rich volcanic glasses, where average concentrations reach about 250 ppm (KREMENETSKIY et al. 1981). This is consistent with the observed tendency of Cs to be retained during the alteration of nuclear waste glasses. For instance, during leaching experiments performed on samples of the British BNFL glass, Cs was found to be retained in the corrosion products almost quantitatively (CURTI 1991, fig.12). Thus, Cs seems to coprecipitate with specific glass alteration products, which ought to be identified.

²³ These concentrations are the averages of a large number of measurements made on samples of Swiss ground waters (NAGRA 1989).

²⁴ Illitisation is the process by which (Na,Ca)-smectite clays are transformed into K-rich clays called illites. Although caesium may be incorporated in the interlayer sites of smectite clays, such uptake is reversible (i.e. it would be due to a ion-exchange reaction, not to a coprecipitation process).

The enrichment of Cs in altered volcanic glasses may be explained in two ways. First, it can be assumed that the amorphous products formed through the alteration process may act as an ideal trap for the large caesium ions, since non-crystalline solids typically form large microstructural cavities where ions as large as Cs⁺ can be accommodated. Alternatively, caesium may concentrate in secondary crystalline phases with suitably large structural sites. Good candidates are *zeolites*²⁵, a class of framework silicates fulfilling both the requisites of being a common alteration product of silica glasses and of possessing large structural sites. Two investigations, dealing with the uptake of Cs by hydrothermally altered volcanic glasses in active geothermal fields, provide important information on this subject. KEITH et al. (1983) showed that hydrothermally altered rhyolites²⁶ at Yellowstone are enriched in Cs and that the main Cs carrier is the zeolite mineral *analcime* (NaAlSi₂O₆ · H₂O). Analcime concentrates were found to contain 1750-4500 ppm Cs, while total rock analyses consistently yielded concentrations by 10-100 times smaller. Similar results were obtained by GOGUEL (1983), who identified *wairakite*, the Ca-analogue of analcime, to be the main Cs carrier (240-4500 ppm). In contrast, associated potassium minerals like *adularia* (KAlSi₃O₈) and illite carried much less Cs (~10 ppm and ~40 ppm, respectively).

The incorporation of Cs⁺ during the precipitation of analcime and wairakite is not a simple isomorphous substitution like the incorporation of divalent cations in calcite. In analcime, the Cs⁺ cations are incorporated in sites normally occupied by water molecules, which fill structural channels typical of zeolite structures. In order to maintain electrical neutrality, for each substituted Cs⁺ ion a site normally occupied by Na⁺ must be left vacant (CERNY 1974). It is this coupled mechanism which facilitates the incorporation of Cs⁺ in this mineral.

Table 6-2: Estimated partition coefficients for the incorporation of Cs in analcime formed in the geothermal field of Yellowstone (USA) based on the data given by KEITH et al. (1983). Surface concentrations are given as mole fractions, species in solution are expressed in molar concentration units (see Equation 3-11).

	lower bound	upper bound
{Cs}	2.9×10^{-3}	7.8×10^{-3}
[Cs]	5.6×10^{-6}	3.8×10^{-7}
{Na}	0.997	0.992
[Na]	9.1×10^{-4}	1.8×10^{-2}
D	0.5	370

²⁵ Zeolites are framework silicates characterised by regular arrays of openings, which make them useful as reaction catalysts and ion exchangers.

²⁶ Rhyolites are silica-rich glassy volcanic rocks with the same bulk composition as granites.

The size of the channels in analcime and wairakite is such that the Cs^+ ions and water molecules just fit their cross-sectional dimensions ($\sim 2.2 \text{ \AA}$, see BARRER 1978). This means that Cs^+ ions are held tightly, once they become imprisoned in the lattice, and cannot be exchanged further²⁷ (smaller ions, in contrast, are free to move into or out of the channels and can thus undergo ion exchange). Thus, the uptake of Cs^+ by analcime can be regarded as a true coprecipitation process. Since the dimension of the channels is variable in the different zeolites, not every zeolite will be capable of immobilising Cs^+ like analcime. The channels of other common zeolites, like chabazite and clinoptilolite, are indeed too large, so that these minerals will act only as exchangers for Cs^+ .

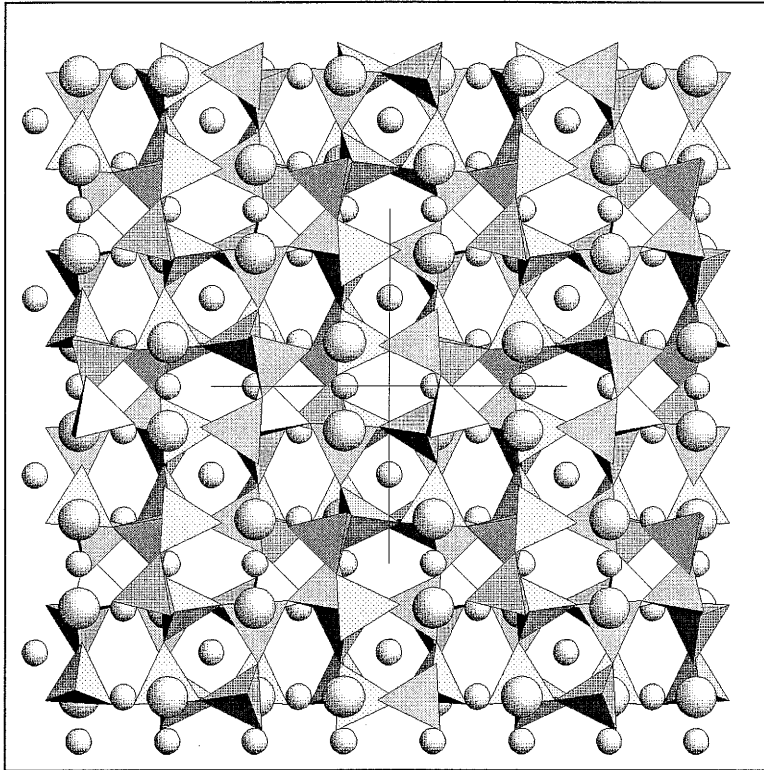


Figure 6-2: The structure of analcime is characterised by a 3-dimensional network of interconnected $(\text{Si,Al})\text{O}_4$ -tetrahedra with “channels” occupied by Na^+ (small spheres) and water molecules (large spheres). Water molecules can be extensively replaced by Cs^+ ions, in which case a corresponding number of Na^+ sites must be left vacant in order to maintain electroneutrality.

²⁷ Although the channel dimensions exceed the ionic size of Cs^+ , its mobility in the channels is strongly limited by electrostatic effects (see DEER et al. 1992, p.522).

The data of KEITH et al. (1983) are detailed enough to allow a crude estimation of the partition coefficient for Cs coprecipitation with analcime at Yellowstone. The data used and the estimated partition coefficients are summarised in Table 6-2. Using the homogeneous distribution law, partition coefficients ranging from 0.5 to 370 were determined.

A Cs-isomorph of analcime exists, the mineral pollucite, with the ideal formula $\text{CsAlSi}_2\text{O}_6$ (CERNY 1974). Thus, one has to deal with the possibility that the Cs solubility in the near-field of the HLW repository may be limited by saturation equilibrium with this mineral. Geochemical evidence suggests, however, that this mineral will not form under repository conditions. Firstly, pollucite is never found pure in nature (approximately 20-50 mole % Na are always present). Secondly, it apparently forms at high temperatures, since it is commonly found as a primary mineral in alkali-rich pegmatites (volcanic rocks crystallising at temperatures far exceeding 100 °C). Finally, pollucite is unstable at earth surface conditions, as it is commonly replaced by a mixture of clay minerals, carbonates and quartz (CERNY 1978). Consequently, pollucite should not form in connection with the release of radioactive Cs from the Swiss HLW repository and the solubility of this radioelement should be rather modelled considering coprecipitation with analcime, which is likely to form during the aqueous corrosion of vitrified waste.

7. Radionuclide coprecipitation in the LLW / ILW repository

7.1 Preliminary remarks

One of the main objectives of this report is to answer the question, whether radionuclide coprecipitation will play a major role during chemical interactions in the near-field of a radioactive waste repository in Switzerland. Given that coprecipitation contributes positively to radiological safety, will this contribution be significant or negligibly small, so that it can be ignored in safety assessment models? How can this contribution be quantified? How do the effects of coprecipitation and sorption compare with each other? These are the points to be clarified in the present chapter.

At the present stage, it is surely premature to develop detailed coprecipitation models specifically designed for integration in a safety assessment. Since only a crude estimation of the role of coprecipitation is required, a *simple*, though *site-specific*, model will be developed to estimate the amounts of radionuclides which could be immobilised through coprecipitation during cement degradation in the L/ILW repository planned at the Wellenberg site. The model focuses on the uptake of safety-relevant radionuclides in secondary calcite, which will precipitate in large amounts due to the reaction of alkaline, Ca-rich cement pore waters with bicarbonate-rich ground waters (see NEALL 1994, NEALL 1996).

Although other equally important radionuclide coprecipitation reactions may take place during cement degradation (e.g. incorporation in ettringite and CSH-phases, see GOUGAR et al. 1996), the total lack of coprecipitation data for these minerals makes any attempt at quantitative modelling a purely academic exercise. The same statement applies to coprecipitation processes taking place during the alteration of vitrified high-level waste. In this case, the phases formed during alteration will be mainly zeolites and clay minerals, for which partition coefficients are not available²⁸.

7.2 Calcite formation during cement degradation

The chemical evolution of cement pore waters in the L/ILW repository has been summarised in NAGRA (1994b) and, in more detail, by NEALL (1996). Accordingly, the initial stage of degradation will be characterised by a very high pH, due to the dissolution of alkali hydroxides, and by relatively small Ca concentrations (~ 1 mM). With increasing supply of ground water, a less alkaline, more Ca-rich solution with intermediate composition and pH will develop. The pH will be initially fixed at 12.5 by portlandite dissolution and will then fall to ~10.5 after this mineral has been consumed.

²⁸ A notable and important exception is the case of Cs in analcime, for which the partition coefficient was estimated in chapter 6. It is thus in principle possible to estimate the retention of Cs due to analcime precipitation, if the amounts of analcime formed during the alteration process can be inferred.

This second type of fluid is thought to be longer-lived than the high pH fluid. Finally, the degradation process will end up with a mildly alkaline fluid (pH ~ 8 - 9).

Abundant calcite precipitation is expected to occur when bicarbonate-rich ground water reacts with the Ca-rich intermediate cement pore fluid. The exact location and extent of the calcite precipitation zone are not predictable, as these will depend on direction and magnitude of fluid advection. However, coupled transport-reaction calculations (Pfungsten, oral communication) and geochemical considerations (NEALL 1996) indicate that calcite will form either in the peripheral zones of the repository or in the adjacent host-rock, so that calcite precipitation can be considered essentially an "in situ" process.

Large amounts of carbonic acid could be produced by the degradation of organic substances in the waste. In this case, calcite would precipitate in situ, since the source of carbonate is in the waste. In summary, the amounts of carbonate precipitated will undoubtedly be very large. According to NEALL (1994), up to 80% of the Ca dissolved from the cement could ultimately precipitate as calcite. This figure corresponds to about 10^9 moles or $\sim 4 \times 10^7$ kg Ca for the whole repository, which is potentially a formidable sink for coprecipitating radionuclides.

7.3 Extrapolation to safety-relevant radionuclides

With few exceptions (Sr, U, Se) there are no laboratory data on the coprecipitation of radionuclides with calcite. The correlations presented in chapter 4 were set up with the idea that they would serve as a guide to estimate the partition coefficients of radionuclides, for which no support from experiments is available. Based on the data analysis presented in chapter 4, an attempt is made to estimate the partition coefficients of the safety-relevant radioelements²⁹ in calcite. These estimates will serve for preliminary model calculations to assess the potential extent of radionuclide coprecipitation following the formation of secondary calcite in the L/ILW repository. The purpose of these calculations is to distinguish radionuclides for which calcite formation is a promising solubility-limiting mechanism from those for which coprecipitation will not significantly affect solution concentration.

7.3.1 Americium, curium

As noted earlier, the most promising guideline for such estimations is the correlation between measured partition coefficients of the trace metals and the solubility of their pure, anhydrous carbonates, presented in Figure 4-6. Unfortunately, the use of this correlation is limited either by the lack of measured solubility products for the solids of interest, or by the fact that some nuclides undergo strong hydrolysis (e.g. Th, Zr),

²⁹ The radioelements for which partition coefficients are estimated here are those considered to be safety-relevant for the L/ILW repository (NAGRA 1994b). The estimations will be necessarily rough due to the inherent uncertainties affecting the analysed data, which derive from kinetic and competition effects (see chapter 4).

which prevents the formation of their carbonates. The correlation can be used, however, to estimate partition coefficients for Am(III), Ni(II) and, indirectly, for Cm(III) in calcite.

For the anhydrous americium carbonate $\text{Am}_3(\text{CO}_3)_2$, a solubility product of $10^{-33.4 \pm 2.2}$ is given in SILVA et al. (1995). This is an extrapolation to zero ionic strength derived from the unweighted average of four independent solubility determinations (three of which, however, are from the same laboratory). The uncertainty assigned to this solubility product arises from the large discrepancy between the values provided by the two laboratories and may be reduced if there are good arguments to decide which one of the two sets of constants is more reliable. The constant determined by ROBOUCH (1989) stems from solubility measurements in solutions of high ionic strength ($I = 3 \text{ M}$), which makes the extrapolation to zero ionic strength questionable. In contrast, the solubility products determined by MEINRATH & KIM (1991a); MEINRATH & KIM (1991b) and RUNDE et al. (1992) stem from experiments conducted in more dilute solutions ($I = 0.1$ to 0.3 M) over a wide pH range (from 6 to 9) and should thus be preferred. The average from these investigations yields a more precise value of the solubility product ($K_{\text{S}0} = 10^{-33.1 \pm 0.4}$), based on which partition coefficients between 200 and 1000 are extrapolated for the coprecipitation of Am with calcite³⁰. These values place americium in the region of Figure 4-6 populated by the partition coefficients of trivalent rare earths, as might be expected independently considering the strong similarity in chemical properties of trivalent actinides and trivalent rare earths.

The solubility of Cm(III) carbonates has not yet been measured. However, on the base of its strong chemical affinity with Am, one can argue that Cm will behave in a similar way to Am during coprecipitation reactions. Therefore partition coefficients between 200 and 1000 are assumed to be good estimates also for curium.

7.3.2 Nickel

The estimation of a partition coefficient for nickel is more problematic. As pointed out by GRAUER (1994), many solubility products for NiCO_3 reported in the literature must be wrong by orders of magnitude, since they differ too largely from the solubility products of carbonates of other transition metals. According to Grauer, the unique reliable determination of the solubility product of NiCO_3 is that of REITERER (1980). Since it was measured at temperatures between 50 and 90°C at $I = 1 \text{ M}$, the solubility product of this compound at zero ionic strength and room temperature can only be estimated by extrapolation. GRAUER 1994 recommends a value of $10^{-11.2 \pm 0.3}$ from which, with the help of the procedure used to construct Figure 4-6, partition coefficients ranging from 0.8 to 6 are estimated for the coprecipitation of nickel with calcite. In Figure 4-6, the partition coefficient of Ni would thus fall in the field populated by other transition metals.

³⁰ The extrapolated values were obtained from straight line equations derived through linear regression analyses of the form: $\log \lambda = m \log (\text{Me}^{2+}) + b$, where (Me^{2+}) is the free metal ion activity in a hypothetical solution at equilibrium with the pure metal carbonate and with a free carbonate activity fixed at 10^{-5} (on the molality scale). Two equations were used, corresponding to the best fit ($m = -0.784$, $b = -4.10$, not shown in Figure 4-6) and to a "worst case" ($m = -0.843$, $b = -5.19$, the "conservative regression line" in Figure 4-6).

7.3.3 Caesium

Cs forms soluble carbonates, similarly to Na and K. Because sodium and potassium partition coefficients are found to be very low (less than 10^{-3}) and because the ionic radius of Cs^+ greatly exceeds that of Ca^{2+} , coprecipitation of caesium with calcite-type carbonates will certainly be insignificant. Cs will therefore not be immobilised by carbonate precipitation; other phases, notably analcime, must be considered as coprecipitation traps for these elements (see chapter 6).

7.3.4 Strontium, radium

Strontium and radium are both alkaline-earth elements and should thus behave in a way similar to calcium. However, divalent strontium and radium ions have ionic radii greatly exceeding the size of Ca^{2+} , a fact which severely limits the possible extent of isomorphous substitution of these elements in calcite. Partition coefficients of Sr^{2+} in calcite have been measured repeatedly under a variety of conditions and are therefore well-known. They were indeed found to be small and fall in a restricted range between 0.04 and 0.4. These values can be directly used for safety assessment purposes.

For reasons of chemical affinity, Ra^{2+} is assumed to have partition coefficients close to those of Sr^{2+} and particularly of Ba^{2+} . This assumption is substantiated by the similar value of the partition coefficients measured for Ba^{2+} and Sr^{2+} in calcite. PINGITORE & EASTMAN (1984) determined a partition coefficient of 0.06 for Ba^{2+} , which falls within the range of partition coefficients determined for Sr^{2+} (0.04- 0.4). Therefore the same range of partition coefficients determined for Sr^{2+} is assumed for Ra^{2+} in calcite (0.04- 0.4).

7.3.5 Selenium

Selenium has a strong chemical affinity with sulphur and, like this element, can occur in several oxidation states (STANTON 1972, BERNER 1995). Stable aqueous species are Se^{2-} (selenide), SeO_3^{2-} (selenite) and SeO_4^{2-} (selenate), each characterised by specific chemical properties. The incorporation of selenium in minerals will therefore depend on its oxidation state. Under reducing conditions selenide will be the stable form. Due to its anionic nature, selenide will tend to replace the carbonate groups in calcite rather than calcium ions. Unfortunately, no experimental data exist which may help in estimating a partition coefficient for selenide in calcite.

If selenium enters the calcite structure as selenite or selenate, it would also substitute for the carbonate groups, as a result of the negative charge of these oxo-anions. The three-dimensional geometry of selenite and selenate, however, makes them unfavourable for substitution for the planar CO_3^{2-} groups (selenate ions have a tetrahedral geometry, while selenite ions are pyramidal with a O-Se-O angle of approximately 100° , see HAWTHORNE et al. 1987). REEDER et al. (1994) carried out a surface analysis investigation on calcites coprecipitated with selenate. They were able

to show with the help of XAFS³¹ analyses that selenium is incorporated as selenate ion in the carbonate sites and not as a free Se⁶⁺ ion. The amount of coprecipitated Se is very small and from their data very small partition coefficients, ranging from 6×10^{-6} to 5×10^{-5} , were calculated. These low values are consistent with the partition coefficients measured for sulphate coprecipitation with calcite, which range from $\sim 10^{-5}$ to 10^{-3} (BUSENBERG & PLUMMER 1985)³².

To summarise, it can be concluded that incorporation of selenite and selenate in calcite and other carbonates will be negligible and that the extent of selenide incorporation into calcite is not known. Considering the strong geochemical affinity between selenium and sulphur, however, it may be assumed that selenate would coprecipitate effectively with secondary sulphates formed during cement degradation and that selenide will be easily incorporated in sulphides, as indicated by the high Se concentrations (up to 1280 ppm) analysed in sedimentary pyrites from Spain (KERSABIEC & ROGER 1977).

7.3.6 Zirconium, tin, molybdenum, technetium

It is presently not possible to estimate partition coefficients for these radioelements in calcite. Nevertheless, their chemical properties suggest that they do not coprecipitate significantly with calcite.

Zr, Sn, Mo and Tc are characterised by oxidation states of +IV or higher and small cationic radii (less than 0.72 Å). Consequently, they have a strong tendency to hydrolyse, a property which hinders the dehydration of the dissolved metal prior to its incorporation in the calcite lattice (see chapter 5). In addition, Mo and Tc easily form stable oxo-anions, which are difficult to incorporate into the lattice of calcite considering their very large dimensions. Finally, with the exception of Zr, no carbonate compounds or complexes are known for these elements, suggesting that there is no chemical affinity between these metals and carbonate.

7.3.7 Palladium

Under reducing conditions only metallic palladium, which is extremely insoluble, will be stable. Above $\sim +200\text{mV}$ (at pH ~ 9), Pd⁰ is oxidised to Pd²⁺ and readily hydrolysed to Pd(OH)₂⁰. Pd²⁺ may also form strong chloride complexes, but these are insignificant in diluted solutions above a pH of ~ 3 (BERNER 1995).

³¹ With XAFS (X-ray Absorption Fine Structure), the absorption of X-rays in a particular region beyond a characteristic elemental absorption peak is analysed. This region is defined by energies 50 to 1000 eV higher than the characteristic absorption peak. The absorption structure of this region is sensitive to both *distance* and *arrangement* of the nearest neighbours, so that this method is particularly suited to determine the coordination of ions in solids.

³² Sulphate is chemically analogous to selenate and also has a tetrahedral geometry.

With a ionic radius of 0.86 Å, Pd²⁺ could, in principle, substitute significantly for Ca²⁺ in the calcite lattice. However, geochemical indications supporting this assumption are completely missing. No chemical or mineralogical textbook mentions the existence of any Pd-carbonate compound (neither complexes nor solids), suggesting a fundamental chemical incompatibility between Pd and carbonate. On the other hand, the lack of carbonate compounds in nature and in the laboratory may be simply a consequence of the low solubility of Pd oxides and sulphides (BERNER 1995), which would prevent Pd from reaching a concentration sufficient for the formation of carbonates. Therefore it is not possible to predict reliably the value of partition coefficients for Pd²⁺ in calcite.

¹¹⁷Pd is present in relatively high concentrations in vitrified HLW waste. Due to its large inventory (~17 moles per waste canister, see NAGRA 1994a) and considering the reducing conditions prevailing in the Swiss HLW repository near-field, Pd could precipitate as a pure (very insoluble) metal. Alternatively, it may coprecipitate with other insoluble metals to form alloys and sulphides, rather than carbonates. Thus, the determination of partition coefficients for this element in calcite seems not to be a critical issue.

7.3.8 Thorium, protactinium, uranium, neptunium, plutonium

These radioelements are expected to occur in the +IV (tetravalent) oxidation state³³ under repository conditions, due to the large amounts of metallic iron which will be present in both repository types planned in Switzerland (a massive cast steel canister in HLW repository and steel drums in the L/ILW repository). Unfortunately, there are no laboratory investigations on the coprecipitation of tetravalent actinides with carbonates. In addition, tetravalent actinides do not form pure anhydrous carbonates, so that the correlation with the solubility products (Figure 4-6) cannot be used. Since, as discussed earlier, the correlation with ionic radius alone is not sufficient for a reliable extrapolation of partition coefficients, an attempt will be made to consolidate such extrapolations with supporting evidence from geochemical data on actinides in natural environments.

Coprecipitation with calcite was investigated in the laboratory for uranyl ions, where uranium is in the oxidised hexavalent form. These experiments yielded low partition coefficients ranging from 0.01 to 0.2 (see Table 4-1), in agreement with the large size of UO₂²⁺ ions. With an ionic radius of 0.89 Å, U(IV) should be in principle incorporated more easily in calcite than uranyl, as should the other tetravalent actinide ions, which have similar ionic radii (0.86 to 0.94 Å). Applying the empirical correlation with ionic size, partition coefficients ranging from ~10 to ~100 would result for the coprecipitation of tetravalent actinides with calcite.

Geochemical evidence in support of this extrapolation, however, is somewhat contradictory. On one hand, the fact that U(IV) and Th(IV) are frequently found in percent amounts in a variety of rare earth carbonates (e.g. bastnäsite, Ln [CO₃]F or ankylite,

³³ Plutonium may occur also in the trivalent oxidation state, in which case it will behave in a similar way as Am(III) and Cm(III).

$\text{Sr}_3\text{Ln}_4[\text{CO}_3]_7[\text{OH}]_4 \cdot 3\text{H}_2\text{O}$ ³⁴ points to a close geochemical affinity between tetravalent actinides (particularly thorium) and trivalent rare earths, indirectly suggesting high partition coefficients for the actinides in calcite. Thorium also forms a variety of complex carbonate salts (KATZIN 1954) and aqueous carbonate complexes (REMY 1949, p.79). Moreover, recent data support the existence of the hydroxyl-free $\text{Th}(\text{CO}_3^{2-})_5^{6-}$ complex (ÖSTHOLS et al. 1994, FELMY et al. 1997), indicating that, under favourable conditions, Th^{4+} can be coordinated by carbonate ions alone (like it would be in the calcite lattice). On the other hand, all tetravalent actinides hydrolyse strongly, which may hinder their incorporation in the calcite lattice (the strongly bound hydroxyls must be detached before the actinides can be incorporated in the calcite lattice). This hypothesis is also consistent with the observation that Th(IV) and U(IV) always form hydrous carbonates, both in nature and in the laboratory.

Fortunately, more conclusive information can be obtained from the literature on U,Th-geochronology, a field in which accurate measurements of isotopic concentrations of U and Th in rocks, minerals and waters are routinely needed for precise age determinations. With the help of carefully selected concentration data (Table 7-1), it was possible to bracket the values of partition coefficients for Th coprecipitated with marine calcites and limestones. The data indicate partition coefficients ranging from ~20 to ~2000, in rough agreement with the extrapolation based on the "ionic size rule". These values have been determined applying the definition of homogeneous partition coefficient (Equation 3-11) and assuming a concentration of 0.01 M for calcium dissolved in seawater.

Some comments on the geochemistry of Th and on the data selected in Table 7-1 are necessary to substantiate this estimation. In contrast to uranium, which is readily oxidised and thus relatively soluble in surface waters, thorium remains in the +IV oxidation state in natural environments. This leads to hydrolysis and consequent strong adsorption of Th(IV) on clay minerals, which explains the extremely low concentrations of dissolved Th in the oceans (WEDEPOHL 1969-1978, section 90-K; COCHRAN 1992; LI 1991). Early measurements of Th concentrations in seawater tended to be higher than indicated in Table 7-1, as a result of the technical difficulties involved in determinations by alpha spectrometry at those times. Recent measurements take advantage from the improved sensitivity of alpha spectrometry and are in agreement with the results obtained using new, extremely sensitive isotope dilution and neutron activation analyses. The range of Th seawater concentrations defined in Table 7-1, used for the estimation of the partition coefficients, represents the large majority of experimental determinations made after 1980 (COCHRAN 1992).

While Th-concentration determinations on total rocks abound in the literature, only two on pure calcites (from corals) could be found (SACKETT & POTRATZ 1963). The average Th-concentration in marine limestones of organic origin given by LI (1991) agree reasonably well with the coral determinations³⁵. Other studies (ADAMS &

³⁴ although the names of such minerals sound rather exotic, they may occur in considerable amounts. Bastnäsite, which is mined as a cerium ore, is found in amounts of millions of tons (BETECHTIN 1974).

³⁵ It should be noted that the partition coefficients of biogenic and inorganic carbonates may differ from each other for a given trace element due to biological fractionation effects (VEIZER 1983b). Generally, however, differences are rather modest (within one order of magnitude) and biogenic calcites tend to have lower partition coefficients than those of inorganic origin (which would lead to conservative estimates for radioelements).

WEAVER 1958, BARANOV et al. 1956) report much higher Th average concentrations in limestones. These data are based on a large number of analyses of impure limestones. The high Th contents can be ascribed to Th adsorbed on the clay fraction of these limestones and are thus not representative for Th concentrations in calcite, which justifies neglecting them.

In summary, the concentration data reported in Table 7-1 support the estimation of Th partition coefficients in calcite made on the base of the ionic size of tetravalent actinides. Thus, partition coefficients in the range 10-100 will be assumed in preliminary model calculations to describe coprecipitation of tetravalent actinides with calcite.

Table 7-1 : Thorium concentrations in seawater, marine limestones and marine calcites. These data were used to estimate partition coefficients for Th(IV) coprecipitation with calcite. Concentrations in seawater are given in molar units, while concentrations in solids are given as mole fractions of Th, assuming that the solid is 100 % calcite.

medium	concentration [M] / mole fraction	remarks	reference
seawater	$2 \cdot 10^{-13}$ - $2 \cdot 10^{-12}$	range defined by most recent measurements (after 1980)	COCHRAN (1992)
	$2 \cdot 10^{-13}$	average value	LI (1991)
	$6 \cdot 10^{-13}$	average value	LIN et al. (1996)
calcite	$4 \cdot 10^{-9}$ / $2 \cdot 10^{-8}$	two single determinations	SACKETT & POTRATZ (1963)
limestones	$4 \cdot 10^{-8}$	average value	LI (1991)

7.4 A model to estimate radionuclide coprecipitation with calcite in the L/ILW repository near-field

Having fixed the values of the partition coefficients for the safety-relevant radioelements, it is now possible to proceed with the development and application of a simple model, which quantifies the distribution of radionuclides between calcite (as a sink for radionuclide coprecipitation), concrete (as a sorbent) and pore solution as a function of the progress of cement degradation.

In the model developed below, it is assumed that the total initial radionuclide inventory is instantaneously and homogeneously dissolved in the water-saturated pore volume of the repository caverns. Instantaneous, reversible sorption of the radionuclides onto

cement phases is accounted for using constant, element-specific distribution coefficients. It is then assumed that an amount of calcite, corresponding to a given percentage of the calcium inventory in the cement³⁶, precipitates within the repository caverns or in the region adjacent to them, thereby removing from solution a fraction of the dissolved radionuclides (to be determined). The amounts of radionuclides coprecipitated with calcite are computed applying the heterogeneous law with the partition coefficients estimated in section 7.3 via a mass balance equation. A fixed Ca concentration in solution is assumed in the model, which is reasonable, since the calcium concentration in the “intermediate phase” will be buffered between ~8 and ~16 mM by saturation equilibrium with portlandite (NEALL 1996). The main results of the calculations are the fractions of radionuclide dissolved, sorbed and coprecipitated.

A number of simplifying assumptions are implicit in this model, which make it unsuitable for safety assessment purposes. For instance, the porosity and sorption properties of the concrete are assumed to remain constant in the course of degradation, radioactive decay and transport are neglected, and instantaneous release of the radionuclide inventory is postulated. In spite of such simplifications, this model remains useful if the objective is merely to estimate, in terms of orders of magnitude, the “potential” of calcite precipitation to reduce radionuclide solution concentrations and, further, to compare the relative contributions of coprecipitation and sorption to the overall retention of radionuclides. In other words, the model calculations will answer the following questions:

1. What percentage of a specific radionuclide inventory may coprecipitate with secondary calcite in the near-field of the L/ILW repository? For which radionuclides are the amounts coprecipitated sufficiently large to cause important reductions in their solution concentration?
2. Can radionuclide coprecipitation “compete” with sorption as a retention mechanism and under what circumstances?

More realistic calculations will be performed in future with the help of a suitable reactive transport model, if the answers to the questions formulated above justify such an effort.

7.5 Model development

The mass balance equation for simultaneous sorption and coprecipitation of a trace element in a closed system, where no external sources of the trace element exist, is given by:

$$[T_{tot}] = [T_s] + [T_c] + [T_f] \quad (7-1)$$

where:

³⁶ Since the amount of precipitated calcite cannot be predicted precisely, two cases were calculated: 50% of the Ca inventory, as a realistic case close to the estimation made by NEALL (1994), and 5% as a conservative case.

- $[T_{tot}]$ is the total concentration of the trace element T [mol m^{-3}],
 $[T_s]$ is the concentration of sorbed trace element [mol m^{-3}],
 $[T_c]$ is the concentration of coprecipitated trace element [mol m^{-3}],
 $[T_f]$ is the concentration of dissolved trace element [mol m^{-3}].

All concentrations are normalised to the (water-saturated) pore volume. In order to express $[T_s]$ as a function of $[T_f]$, a retardation factor R [-], is introduced:

$$R \equiv 1 + K_d \frac{\rho(1-\varepsilon)}{\varepsilon} = \frac{[T_s] + [T_f]}{[T_f]} \quad (7-2)$$

where:

- K_d is the sorption distribution coefficient of the trace element [$\text{m}^3 \text{kg}^{-1}$],
 ρ is the average density of the solids (pores excluded) [kg m^{-3}],
 ε is the average concrete porosity [-].

Substitution of Eq. (7-2) into Eq. (7-1) yields:

$$[T_{tot}] = R [T_f] + [T_c]. \quad (7-3)$$

Consider now the precipitation of a very small amount of calcite, Δn [mol]. Mass conservation requires:

$$\Delta[T_{tot}] = 0, \quad (7-4)$$

and hence, from Eq. (7-3):

$$R \Delta[T_f] = -\Delta[T_c]. \quad (7-5)$$

Applying Doerner-Hoskins' heterogeneous partition law (see also Eq. (3-12)), one obtains:

$$\frac{\Delta[T_c]}{\Delta[C_c]} = \lambda \frac{[T_f] + \Delta[T_f]}{[C_f] + \Delta[C_f]}, \quad (7-6)$$

where:

- $[C_c]$ is the concentration of carrier element (calcium) in the solid [mol m^{-3}],
 normalised to the solution volume,
 $[C_f]$ is the concentration of carrier element (calcium) in solution [mol m^{-3}].

Considering that $\Delta[C_c]$ is equal to the amount of precipitated calcium (Δn , [mol]) divided by the water-filled pore volume (V_p , [m³]), that a constant calcium concentration is assumed ($\Delta[C_f]=0$) and substituting $\Delta[T_c]$ by $-R \Delta[T_f]$ as stated by Eq. (7-5), Eq. (7-6) can be rewritten as follows:

$$\frac{-RV_p \Delta[T_f]}{\Delta n} = \lambda \frac{[T_f] + \Delta[T_f]}{[C_f]}. \quad (7-7)$$

In the limit of $\Delta[T_f]$, $\Delta n \rightarrow 0$ and defining the constant

$$\alpha \equiv \frac{\lambda}{V_p R [C_f]}, \quad (7-8)$$

the following differential equation is obtained, where $[T_f]$ is the dependent variable and n the independent variable:

$$\frac{d[T_f]}{[T_f]} = -\alpha dn. \quad (7-9)$$

The general solution of Eq. (7-9) is:

$$[T_f] = \text{const} \cdot \exp(-\alpha n), \quad (7-10)$$

where *const* is a generic constant to be determined through an appropriate boundary condition. Before any precipitation begins ($n=0$) the entire inventory of a specific trace element, T_0 [mol], will be either adsorbed or dissolved. This condition allows the determination of the integration constant:

$$\text{const} = [T_f]_{n=0} = \frac{T_0}{R V_p}. \quad (7-11)$$

The particular, explicit solution is then:

$$[T_f] = \frac{T_0}{R V_p} \exp\left(-\frac{\lambda n}{R V_p [C_f]}\right). \quad (7-12)$$

Equation (7-12) gives the residual solution concentration of the trace element, after n moles of the carrier element have precipitated, as a function of the partition coefficient

of the retention factor, the latter quantifying sorption of the trace element on a fixed amount of concrete. This expression is the starting point for the determination of the relative proportions of sorbed, dissolved and coprecipitated trace element, as a function of a few simple parameters. The total amounts [mol] of trace element left in solution (T_f), sorbed (T_s) and coprecipitated (T_c) are given by:

$$T_f = \frac{T_0}{R} \exp\left(-\frac{\lambda n}{R V_p [C_f]}\right) \quad (7-13)$$

$$T_s = \frac{(R-1) T_0}{R} \exp\left(-\frac{\lambda n}{R V_p [C_f]}\right) \quad (7-14)$$

$$T_c = T_0 \left\{ 1 - \exp\left(-\frac{\lambda n}{R V_p [C_f]}\right) \right\} \quad (7-15)$$

Expressions for the dissolved, sorbed and coprecipitated *fractions* of the trace element inventory are obtained by dividing Eqs. (7-13) to (7-15) by the total inventory T_0 :

$$x_f \equiv \frac{T_f}{T_0} = \frac{1}{R} \exp\left(-\frac{\lambda n}{R V_p [C_f]}\right) \quad (7-16)$$

$$x_s \equiv \frac{T_s}{T_0} = \frac{(R-1)}{R} \exp\left(-\frac{\lambda n}{R V_p [C_f]}\right) \quad (7-17)$$

$$x_c \equiv \frac{T_c}{T_0} = 1 - \exp\left(-\frac{\lambda n}{R V_p [C_f]}\right) \quad (7-18)$$

The sum of Eqs. (7-16) to (7-18) is equal to one, as it should be.

7.6 Model parameters

The nuclide-independent parameters required to apply the model developed in the previous section are summarised in Table 7-2. Many of the parameters listed in the table are self-explanatory and need no discussion. For the sake of simplicity, it was

assumed that the total repository volume is filled homogeneously with a unique concrete type (the concrete composition defined for cavern type 2 by NEALL (1994), see Tables 3a, 3b and 4 in this reference). Choosing other concrete types has little influence on the results. Only calcium contributed by the cement is considered; other minor sources are neglected. The average density ρ [kg m^{-3}] is defined as the mass of concrete divided by the volume of the solid fraction, excluding the pore volume.

Table 7-3 reports the nuclide-dependent parameters required to run the model: the heterogeneous partition coefficients for coprecipitation, the distribution coefficients for sorption of the radionuclides in the near-field (K_d values) and the initial radionuclide inventories. The K_d values were taken from a database used for safety assessment purposes (Table 2.2-2 in NAGRA 1994b)³⁷. The partition coefficients are best estimates obtained either from experimental data or from geochemical correlations (see section 7-3).

Table 7-2: Summary of parameter values used for the model calculations of radionuclide coprecipitation in the L/ILW near-field.

Parameter	Symbol	Value	Unit	Reference
Total length of caverns	L	1800	m	(1), p.10
Cavern cross-sectional area	A	231.3	m^2	(3), p.32
Repository volume	$V_r = AL$	$4.16 \cdot 10^5$	m^3	-
Average concrete porosity	ε	0.13	-	(2), Table 8
Water-filled pore volume	$V_p = \varepsilon V_r$	$5.41 \cdot 10^4$	m^3	-
Mass of cement in repository	M_c	$1.02 \cdot 10^8$	kg	(1), p. 9
Ca content in cement	x_{Ca}	0.45	kg Ca/ kg cement	(2), Table 4
average concrete density (pores excluded)	ρ	2600	kg m^{-3}	(2), Table 4 and 3a
Ca concentration in pore water	$[C_f]$	8.1	mol m^{-3}	(1), p. 6

References: (1) NEALL (1996); (2) NEALL (1994); (3) NAGRA (1994b)

³⁷ The distribution coefficients of most radionuclides are given as a range of values, to take account of the effects of radionuclide complexation with organic ligands (NAGRA 1994b, pp. 16-29). A specific set of K_d values has been defined for each of the four waste categories to be hosted in the repository (see Table 2.2-2 in NAGRA 1994b). The K_d values of many radionuclides, and particularly of actinides, may decrease considerably as the content of organic substances in the waste increases. The ranges given in Table 7-3 are defined by the values associated with the SMA-1 and SMA-2 waste types (i.e. the waste types with the smallest content of organic substances). The K_d values for the organic-rich SMA-3 and SMA-4 waste types were neglected, since most of the radiological inventory is associated to the SMA-1 and SMA-2 waste types.

Table 7-3: Partition coefficients, distribution coefficients for sorption on cement phases (after Table 2.2-2 in NAGRA 1994b) and initial radionuclide inventories in the L/ILW repository (sum of all radioactive isotopes of each element, calculated from data in Table 2.2-8 in NAGRA 1994b). Column 5 reports model pore water concentrations obtained by dividing each element's radionuclide inventory by the product of pore volume and retardation factor; column 6 gives indicative values of background concentrations in the ground water (these were obtained from analytical data given by SCHOLTIS & DEGUELDRE 1996 and by NAGRA 1989).

Element	Partition coefficient, [-]	Distribution coefficient, K_d [$\text{m}^3 \text{kg}^{-1}$]	Initial radiological inventory [mol]	Radionuclide concentration [M]	Background concentration [M]
Fe	2.0 - 7.7	10^{-2} - 10^{-1}	1.25	$1.3 \cdot 10^{-11}$ - $1.3 \cdot 10^{-10}$	10^{-6} - $2 \cdot 10^{-4}$
Co	2.0 - 8.0	10^{-2} - 10^{-1}	2.47	$2.6 \cdot 10^{-11}$ - $2.6 \cdot 10^{-10}$	10^{-10} - 10^{-7}
Ni	0.8 - 6.0	10^{-2} - 10^{-1}	9100	$9.7 \cdot 10^{-8}$ - $9.7 \cdot 10^{-7}$	10^{-9} - 10^{-6}
Sr	0.04 - 0.08	10^{-3}	0.13	$1.3 \cdot 10^{-10}$	10^{-6} - 10^{-4}
Sm	260 - 2280	10^{-1} - 5	0.0034	$7.2 \cdot 10^{-16}$ - $3.6 \cdot 10^{-14}$	$< 10^{-10}$
Ra	0.05 - 0.07	$5 \cdot 10^{-2}$	0.29	$6.2 \cdot 10^{-12}$	no data available
Th	10 - 100	10^{-1} - 5	$6.4 \cdot 10^{-6}$	$1.4 \cdot 10^{-18}$ - $6.8 \cdot 10^{-17}$	10^{-11} - 10^{-10}
Pa	10 - 100	10^{-1} - 5	$8.4 \cdot 10^{-8}$	$1.8 \cdot 10^{-20}$ - $8.9 \cdot 10^{-19}$	-
U	10 - 100	10^{-1} - 5	1630	$3.5 \cdot 10^{-10}$ - $1.7 \cdot 10^{-8}$	10^{-11} - 10^{-9}
Np	10 - 100	10^{-1} - 5	0.194	$4.1 \cdot 10^{-14}$ - $2.1 \cdot 10^{-12}$	-
Pu	10 - 100	10^{-1} - 5	2.32	$4.9 \cdot 10^{-13}$ - $2.5 \cdot 10^{-11}$	-
Am	200 - 1000	10^{-1} - 5	1.65	$3.5 \cdot 10^{-13}$ - $1.8 \cdot 10^{-11}$	-
Cm	200 - 1000	10^{-1} - 5	0.0022	$4.7 \cdot 10^{-16}$ - $2.3 \cdot 10^{-14}$	-

7.7 The effect of stable and natural radioactive isotopes

In the model developed in section 7.5, the presence of dissolved stable or natural radioactive isotopes, which may affect the coprecipitation of some radionuclides, is neglected³⁸: only radionuclide inventories in the waste are considered. An important source of stable nuclides is, for instance, the ground water flowing through the repository caverns. If the concentration of dissolved stable isotopes is much larger than that contributed by the radioactive isotopes released from the waste, then coprecipitation will be essentially controlled by the concentration of the stable isotopes. In this case, the partition law predicts the following effects: 1) a larger amount of trace element would coprecipitate compared with the case where only radioactive isotopes from the waste inventory are present; 2) on the other hand, only a fraction of the coprecipitated element will be in the form of radionuclides.

Table 7-3 lists the initial concentrations of safety-relevant elements in the cement pore water (calculated assuming that radionuclides in the waste are instantaneously dissolved and sorbed) and the range of concentrations expected in natural ground waters. A comparison reveals immediately that in several cases ground water concentrations greatly exceed the concentrations obtained dissolving the corresponding radionuclide inventories. This implies that the effects of stable isotopes on the amount of radionuclide coprecipitation cannot be a priori neglected, so that an improved model is needed.

Stable isotopes may also originate from the degradation of the solid materials in the repository (including the cement). For instance, the radionuclide inventory of iron is only 1.25 moles, resulting in a small average concentration of $\sim 10^{-8}$ M in the pore water. However, there are at least 10^9 moles of stable isotopes of iron in the repository (e.g. steel containers). It is clear that the total iron concentration in solution will be governed by the corrosion of the steel canisters, not by the release of radioactive ^{60}Fe from the waste. Under such circumstances, iron cannot be treated as a trace element like other radionuclides and the precipitation of pure iron phases must be considered. The amount of radioactive Fe effectively coprecipitated will be proportional to the ratio of radioactive to stable iron isotopes in solution. For the model calculations, we assumed that the iron concentration is limited by the solubility of $\text{Fe}(\text{OH})_2$, which results in a total Fe concentration of 2.4×10^{-4} M in the intermediate cement pore water.

Similar arguments can be applied to predict the influence of stable nickel. Nickel is an important alloy component of stainless steel used in the construction of nuclear power plants, so that many hundreds tons of stable Ni will be present in the repository besides about 0.5 tons radioactive Ni. The solubility of Ni under such conditions is likely to be controlled by pure Ni-oxyhydroxides or basic hydroxo-carbonates. Using the laboratory data reported by OSWALD & ASPER (1977), the concentration of Ni in equilibrium with pure $\text{Ni}(\text{OH})_2$, at pH-values between 11 and 13, ranges from $\sim 10^{-7}$ to $\sim 10^{-6}$ M. Therefore a Ni concentration of 10^{-6} M can be taken as upper limit for the model calculations presented in this report.

³⁸ Obviously, such effects need not to be considered for transuranic radionuclides (Pu, Am, Np, Cm), which have neither stable nor natural radioactive isotopes.

In order to include the effect of stable isotopes, the previous model is modified as follows. It is assumed that the total concentration of a generic trace element in solution, $[T_f]$, is fixed at a constant value (imposed by the solubility of a solid phase or by continuous supply from the ground water). A mass balance is then set up, as in Equation (7-1), but only for the radionuclide fraction, N , of the element:

$$[N_{tot}] = [N_s] + [N_c] + [N_f] \quad (7-19)$$

where:

- $[N_{tot}]$ is the total radionuclide concentration in the waste [mol m^{-3}],
- $[N_s]$ is the concentration of sorbed radionuclides [mol m^{-3}],
- $[N_c]$ is the concentration of coprecipitated radionuclides [mol m^{-3}],
- $[N_f]$ is the concentration of dissolved radionuclides [mol m^{-3}].

Coprecipitation obeys again the heterogeneous partition law, but since constant concentrations of both trace and carrier elements are postulated, the coprecipitate will be homogeneous with respect to the *total* trace element (that is, the concentration of radioactive plus stable isotopes of a given element will be constant in the solid, although the concentration of the radioisotopes in the solid may vary as precipitation progresses). Therefore, one can apply directly the homogeneous law and write:

$$\lambda = D = \frac{[T_c][C_f]}{[T_f][C_c]} \quad (7-20)$$

The solution concentrations $[C_f]$ and $[T_f]$ are constant, but the concentrations in the solid $[C_c]$, $[T_c]$ are not, since these are normalised to the (fixed) pore volume and thus increase as precipitation progresses ($[C_c]$, $[T_c]$ would, however, be constant if they were normalised to the *amount* of solid precipitated). $[C_c]$ and $[T_c]$ are thus related to the amount of calcite precipitated, n [mol]:

$$[C_c] + [T_c] = \frac{n}{V_p} \quad (7-21)$$

Combining Equations (7-21) with (7-20) and rearranging:

$$[T_c] = \frac{n\beta}{V_p(1+\beta)}, \quad \beta \equiv \lambda \frac{[T_f]}{[C_f]} \quad (7-22)$$

Now, consider a trace element in the repository consisting of a radionuclide inventory, N_{tot} , and a proportion of stable isotopes (determined by the "unlimited" supply from an external reservoir, e.g. a dissolving solid), so that the *total* trace element concentration

is buffered to a constant value. At any time during precipitation, the ratio of radionuclide to total trace element, F [-], will be identical in solution and *at the surface* of the precipitating solid (isotope fractionation effects being negligible). This ratio will be highest as precipitation starts, when the entire radionuclide inventory is assumed to be dissolved or adsorbed, and will progressively decrease as radionuclides coprecipitate with calcite. This implies that the calcite will have heterogeneous composition with respect to the radionuclides, although it will be homogeneous with respect to the *total* trace element. The ratio of radionuclides to total element at any stage of the precipitation is given by:

$$F(n) = \frac{[N_f]}{[T_f]} = \frac{d[N_c]}{d[T_c]} \quad (7-23)$$

Using the mass balance equation (7-19) and the retention factor R one obtains:

$$d[N_{tot}] = R d[N_f] + d[N_c] = 0 \quad (7-24)$$

Combining Equation (7-24) with Equation (7-23):

$$d[N_c] = -R d[N_f] = -R [T_f] dF \quad (7-25)$$

From Equations (7-22) and (7-23) one gets:

$$d[N_c] = F d[T_c] = F \frac{\beta}{V_p (1 + \beta)} dn \quad (7-26)$$

Equating Equations (7-25) with (7-26) and defining the constant

$$A \equiv \frac{\lambda}{RV_p [C_f] \left(1 + \lambda \frac{[T_f]}{[C_f]} \right)} \quad (7-27)$$

one obtains the differential equation:

$$\frac{dF}{dn} = -A F \quad (7-28)$$

with solution:

$$F(n) = F_0 \exp(-An) \quad (7-29)$$

The integration constant, F_0 , is given by the initial condition:

$$F|_{n=0} \equiv F_0 = \frac{N_0}{R V_p [T_f]} \quad , \quad (7-30)$$

where $N_0 = [N_{tot}] V_p$ is the initial radionuclide inventory of the element T . It is then straightforward to derive expressions for the concentrations of dissolved, adsorbed and coprecipitated radionuclides:

$$[N_f] = F(n) [T_f] = \frac{1}{R} \frac{N_0}{V_p} \exp(-An) \quad (7-31)$$

$$[N_s] = (R-1) F(n) [T_f] = \frac{(R-1)}{R} \frac{N_0}{V_p} \exp(-An) \quad (7-32)$$

$$[N_c] = \int_0^{[T_c]} F d[T_c] = \frac{\beta}{V_p (1+\beta)} \int_0^n F dn = \frac{\beta F_0}{V_p (1+\beta)} \int_0^n \exp(-An) dn = \frac{N_0}{V_p} [1 - \exp(-An)]. \quad (7-33)$$

Finally, one can easily obtain explicit expressions analogous to Equations (7-16) to (7-18) for the dissolved, adsorbed and coprecipitated radionuclide fractions:

$$x_f \equiv \frac{N_f}{N_0} = \frac{1}{R} \exp \left(\frac{-\lambda n}{R V_p [C_f] \left(1 + \lambda \frac{[T_f]}{[C_f]} \right)} \right) \quad (7-34)$$

$$x_s \equiv \frac{N_s}{N_0} = \frac{R-1}{R} \exp \left(\frac{-\lambda n}{R V_p [C_f] \left(1 + \lambda \frac{[T_f]}{[C_f]} \right)} \right) \quad (7-35)$$

$$x_c \equiv \frac{N_c}{N_0} = 1 - \exp \left(\frac{-\lambda n}{R V_p [C_f] \left(1 + \lambda \frac{[T_f]}{[C_f]} \right)} \right). \quad (7-36)$$

A comparison of Equations (7-16) to (7-18) with Equations (7-34) to (7-36) readily indicates that the latter differ from the corresponding expressions of the simpler model only by the term $1 + (\lambda [T_f] / [C_f])$ in the exponent, which is missing in Equations (7-

16) to (7-18). Thus, both models will give the same results if the criterion $\lambda[T_f] \ll [C_f]$ is satisfied. In other words, the two models will yield different results only if the product of partition coefficient and total trace element concentration is comparable to, or larger than, the concentration of calcium in the pore water. In this case, the fraction of radionuclide coprecipitated, x_c , must decrease due to the presence of a background concentration of stable isotopes. *That is, the effect of stable isotopes, if any, is to decrease the efficiency of radionuclide coprecipitation.* This effect must therefore be evaluated, since it acts negatively.

An inspection of the data in Table 7-3 reveals that for all elements but iron, the products of the partition coefficient and the corresponding background concentration is much smaller than the assumed calcium concentration of 8.1×10^{-3} M. For all these elements the two models produce identical results. For iron, the calculations with the improved model lead to results differing by only 0.2 % from those obtained applying the first model. Therefore, the presence of stable isotopes should not significantly affect the incorporation of trace radionuclides in secondary calcite.

This straightforward conclusion must, however, be taken with caution. The models presented here are too simplistic to predict secondary chemical effects; their results should be always analysed from a certain distance through the lens of geochemical common sense. For instance, if iron concentrations as high as $\sim 10^{-4}$ M are established by saturation equilibrium with $\text{Fe}(\text{OH})_2$, the secondary carbonates formed will contain a large proportion of iron; they will be no longer pure calcites, but ferroan calcites with slightly different lattice parameters. Under these conditions, the partition coefficients of *all* radionuclides may be affected. It is not possible, at the present state of knowledge, to predict the magnitude of such effects, although there are indications that they should not be large.

The previous statements trace clear limits to the applicability of the results given in the following section. Again, it is recalled that these calculations have the unique objective to determine the *potential* of coprecipitation as a retention mechanism during the cement degradation process and to evaluate the relative efficiencies of coprecipitation and sorption; the results should not be used for other purposes.

7.8 Results: is sorption or coprecipitation more efficient?

The results of the model calculations are summarised in Table 7-4, in which the distribution of the various radionuclides between adsorbed, solid and aqueous phases are reported for two parameter combinations.

The results indicate that substantial fractions of *all* radionuclide inventories would coprecipitate if 50% of the calcium available in the cement were degraded to calcite. Using the best estimates of the partition coefficients, the percentage of the inventory coprecipitating with calcite is found to exceed 99% for all radioelements but Ra. For Ra the percentage coprecipitated is small (due to the very small partition coefficient and inventory) but nevertheless significant and comparable to the amount adsorbed. If conservative estimates of the partition coefficients are used, the coprecipitated fractions of many radionuclides decrease more or less considerably. However, for Sm, Am and

On the conservative partition coefficients are still sufficiently high to guarantee that these nuclides are almost quantitatively fixed in calcite.

Table 7- 4: Results of model calculations to estimate the amounts of coprecipitated, adsorbed and dissolved radionuclides after precipitation of 50% of the calcium inventory of cement as calcite. The results were obtained from the improved model, taking into account the effect of stable isotopes. However, only for Fe do the two models yield different results. Empty cells denote percentages of less than 10^{-10} .

Element	Case 1 (combines low K_d and high λ of Table 7-3)			Case 2 (combines high K_d and low λ of Table 7-3)		
	% adsorbed	% coprecip.	% dissolved	% adsorbed	% coprecip.	% dissolved
Fe	-	100	-	24	76	-
Co	-	100	-	22	78	0.01
Ni	-	100	-	55	45	0.03
Sr	0.3	99.7	0.02	5.6	94.1	0.3
Sm	-	100	-	2	98	$2 \cdot 10^{-9}$
Ra	8.9	10	0.1	92.7	7.2	0.1
Th, Pa, U, Np, Pu (IV)	-	100	-	86	14	0.001
Am, Cm (III)	-	100	-	5	95	-

The prediction that many radionuclides should be preferentially retained through coprecipitation rather than through sorption might at first sight be surprising. However, this result appears logical if one considers the way in which the two processes interact. While the adsorbed fraction is proportional to the exposed surface area of sorbing solids, which is assumed to be constant, the coprecipitated fraction is proportional to the amount of precipitated solid, which *increases* as degradation proceeds. Before calcite precipitation starts, all radionuclides will be either dissolved or adsorbed. During precipitation radionuclides are continuously removed from solution, so that an increasing amount of radionuclides must desorb in order to restore sorption equilibrium. To put it in another way, coprecipitation causes the displacement of the adsorbed radionuclides from the sorbent. Thus, coprecipitation is favoured when very large amounts of secondary solid are formed, while sorption will be the dominant retention mechanism when only small amounts of solids are formed.

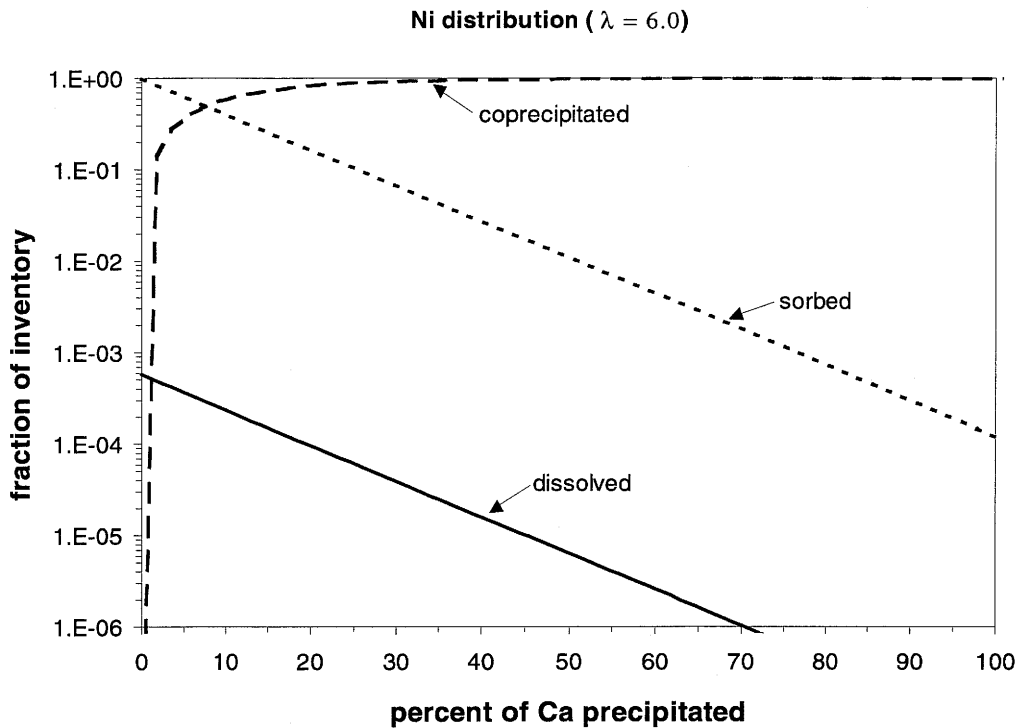


Figure 7-1: Calculated distribution of the Ni inventory as a function of the amount of secondary calcite precipitated, expressed as percent of the total calcium inventory in cement.

The “pumping effect” of coprecipitation is evident in Figure 7-1, where the dissolved, adsorbed and coprecipitated fractions of Ni are plotted as a function of the amount of calcium precipitated, assuming a partition coefficient of 6. Initially, almost the entire waste inventory of Ni is adsorbed; after ~10% of the calcium in the cement has precipitated as calcite, half of the Ni is adsorbed and half has coprecipitated with calcite (intersection of the 2 curves). Finally, after ~40% of the Ca is converted in calcite, almost the entire Ni inventory is fixed in the secondary calcite. The proportion of Ni in solution at any time is very small, but not constant. Since it is proportional to the amount adsorbed, the Ni concentration in solution is highest when precipitation starts ($\sim 10^{-7}$ M, corresponding to ~0.06 % of the inventory) and decreases to a minimum of $\sim 10^{-11}$ M after precipitation of all available Ca as calcite (not shown in the plot). **After precipitation of 50% of the initial Ca as calcite, the dissolved Ni concentration has decreased by about 2 orders of magnitudes.** This result is particularly important in view of safety analyses, since radiological doses ultimately depend on the solution concentration of a radionuclide, not on the amount coprecipitated. Coprecipitation may thus be effective as a mechanism reducing radionuclide solution concentrations, on which their mobility depends.

7.9 Generalisation of the model

In order to determine the general requirements for efficient radionuclide coprecipitation during calcite formation in the L/ILW repository, the key model parameters (n , K_d and λ) were varied systematically over the range of expected values. The results are summarised in three-dimensional surface plots (Figure 7-2 and 7-3). Figure 7-2 shows the fraction of radionuclide inventory coprecipitated as a function of K_d and λ , while Figure 7-3 shows the dependency of the radionuclide solution concentration on the same two parameters, expressed by means of a *reduction factor*, to be defined later in this chapter. Two cases have been investigated: precipitation of 50% and 5% of the total calcium available in the cement phases as secondary calcite.

An important feature emerging from Figure 7-2 is that the amount of coprecipitated radionuclides increases as the amount sorbed on the cementitious material decreases. For instance, the upper plot of Figure 7-2 indicates that coprecipitation will be incomplete, in spite of the high partition coefficients, if tetravalent actinides are strongly adsorbed on the cementitious material ($K_d = 5 \text{ m}^3/\text{kg}$). Conversely, if adsorption were one order of magnitude lower, coprecipitation of tetravalent actinides would be quantitative. Thus, an important conclusion from this modelling exercise is that radionuclide sorption and coprecipitation are not independent of each other. For any radionuclide, coprecipitation will be the more effective the weaker its adsorption on cement phases is.

The interdependency between sorption and coprecipitation can be understood considering that the radionuclide solution concentration increases as the retention factor, R [-], is reduced (see Eq. (7-12)). The higher the radionuclide concentration in solution, the larger the amount incorporated in calcite through coprecipitation, according to the partition law. Thus, including coprecipitation in safety assessment models is likely to bring the largest benefits in the case of reduced sorption: a) for radionuclides with high partition coefficients and low associated K_d values; b) for systems with high water-rock ratios, e.g. open fractures³⁹. The relevance of the former case is, however, questionable: as discussed in section 4.4.6, partition coefficients and sorption parameters are likely to be correlated for some radionuclides. On the other hand, at advanced stages of cement degradation K_d values may be reduced due to the large amounts of secondary calcite replacing the dissolved CSH-gel in the cement.

Another important conclusion drawn from Figure 7-2 is that coprecipitation is always inefficient for radionuclides with a partition coefficient of less than 0.01, even if no sorbent were present. Thus, coprecipitation is likely to bring little or no benefit in safety assessment calculations for all those radionuclides with a partition coefficient of less than this value (e.g. Ra). Finally, Figure 7-2 (bottom) shows that trivalent actinides could coprecipitate quantitatively even if only 5% of the available Ca were converted to calcite, provided the K_d values are on the lower end of the assumed range. These are undoubtedly the radionuclides for which coprecipitation with calcite should bring the largest benefits.

³⁹ The retention factor R , on which the trace element solution concentration depends according to Equations (7-2) and (7-12), decreases with increasing porosity and decreasing K_d . A decrease in K_d may result from changes in the mineralogy (alteration products replacing the dissolved primary cement phases) or from a reduction of the exposed surface area.

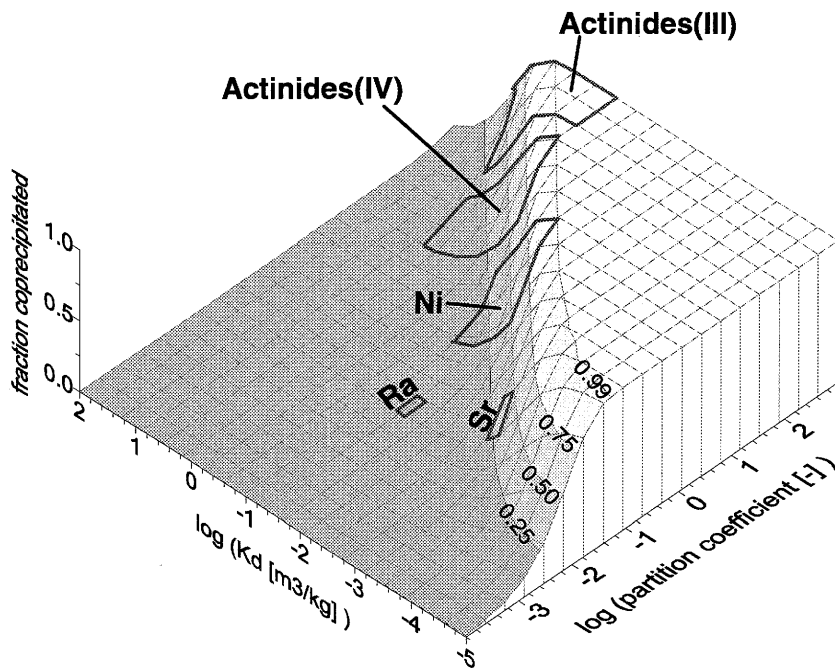
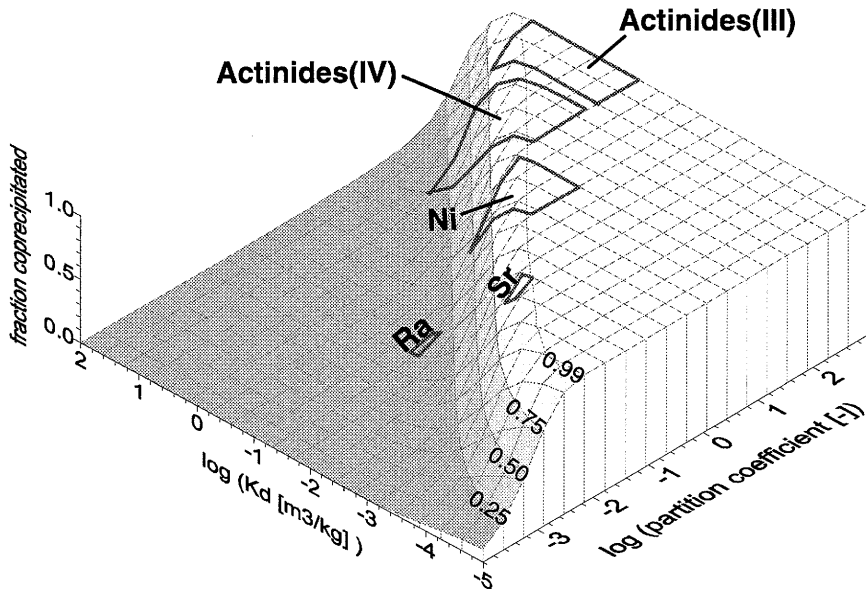


Figure 7-2: Three dimensional combined surface and contour plots of the fraction of the inventory coprecipitated as a function of K_d and λ , assuming that 50% (upper plot) or 5% (lower plot) of the Ca stored in the cement of the planned L/ILW repository precipitates as calcite.

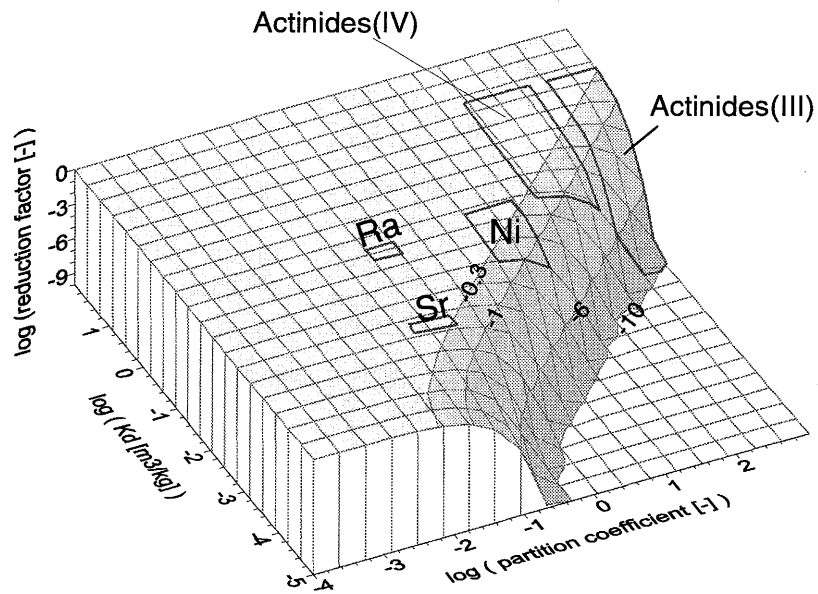
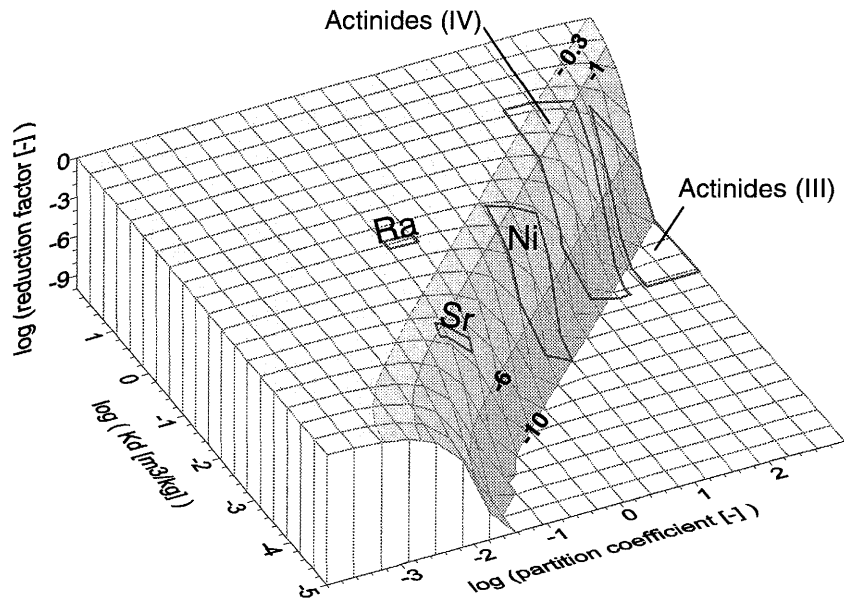


Figure 7-3: Three dimensional surface and contour plots showing the reduction in radionuclide solution concentration as a function of K_d and λ , assuming that 50% (upper plot) or 5% (lower plot) of the Ca in the cement of the planned L/ILW repository precipitates as calcite. The z-axis gives the ratio, on a logarithmic scale, of the concentration calculated assuming simultaneous sorption and coprecipitation, to the concentration obtained assuming sorption, but no coprecipitation of the radionuclide (see detailed explanation in text).

From the point of view of safety assessment, the plots of Figure 7-3 are more relevant, since they show the effects of coprecipitation on the solution concentration of radionuclides, which directly affects their mobility. The reduction factor r_f [-] plotted in Figure 7-3 is obtained from Equations (7-16) and (7-18) in the following way.

Defining:

$$E \equiv \exp\left(-\frac{\lambda n}{R V_p [C_f]}\right), \quad (7-37)$$

Equations (7-16) and (7-18) reduce to:

$$x_f = \frac{E}{R} \quad (7-38)$$

$$x_c = 1 - E \quad (7-39)$$

from which one obtains:

$$x_f = \frac{1}{R}(1 - x_c). \quad (7-40)$$

We further define x_f^0 as the inventory fraction dissolved *before any precipitation starts*, that is when only sorption acts as a retention mechanism. Under such circumstances $x_c = 0$. Thus, from Equation (7-40):

$$x_f^0 = \frac{1}{R}. \quad (7-41)$$

The reduction factor r_f [-] plotted in Figure 7-3 is simply obtained by dividing Equation (7-40) with Equation (7-41):

$$r_f \equiv \frac{x_f}{x_f^0} = 1 - x_c = E. \quad (7-42)$$

The quotient r_f expresses the decrease in solution concentration of a radionuclide due to coprecipitation alone. In other words, it indicates (of course only for the closed-system model developed in this chapter), how much the solution concentration of a radionuclide is reduced compared with the case when only sorption on cement acts as a retention mechanism. For instance, in the plots of Figure 7-3 the -1.0 contour line ($\log r_f = -1$) defines the positions of λ, K_d -combinations for which the radionuclide solution concentration is decreased by one order of magnitude due to coprecipitation of n moles calcite. The -0.3 contour line defines λ, K_d -combinations for which the solution concentration is reduced to half the value it would have if no calcite would precipitate ($n=0$)⁴⁰.

⁴⁰ The absolute concentrations of dissolved radionuclides for $n=0$ are given in Table 7-3, column 5.

Since the reduction factor is equal to the exponential term expressed in Equation (7-37), it depends essentially on the number of moles of calcite formed, n . The other parameters appearing in the exponential term are either fixed or are independent variables. The dependency on n is illustrated by the two cases considered in the two plots, where precipitation of 50% and 5% of the Ca-inventory in the cement are assumed. Obviously, for $n=0$ the plot would be a planar, horizontal surface at height $\log r_f = 0$. With increasing calcite precipitation, the depressed region, in which radionuclide solution concentrations are significantly reduced due to coprecipitation, increases in size. The lower plot in Figure 7-3 shows that even if only 5% Ca of the cement precipitates as calcite, the solution concentration of many radionuclides would decrease substantially. If extensive carbonation of the cement is assumed (upper plot), significant reductions of the solution concentrations are predicted also for Ni and Sr. In contrast, coprecipitation of Ra with calcite will not result in decreased solution concentrations, even if very large amounts of calcite precipitate.

7.10 Coprecipitation of ^{14}C with calcite

An important, not yet discussed topic is that of ^{14}C coprecipitation with calcite. This subject is treated here separately because it differs in at least two points from the other cases. First, carbon is a main component of calcite, so that any ^{14}C attached to a carbonate ion will coprecipitate with a partition coefficient close to one⁴¹. Second, there are two sorts of ^{14}C in the radionuclide inventory, which differ in both sorption and coprecipitation properties (NAGRA 1994b): inorganic ^{14}C (82 moles), which will be dissolved mainly as carbonate, and ^{14}C present in organic molecules (33 moles). Safety assessment calculations indicate that, for the reference scenario, ^{14}C of organic origin determines the calculated dose maximum, as a result of conservative assumptions made on the sorption properties of organic substances (a K_d value of zero was assumed). In contrast, the contribution of the well-sorbed ($K_d = 1 \text{ m}^3 \text{ kg}^{-1}$) inorganic ^{14}C to the total calculated dose appears to be insignificant. Therefore coprecipitation of organic ^{14}C is the major concern.

Unfortunately, little is known on the nature and properties of organic compounds concentrated in the L/ILW waste (see VAN LOON & HUMMEL 1995). It is thus not possible to fix reliable values for sorption and coprecipitation parameters. The incorporation of organic ^{14}C in calcite will depend on a number of factors, like the nature and molecular weight of the degradation products, their charge and the relative amounts of radioactive and stable dissolved organic carbon. None of these is quantifiable on the base of current knowledge.

It may be speculated, however, that partition coefficients approaching zero may apply to high-molecular polymeric species. For such compounds, even the partition-law approach, used to describe incorporation of trace metals, may be questioned, since polymeric species are too bulky for isomorphous substitution.

⁴¹ The partition coefficient of ^{14}C will slightly differ from unity due to isotopic fractionation effects with ^{12}C .

In summary, it is still an open question whether coprecipitation of organic ^{14}C with calcite could be an effective mechanism for reducing the calculated doses. An answer will only be possible if detailed information on the nature and sorption/coprecipitation properties of organic degradation products will become available.

7.11 Conclusions

The model calculations presented in this chapter indicate that an important fraction of the radionuclide inventory in the L/ILW waste could be fixed through coprecipitation reactions with secondary calcite during the degradation of cementitious materials. The solution concentrations of several safety-relevant radionuclides could be reduced by orders of magnitude as a result of coprecipitation with secondary calcite. These results are robust to variations of material properties (porosity and density of the concrete) and of the calcium concentration in the pore water, within the uncertainty limits of these parameters.

The extent of radionuclide coprecipitation will critically depend on both extent and rate of calcite formation during the degradation process. Precipitation of sufficient amounts of this mineral is a necessary requirement for an effective reduction of radionuclide solution concentrations. In the specific case of a repository in the Wellenberg region, there is no doubt that very large amounts of secondary carbonate minerals will form upon interaction with Na-HCO_3^- ground water or with carbonate originating from the degradation of organic substances, so that the assumption that 50% of the Ca in the repository will precipitate as calcite is by no means unrealistic. Even if only 5% of the Ca were converted to calcite, the solution concentration of some radionuclides with high partition coefficients (particularly of trivalent actinides) could be substantially reduced.

Another important requirement for the effective coprecipitation of radionuclides with calcite is that the calcium and the radionuclides must be released simultaneously. Due to the large heterogeneity of materials and wastes in the repository, it is however difficult to foresee whether this requirement will be fulfilled or not. For instance, calcium release, and consequently calcite precipitation rates, could be relatively slow in the initial stages of cement degradation, due to the small Ca concentrations imposed during the initial high-pH phase (Neall 1995). If the degradation of the radioactive waste is fast compared to calcium dissolution, most radionuclides could then migrate through the engineered barriers, avoiding coprecipitation and retarded only by sorption⁴². Such scenarios will, however, remain speculative until reliable source term models for radionuclide release from each waste type will become available.

⁴² The precise duration of the high pH phase is currently unknown. NEALL (1995) argues that this phase may last thousands of years or be of very short-lived.

8. Summary, conclusions and recommendations

8.1 Models for the quantitative description of coprecipitation processes

Two model types are commonly used to describe coprecipitation processes: a) thermodynamic solid-solution models and b) models based on empirical partition “laws”.

The application of solid-solution models is currently limited by the following inherent problems: a) since solid-solution models rely entirely on equilibrium thermodynamics, they cannot account for the effects of fast precipitation kinetics and can strictly be applied only to systems where all reactions involved are sufficiently slow; b) the simplest thermodynamic model, the so-called *ideal solid-solution model*, was found to be inadequate for simple cases of binary carbonate solid solutions (coprecipitation of Mg, Sr, Fe and Mn with calcite). More complex thermodynamic models have not been tested in this report. This task will be accomplished, if necessary, at a later stage of the project.

Partition-law models are free of some shortcomings mentioned above by virtue of their empirical nature and are thus more flexible. It is the classical approach used by the pioneers of radiochemistry and is still widely used. The flexibility of partition models is paid for with strong limitations in their predictive power, due to the fact that partition coefficients depend on a variety of physicochemical parameters. These limitations can be overcome by carrying out coprecipitation experiments under the specific conditions of interest, or by carrying out systematic laboratory investigations to explore the dependency of a specific partition coefficient on the key physicochemical parameters.

Systematic investigations on coprecipitation are time-consuming and need accurate laboratory work; up to date such extensive work has been carried out only for the incorporation of metals in calcite. In spite of these difficulties, the author is convinced that the partition-law approach, when supported by appropriate laboratory data, is a practicable way to model coprecipitation of radionuclides successfully.

8.2 Factors affecting radionuclide coprecipitation

The coprecipitation of metals with carbonate minerals was found to depend on various physicochemical factors. It is useful here to distinguish between factors controlling the selectivity of a given host mineral for the various trace elements (why some trace elements are incorporated in a host mineral more easily than others) and factors controlling the variation of a specific partition coefficient (why the partition coefficient of a single trace element in a given host mineral is subject to variations).

In the former category are elemental properties like ionic radius and charge, electronic configuration, the tendency of an ion to form carbonate minerals and to adsorb on the

surface of carbonate crystals. The analysis of the coprecipitation data from the open literature shows reasonable correlations with most of the properties listed above.

Ionic charge does not correlate with the partition coefficient, at least as long as only trace amounts of the ion are incorporated in the host phase. In contrast, partition coefficients in calcite depend in most cases on the radius of the coprecipitating ion. Cations with a ionic radius greatly exceeding the size of Ca^{2+} are weakly incorporated, while most, but not all, cations with a radius similar or slightly smaller than that of Ca^{2+} coprecipitate efficiently. Notable exceptions to this rule are found for Na^+ and Mg^{2+} ; these cations remain preferentially in solution although they would fit well in the Ca^{2+} sites of calcite.

If the partition coefficients of the various ions are plotted against the solubilities of their pure carbonates, a well-defined linear correlation emerges, from which low partition coefficients are predicted for cations forming soluble carbonates and high partition coefficients for cations forming insoluble carbonates (*Fajans' rule*). This correlation successfully predicts the partition coefficients of Na^+ and Mg^{2+} , for which anomalously low values have been determined experimentally. *Fajans' rule* was thus selected as the main tool for the estimation of partition coefficients of radionuclides in calcite (e.g. for Ni^{2+} and Am^{3+}).

A good correlation also emerged between partition coefficients and selectivity coefficients of transition metals, but the scarcity of experimental data of metal sorption on calcite presently limits its predicting power.

Among the factors influencing the magnitude of partition coefficients for a specific trace element, the rate of precipitation (or recrystallisation) and competition effects at the solution-mineral interface seem to be the most important. On the contrary, the dependency on temperature was found to be negligible.

Partition coefficients vary by up to one-two orders of magnitude over a range of six orders of magnitude in the precipitation rate. The partition coefficients of Cu^{2+} and Zn^{2+} in calcite were also found to depend on the extent of complexation with some organic and inorganic ligands. Whenever strong, non-sorbing complexes are formed with dissolved Cu^{2+} or Zn^{2+} ions, partition coefficients decrease significantly. The extent to which coprecipitation is reduced depends on both ligand concentration and stability of the complex. This effect could play an important role during coprecipitation reactions in the L/ILW repository environment, due to the release of a variety of organic substances stored in the waste.

Since adsorption reactions are strongly pH-dependent, it is easy to foresee that pH could indirectly have an influence on the magnitude of partition coefficients. Unfortunately, coprecipitation studies carried out over a pH-range large enough to cover strongly alkaline conditions are completely missing. Most partition coefficients were determined in a very restricted pH range (essentially 7 to 10). To fill this gap could be one of the major tasks in the future.

8.3 Estimation of partition coefficients for radionuclides

Partition coefficients for radionuclides coprecipitating with calcite were estimated with the help of geochemical correlations established through the analysis of literature data. All the available information was used in order to build confidence in the estimated values. For instance, the high partition coefficients estimated for the trivalent actinides Cm^{3+} and Am^{3+} are corroborated by the high partition coefficients *measured* for the chemically analogous trivalent rare-earths. It must be stressed again that our estimations do not account for possible variations caused by hyperalkalinity or complex formation; hence these values should be used only for preliminary assessments. Nevertheless, carbonate precipitation in the planned Wellenberg repository will essentially occur in response to a neutralisation reaction (hyperalkaline cement pore water reacting with near-neutral ground water) so that at least a fraction of the radionuclides will coprecipitate at moderate pH (~ 8-10), a range for which the partition coefficients estimated in this report should apply.

8.4 The role of coprecipitation as a retention mechanism

The main question, whether radionuclide coprecipitation is a potentially safety-relevant retention mechanism, could be answered through simple model calculations based on the estimated partition coefficients. According to such calculations, important amounts of radionuclides could be trapped in secondary calcite during cement degradation in the L/ILW repository at Wellenberg. This conclusion is reached even assuming conservative partition coefficients.

The model calculations indicate that, under reducing conditions, coprecipitation reactions could bind important amounts of Am, Cm, Sm, Np and Pu and U in secondary calcite. Considerable fractions of the Ni, Sr, Fe and Co radiological inventories may also remain trapped in calcite, while only small fractions of the Se, Ra, Th and Pa inventories are expected to coprecipitate. The calculations also show that coprecipitation is complementary to sorption: coprecipitation is most effective when radionuclides are weakly sorbed (and vice versa). This effect could become important in systems with high water-rock ratios (e.g. open fractures), or if the sorption capacity of the near-field decreases due to mineralogical transformations (e.g. precipitation of alteration products at the expense of primary cement phases). Further, it is clear that a necessary requirement for efficient coprecipitation is that *large amounts* of secondary solids must form. Coprecipitation will be unimportant if only minor amounts of secondary solids precipitate, or if precipitation / recrystallisation rates are slow compared with radionuclide transport rates in solution.

Comparable predictions for the HLW repository have not been attempted, although there is little doubt that coprecipitation could be an important retention mechanism also in this repository type. Unfortunately, it is difficult to determine with sufficient confidence which of many possible secondary phases (and how much of each) will form during alteration reactions in the HLW repository. In addition, even if such information were available, the corresponding partition coefficients are unknown. A possible exception is Cs, which is known to partition strongly in the sodium silicate *analcime*, a typical secondary product of silica glasses. If the amount of analcime

formed during the alteration of waste glass can be estimated, then it is in principle possible to evaluate the effects of Cs coprecipitation with this phase. This would be valuable, as ^{135}Cs is one of the most significant isotopes for HLW waste.

8.5 A road map for future work

Current knowledge of radionuclide coprecipitation processes is poor and scanty. It is evident that any decision to pursue investigations on this topic, with the final objective being to include radionuclide coprecipitation in future safety assessment models, needs a careful evaluation.

The effort needed to bring the knowledge of radionuclide coprecipitation to a level comparable to our current knowledge of radionuclide sorption is very large. On the other hand, if a more modest and specific objective is pursued, like that of incorporating radionuclide coprecipitation with only the dominant and best characterised secondary phases in future safety assessments, the effort required should be affordable. In this case, work could go in two directions: 1) modelling work, to provide a detailed understanding of the potential of radionuclide coprecipitation in a repository-specific situation and to develop computational tools for future safety assessment models; 2) experimental work aiming at determining reliable partition coefficients for radionuclides under relevant conditions.

Modelling work:

The first step would be to implement the partition law in the coupled reactive transport code MCOTAC (PFINGSTEN 1994). This task could be accomplished within a few months and should be relatively straightforward. With a source-term model for the release of radionuclides, such an implementation would allow to predict, by means of a "backdoor approach", the effects of calcite precipitation on the release rates of radionuclides from the repository. This approach would yield more realistic results than the preliminary calculations presented in this report. Specifically, it would be possible to quantify the effect of transport parameters (e.g. diffusive vs. advective transport). Problems may arise, however, in defining a realistic source term function for radionuclide release from the waste, due to the heterogeneity of the repository materials. In a first step, the very simple assumption that each radionuclide is released in proportion to the mass of degraded cement would be made. In a second step, appropriate concepts should be developed in order to integrate coprecipitation in safety assessment models.

Additional modelling work should be performed to test complex solid solution models against the available coprecipitation data. Although such models are already available, attempts to verify their validity by comparing model predictions with experimental data are, surprisingly, very rare. The hope is to find a model of general validity, applicable with some confidence to different chemical conditions, thus overcoming the uncertainties involved in extrapolating data from empirical partition models to conditions differing from those prevailing in the experiments.

Experimental work:

A more pragmatic, but surely more expensive and time-consuming, approach would require coprecipitation experiments specifically designed for the needs of radioactive waste management problems. In the case exemplified in this report, this would mean that calcite coprecipitation experiments should be performed directly with safety-relevant radionuclides, over the pH-range and with solution compositions relevant for repository conditions.

The first step would be to gain expertise in the techniques needed for carrying out chemostatic coprecipitation experiments with carbonate minerals. These techniques were developed during the past 10-15 years by a small group of marine geochemists in the U.S. and Canada and are still used, judging from the frequency of recent publications. Therefore, it should not be difficult to arrange a "technology transfer" to the community of geochemists involved in radioactive waste disposal within a reasonable time (~ 1 man-year).

In a second step, the experimental techniques should be refined to comply with the need for repository-relevant conditions. For instance, the coprecipitation experiments would have to be carried out directly with the radionuclides of interest and also in hyperalkaline solutions, in order to explore the pH-dependency of partition coefficients. Further, techniques must be developed and tested for measuring precisely very low radiotracer concentrations in solution and in the precipitate. Although the author of this report has little expertise in experimental chemistry, it is not difficult to argue that this preparation phase would be very time-consuming (> 1 man-year ?).

Once these techniques are mastered in detail, it will be possible to determine the partition coefficients of safety-relevant radionuclides in calcite. This phase will also be time-consuming, because a long series of experiments will be needed for each radionuclide in order to determine the dependency of the partition coefficient on all critical parameters (rate of precipitation, pH, concentration of organic ligands). Therefore these experiments should involve first those radionuclides, for which most benefits are expected in terms of safety assessment results.

8.6 Concluding remarks

In summary, it can be stated that a very large workload is needed in order to gain sufficient knowledge of radionuclide coprecipitation processes to justify including them in safety assessment models. Although safety assessments may be carried out ignoring (conservatively) radionuclide coprecipitation, there is no objective reason to explain why this process, which will limit together with sorption the solution concentrations of many radionuclides, has been widely neglected in the field of radioactive waste disposal. The frequently heard objection, that coprecipitation is too complex for a quantitative treatment, is not acceptable in view of the results presented in this report. Moreover, one should consider that radionuclide sorption processes, which are equally complex, were also poorly understood two decades ago. Now, after careful and continuous work by many investigators, a sufficiently high level of understanding has been reached to justify incorporation of this process in safety assessments. The basic questions to ask therefore is: are we satisfied with the incomplete and biased safety models

currently used, or should we try to fill this major gap in our model representations by including the process of radionuclide coprecipitation?

It is the author's conviction that this objective should be pursued. If we succeed, we will have developed a more realistic tool for describing geochemical processes in the repository near-field. In particular, it will be possible to abandon the problematic "solubility limit" approach, which often relies on the solubility of hypothetical pure radionuclide solids. The concentrations of most radionuclides in radioactive wastes are so low that the formation of pure solids is very unlikely: precipitation of radionuclides as dispersed trace elements in large masses of alteration products (like calcite, CSH phases in the L/ILW repository and clay minerals or zeolites in the HLW repository) will be the dominant process limiting their concentrations in solution.

Acknowledgements

The author is indebted to Drs. I. Puigdomenech (KTH, Stockholm), J.F. Pearson, U. Berner, W. Hummel and A. Thoenen (PSI), I.G. McKinley and B. Schwyn (NAGRA) for their careful reviewing work and helpful suggestions, through which both contents and form of this report could be substantially improved. The partial financial support by the Swiss National Cooperative for the Disposal of Radioactive Waste (NAGRA) is gratefully acknowledged.

References

- ADAMS, J.A.S. & WEAVER, C.E. 1958: Thorium to uranium ratios as indicators of sedimentary processes: example of concept of geological facies. *Bulletin of the American Association of Petroleum Geologists* 42(2), 387-430.
- BARANOV, V.I., RONOVA, A.B. & KUNASHOVA, K.G. 1956: Geochemistry of dispersed thorium and uranium in clays and carbonate rock of the Russian platform. *Geochemistry* (3), 227-235.
- BARRER, R.M. 1978: Cation-exchange equilibria in zeolites and feldspathoids. *In*: "Natural zeolites", L.B. Sand and F.A. Mumpton eds., Pergamon press, Oxford, 385-395.
- BERNER, U. 1995: KRISTALLIN I: Estimates of solubility limits for safety relevant radionuclides, Paul Scherrer Institute, Villigen, Switzerland, PSI Report Nr. 95-07 and NAGRA, Wettingen, Switzerland, Nagra Technical Report NTB 94-08.
- BERTHELOT, M. 1872: On the law which governs the distribution of a substance between two solvents. *Ann. Chim. Phys.* 26, 4th Ser., 408-417.
- BESSET, F. 1978: Localisations et répartitions successives du nickel au cours de l'altération latéritique des péridotites de Nouvelle-Calédonie, Université des Sciences et Techniques du Languedoc (Montpellier II), Mémoires du Centre d'Etudes et de Recherches Géologiques et Hydrologiques, Tome XV.
- BETECHTIN, A.G. 1974: *Lehrbuch der speziellen Mineralogie*. 6. ed., VEB Deutscher Verlag für Grundstoffindustrie, Leipzig, 683 p.
- BISH, D.L. 1978: Anion-exchange in takovite: applications to other hydroxide minerals. *Bulletin du B.R.G.M., Section II* 2(3), 293-301.
- BRINDLEY, G.W. 1978: The structure and chemistry of hydrous nickel-containing silicate and aluminate minerals. *Bulletin du B.R.G.M., Section II* 2(3), 234-245.
- BRUNO, J., DEPABLO, J., DURO, L. et al. 1995: Experimental study and modeling of the U(VI)-Fe(OH)₃ surface precipitation/ coprecipitation equilibria. *Geochimica et Cosmochimica Acta* 59(20), 4113-4123.
- BRUNO, J., DURO, L., JORDANA, S. et al. 1996: Revisiting Poços de Caldas - Application of the co-precipitation approach to establish realistic solubility limits for performance assessment, Swedish Nuclear Fuel and Waste Management Co., Stockholm, Sweden, SKB 96-04.
- BUSENBERG, E. & PLUMMER, L.N. 1985: Kinetic and thermodynamic factors controlling the distribution of SO₄²⁻ and Na⁺ in calcites and selected aragonites. *Geochimica et Cosmochimica Acta* 49, 713-725.
- CERNY, P. 1974: The present status of the analcime-pollucite series. *Canadian Mineralogist* 12, 334-341.

- CERNY, P. 1978: Pollucite and its alteration in geological occurrences and in deep-burial radioactive waste disposal. *Scientific Basis for Nuclear Waste Management I*, G. J. McCarthy, ed., Plenum press, 231-236.
- COCHRAN, J. K. 1992: The oceanic chemistry of the uranium and thorium- series nuclides. *In*: "Uranium- series disequilibrium: applications to earth, marine, and environmental sciences", M. Ivanovich and R.S. Harmon eds., Clarendon Press, Oxford, 334-395.
- COREY, R. B. 1981: Adsorption vs. precipitation. *In*: "Adsorption of Inorganics at solid-liquid interfaces", M.A. Anderson and A.J. Rubin eds., Ann Arbor Science, 161-182.
- CROCKET, J.H. & WINCHESTER, J.W. 1966: Coprecipitation of zinc with calcium carbonate. *Geochimica et Cosmochimica Acta* 30, 1093-1109.
- CURIE, M. 1912: *Die Radioaktivität*, Akademische Verlagsgesellschaft M.B.H., Leipzig.
- CURTI, E. 1991: Modelling the dissolution of borosilicate glasses for radioactive waste disposal with the PHREEQE/GLASSOL code: theory and practice, Paul Scherrer Institut, Villigen and Würenlingen, Switzerland, PSI report Nr. 86 and NAGRA, Wettingen, Switzerland, Nagra Technical Report NTB 91-08.
- DAVIS, J.A., FULLER, C.C. & COOK, A.D. 1987: A model for trace metal sorption processes at the calcite surface: adsorption of Cd^{2+} and subsequent solid solution formation. *Geochimica et Cosmochimica Acta* 51, 1477-1490.
- DEER, W.A., HOWIE, R.A. & ZUSSMAN, J. 1992: *The rock-forming minerals*, Longman, 2nd ed., 696 p.
- DEGUELDRE, C., SCHOLTIS, A., PEARSON, J., JR. and LAUBE, A. (1997): Effect of the conditions of groundwater sampling on its chemistry and colloids. Submitted to *Water Resources Research*.
- DOERNER, H.A. & HOSKINS, W.M. 1925: Co-precipitation of radium and barium sulphates. *J. Amer. Chem. Soc.* 47, 662-675.
- DROMGOOLE, E.L. & WALTER, L.M. 1990: Iron and manganese incorporation into calcite: effects of growth kinetics, temperature and solution chemistry. *Chemical Geology* 81, 311-336.
- FELMY, A.R., RAI, D. et al. 1997: Thermodynamic models for highly charged aqueous species: solubility of Th(IV) hydrous oxide in concentrated NaHCO_3 and Na_2CO_3 solutions, *Journal of Solution Chemistry*, 26(3), 233-248.
- GLYNN, P.D. & REARDON, E.J. 1990: Solid-solution aqueous-solution equilibria: thermodynamic theory and representation. *American Journal of Science* 290, 164-201.

- GOGUEL, R. 1983: The rare alkalies in hydrothermal alteration at Wairakei and Broadlands, geothermal fields, N.Z. *Geochimica et Cosmochimica Acta* 47, 429-437.
- GOLDSCHMIDT, V.M. 1954: *Geochemistry*, Oxford University Press, Fair Lawn (U.S.A).
- GOUGAR, M.L.D., SCHEETZ, B.E. & ROY, D.M. 1996: Ettringite and C-S-H Portland cement phases for waste ion immobilization: a review. *Waste Management* 16 (4), 295-303.
- GRAUER, R. 1988: Zum chemischen Verhalten von Montmorillonit in einer Endlagerverfüllung, Paul Scherrer Institut, Villigen and Würenlingen, PSI report Nr. 11 and NAGRA, Wettingen, Switzerland, Nagra Technical Report NTB 88-24.
- GRAUER, R. 1994: Bereinigte Löslichkeitsprodukte von M(II) - Schwermetallkarbonaten, Paul Scherrer Institut, Villigen and Würenlingen, internal technical report TM-44-94-05.
- GRAUER, R. & SCHINDLER, P. 1972: Die Löslichkeitskonstanten der Zinkhydroxidchloride - ein Beitrag zur Kenntnis der Korrosionsprodukte des Zinks. *Corrosion Science* 12, 405 - 414.
- GRENTHE, I., FUGER, J., KONINGS, R. J. M. et al. 1992: Chemical thermodynamics of uranium, Nuclear Energy Agency (OECD), Elsevier, Amsterdam, 715 p.
- HAHN, O. 1936: *Applied Radiochemistry*, Cornell Univ. Press, Ithaca (U.S.A.), 278 p.
- HAWTHORNE, F.C., GROAT, L.A. & ERCIT, T.S. 1987: Structure of cobalt diselenite. *Acta Crystallographica* C43, 2042-2044.
- HYDE, E.K. 1954: Radiochemical separation of the actinide elements. In: "The actinide elements", G.T. Seaborg and J.J. Katz eds. , McGraw-Hill, New York, 542-595.
- KATZ, A. 1973: The interaction of magnesium with calcite during crystal growth at 25-90 °C and one atmosphere. *Geochimica et Cosmochimica Acta* 37, 1563-1586.
- KATZ, A., SASS, E., STARINSKY, A. et al. 1972: Strontium behavior in the aragonite-calcite transformation: an experimental study at 40-98 °C. *Geochimica et Cosmochimica Acta* 36, 481-496.
- KATZIN, L.I. 1954: The chemistry of thorium. In: "The actinide elements", G.T. Seaborg and J.J. Katz eds., McGraw-Hill, New York, 66-102.
- KEELE, R.A. & NICKEL, E.H. 1974: The geology of a primary millerite-bearing sulfide assemblage and supergene alteration at the Otter Shoot, Kambalda, Western Australia. *Economic Geology* 69, 1102-1117.
- KEITH, T. E. C., THOMPSON, J. M. & MAYS, R. E. 1983: Selective concentration of cesium in analcime during hydrothermal alteration, Yellowstone National Park, Wyoming. *Geochimica et Cosmochimica Acta* 47, 795-804.

- KERSABIEC, A.M. & ROGER, G. 1977: Eléments en traces dans les pyrites de la province de Huelva (Espagne). In: "Origin and distribution of the elements", L. H. Ahrens ed., Pergamon Press, Oxford, p. 673.
- KINSMAN, D.J.J. & HOLLAND, H.D. 1969: The co-precipitation of cations with CaCO_3 - IV. The co-precipitation of Sr^{2+} with aragonite between 16° and 90 °C. *Geochimica et Cosmochimica Acta* 33, 1-17.
- KITANO, Y., OKUMURA, M. & IDOGAKI, M. 1980: Abnormal behaviors of copper(II) and zinc ions in parent solution at the early stage of calcite formation. *Geochemical Journal* 14, 167-175.
- KITANO, Y. & OOMORI, T. 1971: The coprecipitation of uranium with calcium carbonate. *Journal of the Oceanographical Society of Japan* 27(1), 34-42.
- KITANO, Y., TOKUYAMA, A. & KANAMORI, N. 1968: Measurement of the distribution coefficient of zinc and copper between carbonate precipitate and solution. *The Journal of earth sciences (Nagoya university)* 16, 1-102.
- KLEBER, W. 1975: Einführung in die Kristallographie. 13. ed., VEB Verlag Technik, Berlin, 392 p.
- KRAUSKOPF, K.B. 1979: Introduction to geochemistry. 2nd ed., McGraw-Hill, New York, 617 p.
- KREMENETSKIY, A.A., YUSHKO, N.A. & BUDYANSKIY, D.D. 1981: Geochemistry of the rare alkalis in sediments and effusives. *Geochemistry International* 17, 54-72.
- KUHNEL, R.A., ROORDA, H.J. & STEENSMA, J.J.S. 1978: Distribution and partitioning of elements in nickeliferous laterites. *Bulletin du B.R.G.M., Section II* 2(3), 191-206.
- LI, Y.H. 1991: Distribution patterns of the elements in the ocean: a synthesis. *Geochimica et Cosmochimica Acta* 55, 3223-3240.
- LIN, J.C., BROECKER, W.S., ANDERSON, R.F. et al. 1996: New $^{230}\text{Th}/\text{U}$ and ^{14}C ages from lake Lahontan carbonates, Nevada, USA, and a discussion of the origin of initial thorium. *Geochimica et Cosmochimica Acta* 60(15), 2817-2832.
- LORENS, R.B. 1978: A study of biological and physical controls on the trace metal content of calcite and aragonite. Ph.D. thesis, University of Rhode Island.
- LORENS, R.B. 1981: Sr, Cd, Mn and Co distribution coefficients in calcite as a function of calcite precipitation rate. *Geochimica et Cosmochimica Acta* 45, 553-561.
- MAKSIMOVIC, Z. 1978: Nickel in karstic environment: in bauxites and in karstic nickel deposits. *Bulletin du B.R.G.M., Section II* 2(3), 173-183.

- McKINLEY, I.G. & WEST, J.M. 1987: Radionuclide retardation in the Near- and Far-field of a HLW repository. In: "The geological disposal of high level radioactive wastes", D.G. Brookins, ed., Theophrastus Publications, S.A., Athens, pp. 445-458.
- MEECE, D.E. & BENNINGER, L.K. 1993: The coprecipitation of Pu and other radionuclides with CaCO₃. *Geochimica et Cosmochimica Acta* 57, 1447-1458.
- MEINRATH, G. & KIM, J.I. 1991a: The carbonate complexation of the Am(III) ion. *Radiochimica Acta* 52/53, 29-34.
- MEINRATH, G. & KIM, J.I. 1991b: Solubility products of different Am(III) and Nd(III) carbonates. *Eur. J. Solid State Inorg. Chem.* 28, 383-388.
- MUCCI, A. 1986: Growth kinetics and composition of magnesian calcite overgrowths precipitated from seawater: quantitative influence of orthophosphate ions. *Geochimica et Cosmochimica Acta* 50, 2255-2265.
- MUCCI, A. & MORSE, J.W. 1983: The incorporation of Mg²⁺ and Sr²⁺ into calcite overgrowths: influences of growth rate and solution composition. *Geochimica et Cosmochimica Acta* 47, 217-233.
- MÜLLER-VONMOOS, M. & KAHR, G. 1983: Mineralogische Untersuchungen von Wyoming Bentonit MX-80 und Montigel, NAGRA, Wettingen, Switzerland, Nagra Technical Report NTB 83-12.
- NAGRA 1989: Hydrochemische Analysen, NAGRA, Wettingen, Nagra unpublished report, 9 volumes, unpagued.
- NAGRA 1994a: Kristallin I - Safety assessment report, NAGRA, Wettingen, Switzerland, Nagra Technical Report NTB 93-22.
- NAGRA 1994b: Bericht zur Langzeitsicherheit des Endlagers SMA am Standort Wellenberg, NAGRA, Wettingen, Switzerland, Nagra Technical Report NTB 94-06.
- NEALL, F.B. 1994: Modelling of the near-field chemistry of the SMA repository at the Wellenberg site, Paul Scherrer Institute, Villigen, Switzerland, PSI Report Nr. 94-18 and NAGRA, Wettingen, Switzerland, Nagra Technical Report NTB 94-03.
- NEALL, F.B. 1996: The pH and composition of fluids arising from a cementitious repository - implications for a high pH-plume, Paul Scherrer Institut, Villigen and Würenlingen, internal technical report TM-44-95-07.
- NERNST, W. 1891: Distribution of a substance between two solvents and between solvent and vapor. *Z. Phys. Chem.* 8, 110-139.
- NEWMAN, A.C.D., ed., 1987: Chemistry of clays and clay minerals, Longman, Harlow (England), 480 p.
- NORDSTROM, D.K. & MUNOZ, J.L. 1985: Geochemical thermodynamics. 1st ed., Benjamin/Cummings Publishing Company, Inc., Menlo Park (U.S.A.), 477 p.

- OKUMURA, M. & KITANO, Y. 1986: Coprecipitation of alkali metal ions with calcium carbonate. *Geochimica et Cosmochimica Acta* 50(1), 49-58.
- ÖSTHOLS, E., BRUNO, J. & GRENTHE, I. 1994: On the influence of carbonate on mineral dissolution: III. The solubility of microcrystalline ThO₂ in CO₂-H₂O media. *Geochimica et Cosmochimica Acta* 58(2), 613-623.
- OSWALD, H.R. & ASPER, R. 1977: Bivalent metal hydroxides. In: "Preparation and crystal growth of materials with layered structures", R. M. A. Lieth ed., D. Reidel Publishing Company, Dordrecht, Holland, 71-140.
- PAQUETTE, J. & REEDER, R.J. 1995: Relationship between surface structure, growth mechanism, and trace element incorporation in calcite. *Geochimica et Cosmochimica Acta* 59(4), 735-749.
- PEARSON, F.J., JR., BERNER, U. & HUMMEL, W. 1992: NAGRA thermochemical database - II. Supplemental data, NAGRA, Wettingen, Switzerland, Nagra Technical Report NTB 91-17.
- PFINGSTEN, W. 1994: Modular coupling of transport and chemistry: theory and model applications, Paul Scherrer Institut, Villigen and Würenlingen, PSI report Nr. 94-15 and NAGRA, Wettingen, Switzerland, Nagra Technical Report NTB 94-19.
- PIETSCH, E., ed. 1938: Gmelins Handbuch der anorganischen Chemie: Caesium. 8th ed., Deutsche Chemische Gesellschaft, Weinheim.
- PINGITORE, N.E. & EASTMAN, M.P. 1984: The experimental partitioning of Ba²⁺ into calcite. *Chemical Geology* 45, 113-120.
- PINGITORE, N.E. & EASTMAN, M.P. 1986: The coprecipitation of Sr²⁺ with calcite at 25°C and 1 atm. *Geochimica et Cosmochimica Acta* 50, 2195-2203.
- READ, D. & FALCK, W.E., eds. 1996: CHEMVAL2 - A coordinated research initiative for evaluating and enhancing chemical models in radiological risk assessment (Final report), European Commission, Brussels, Chapter V.
- REEDER, R.J., LAMBLE, G.M., LEE, J.F. et al. 1994: Mechanism of SeO₄²⁻ substitution in calcite: An XAFS study. *Geochimica et Cosmochimica Acta* 58, 5639-5646.
- REITERER, F. 1980: Löslichkeitskonstanten und freie Bildungsenthalpien neutraler Uebergangsmetallcarbonate. Ph.D. thesis, Montanuniversität Leoben.
- REMY, H. 1949: Lehrbuch der anorganischen Chemie. 5th ed., akademische Verlagsgesellschaft Geest & Portig K.-G., Leipzig, 841 p.

- ROBOUCH, P. 1989: Contribution à la prévision du comportement de l'américium, du plutonium et du néptunium dans la géosphère; données chimiques. Ph.D. thesis, Ecole Européenne des Hautes Etudes des Industries Chimiques de Strasbourg, Report CEA-R-5473, Commissariat à l'Energie Atomique, Gif-sur-Yvette, France, 216 p.
- ROSEMBERG, F. 1984: Geochemie und Mineralogie lateritischer Nickel- und Eisenerze in Lokris und auf Euböa, Griechenland. Ph.D. thesis, University of Hamburg, Germany, 169 p.
- RUNDE, W., MEINRATH, G. & KIM, J.I. 1992: A study of solid-liquid phase equilibria of trivalent lanthanide and actinide ions in carbonate systems. *Radiochimica Acta* 58/59, 93-100.
- SACKETT, W.M. & POTRATZ, H.A. 1963: Dating of carbonate rocks by ionium-uranium ratios. In: "Subsurface geology of Eniwetok atoll", Geol. Surv. Professional Paper 260-BB, 1053-1066.
- SCHOLTIS, A. & DEGUELDRE, C. 1996: Spurenelementgehalte im Na-HCO₃ Grundwasser der SB6 am Wellenberg, unpublished report, NAGRA, Wettingen, Switzerland.
- SHANNON, R.D. 1976: Revised effective ionic radii and systematic studies of interatomic distances in halides and chalcogenides. *Acta Crystallographica* A32, 751-767.
- SILVA, R.J., BIDOGLIO, G., RAND, M.H. et al. 1995: Chemical thermodynamics of americium, Nuclear Energy Agency (OECD), Elsevier, Amsterdam, 374 p.
- SMITH, R.M. & MARTELL, A.E. 1976: Critical stability constants: inorganic complexes, Plenum Publishers, New York, 257 p.
- STANTON, R.L. 1972: Ore petrology. 1st ed., McGraw-Hill, New York, 713 p.
- STAUDT, W.J., REEDER, R.J. & SCHOONEN, M.A.A. 1994: Surface structural controls on compositional zoning of SO₄⁻² and SeO₄⁻² in synthetic calcite single crystals. *Geochimica et Cosmochimica Acta* 58(9), 2087-2098.
- STIPP, S.L., EGGLESTONE, C.M. & NIELSEN, B.S. 1994: Calcite surface structure observed at microtopographic and molecular scales with atomic force microscopy (AFM). *Geochimica et Cosmochimica Acta* 58, 3023-3033.
- STIPP, S.L., HOCELLA, M.F., JR. et al. 1992: Cd²⁺ uptake by calcite, solid-state diffusion, and the formation of solid-solution: interface processes observed with near-surface sensitive techniques (XPS, LEED, and AES). *Geochimica et Cosmochimica Acta* 56, 1941-1954.
- STUMM, W. & MORGAN, J.J. 1996: Aquatic chemistry. 3rd ed., Wiley & Sons, Inc., New York, 1022 p.

- TERAKADO, Y. & MASUDA, A. 1988: The coprecipitation of rare-earth elements with calcite and aragonite. *Chemical Geology* 69, 103-110.
- TESORIERO, A.J. & PANKOW, J.F. 1996: Solid solution partitioning of Sr^{2+} , Ba^{2+} , and Cd^{2+} to calcite. *Geochimica et Cosmochimica Acta* 60(6), 1053-1063.
- THOENEN, T. 1997: The effect of sulfidic groundwater on the solubility of Ni: A preliminary study. Paul Scherrer Institut, Villigen and Würenlingen, internal technical report TM-44-97-03.
- THORNER, M.R. & NICKEL, E.H. 1976: Supergene alteration of sulphides. III. The composition of associated carbonates. *Chemical Geology* 17, 45-72.
- TITS, J. 1994: Immobilisation of radioelements by CSH phases: a literature survey, Paul Scherrer Institut, Villigen and Würenlingen, internal technical report TM-44-94-03.
- TITS, J., BAEYENS, B. & BRADBURY, M. (in prep.): Sorption of americium on calcite under alkaline conditions, Paul Scherrer Institute, Villigen and Würenlingen, Switzerland.
- VAN LOON, L. V. & HUMMEL, W. 1995: The radiolytic and chemical degradation of organic ion exchange resins under alkaline conditions: effects on radionuclide speciation, Paul Scherrer Institut, Villigen, Switzerland, PSI Report Nr. 95-13 and NAGRA, Wetingen, Switzerland, Nagra Technical Report NTB 95-08.
- VEIZER, J. 1983a: Chemical diagenesis of carbonates: theory and application of trace element technique. In: "Stable isotopes in sedimentary geology", SEPM Short course No. 10, Society of economic paleontologists and mineralogists, Ottawa, pages 3-1 to 3-100.
- VEIZER, J. 1983b: Trace elements and isotopes in sedimentary carbonates. In: "Carbonates: mineralogy and chemistry", *Reviews in Mineralogy* 11, R.J. Reeder ed., Mineralogical Society of America, Washington, D.C., 265-299.
- WEAST, R.C. 1977: Handbook of chemistry and physics, 58th ed., CRC Press, Inc., Cleveland (U.S.A.).
- WEDEPOHL, K.H., ed. 1969-1978: Handbook of geochemistry, Springer Verlag.
- WESTALL, J., ZACHARY, J.L. & MOREL, F.M.M. 1976: MINEQL, a computer program for the calculation of chemical equilibrium composition of aqueous systems. Mass. Inst. Tech. Dept. Civil Eng. Tech. Note 18, 91 p.
- WHITE, J.S., HENDERSON, E.P. & MASON, B. 1967: Secondary minerals produced by weathering of the Wolf Creek meteorite. *American Mineralogist* 52, 1190-1197.
- ZACHARA, J.M., COWAN, C.E. & RESCH, C.T. 1991: Sorption of divalent metals on calcite. *Geochimica et Cosmochimica Acta* 55, 1549-1562.

- ZHONG, S. & MUCCI, A. 1995: Partitioning of rare earth elements (REEs) between calcite and seawater solutions at 25°C and 1 atm, and high dissolved REE concentrations. *Geochimica et Cosmochimica Acta* 59(3), 443-453.
- ZWICKY, H.U., GRAMBOW, B., MAGRABI, C., et al. 1989: Corrosion behaviour of British Magnox waste glass in pure water. *Scientific Basis for Nuclear Waste Management XII*, Berlin, W. Lutze and R. C. Ewing, eds., Materials Research Society, 129-136.